BEHAVIOR OF EXCITED MERCURY ATOMS IN THE PREIONIZED MERCURY VAPOR FLOW

Masahiro Nishikawa

BEHAVIOR OF EXCITED MERCURY ATOMS IN THE PREIONIZED MERCURY VAPOR FLOW

Masahiro Nishikawa

Preface

In this monograph are collected the fruits of the studies made by the author under the supervision of Professor Tokuo Suita in the postgraduate course of Osaka University. All the researches were performed in the Department of Nuclear Engineering, Faculty of Engineering, Osaka University.

September 29, 1971

Masahiro Nishikawa

Contents

Chapter 1.

Introduction

Studies of behavior of excited and charged particles in a preionized gas flow have been performed in a flowing afterglow on the basis of measurement of the reaction rates at which the active species in the carrier gas decrease downstream. The steady state flowing afterglow method has been developed by the Environmental Science Service Administration (E.S.S.A.) group at Boulder, Colorado, U.S.A. (Fehsinfeld et al. 1966) for one of the measurement methods to obtain reliable information on various reactions between the active species at thermal energy or suprathermal energy i.e. ion-neutral reaction, electron-neutral reaction, the reaction between atoms with the excited state and the ground state and so forth. Such collision phenomena at thermal or suprathermal region can be found to be common in discharges, plasmas and moreover, ionospheres of celestial bodies like the earth and the other planets. Hitherto by observations of the atomic light emitted from a pulsed afterglow, which is resolved on time, many results as to ion-neutral reaction and recombination process have been obtained, however, these accuracies are not always satisfactory. The steady state flowing afterglow method replaces time resolution with spatial resolution so that a noted

plasma condition can be selected spatially and a reactant in the ground state can be introduced into the afterglow plasma.

This experimental method is almost similar to that of the formation and detection of nonequilibrium ionization in the closed cycle MHD generator. In order to attain an appropriate electric conductivity of the working fluid, d.c. and r.f. discharge are excited at the inlet of the generator channel with seeding materials such as cesium and potassium at the upper flow. For such preionization technique, the ion concentration which can be achieved with a given ionization source may be probably limited in the recombination and the diffusion. Thus the loss processes of charged particles in the channel have been discussed in a large number of papers.

In the field of the quantum electronics, with development of lasers the studies of relaxation mechanism in excited laser levels have been discussed frequently. The destruction of lower excited states in discharge plasma containing molecular impurities is of great interest in connection with the problem of creating a medium with a negative absorption coefficient that is a laser action. It will be difficult to isolate and evaluate the role of quenching by the impurities in the pulsed afterglow because the impurities change the electrokinetic characteristics of the discharge.

The various informations drawn from observation of the afterglow are necessary to investigate collision processes at low energy and those rate constants are useful for seeking to design direct energy convertors, the possibility of ion propulsion units and the like.

The afterglow following a pulsed discharge in mercury vapor has been investigated by many persons and it has been reported that the intensity of the spectral emission exhibited a complicated decay on the whole, i.e. an initial rapid decay followed by a decrease with slow decay constant. By R.Anderson and E.Steep it is assumed that the main processes governing the initial decay are spontaneous radiative decay of the mercury states excited by electrons, and the slow rate of decay is probably controlled by dissociative recombination of molecular mercury.

In this thesis, the steady state flowing mercury afterglow by d.c. discharge which is locally excited is performed and decrease in intensity of the mercury lines emitted from the afterglow was measured from the discharge source to the stream spectroscopically. The axial intensity distribution also exhibited rapid decrease near the source followed by slow decrease somewhat distant from the source. From the dependences of these intensity decreases on the charged particle concentration and on the static pressure of vapor flow, the

collision processes in the afterglow plasma are investigated and those rate constants are estimated. The arrangement of the d.c. discharge electrodes is employed in order to clarify the domain of the ionizing source, which is discussed in Chapter 2.

In Chapter 3, rapid decrease in intensity of mercury lines is described in connection with the diffusion of electrons and the electron attachment, which may be interpreted as the production process of temporary negative ions shown by U.Fano and J.W.Cooper. The experimental checks are described in Chapter 4.

From decrease in the metastable atom density distant from the discharge source, the diffusion and the conversion from metastable atoms to metastable diatomic molecules are discussed in Chapter 5.

In Chapter 6, it is described that slow decrease in intensity of mercury lines distant from the discharge source is related to that in the charged particle concentration due to the dissociative recombination. The conversion from atomic mercury ions to molecular ions is also discussed.

In order to make the dissociative recombination described in Chapter 6 clear, hydrogen molecule in the ground state is introduced into the afterglow plasma where the intensity decreases slowly. From quenching of the radiation due to hy-

drogen molecule, the depopulation and the cascade transition of mercury excited atoms which are dissociated from the recombined molecules are examined and further, the quenching cross section and the transition probability are estimated in Chapter 7.

Finally the summary of this thesis is described collectively in Chapter 8.

Chapter 2.

D.C. Discharge in the Mercury Vapor Flow*

For the study of steady state mercury flowing afterglow a d.c. discharge is used as an ionization source and this discharge is caused by a d.c. electric field applied perpendicular to the flow direction. The mechanism of electron release as well as ion release from the discharge source is interpreted.

The electron density and temperature near the discharge source by means of the triple probe method and the line intensity emitted from excited mercury atoms are measured for each discharge current, and it is found that the intensity and the electron density increase linearly with the discharge current when the electron temperature is almost constant.

2-1 Introduction

The intensity distribution of steady state flowing afterglow is generally found to depend on the concentrations and temperatures of the active species, especially on the electron density and temperature. For instance, if the after-

---

*Part of the contents is presented in Journal of the Physical Society of Japan, Vol.30, No.2, P.528-536, February, 1971.

glow plasma is in the recombination region, decrease in the electron density n_e depends on the initial electron density $n_e(0)$, and the intensity decrease is proportional to αn_e^2 .

Assuming one dimensional flow, the rate equation can be written as

$$v_f \frac{\partial n_e}{\partial x} = - \alpha n_e^2 \quad , \qquad (2-1)$$

where v_f, α and x are the flow velocity, the recombination coefficient and the distance from the discharge source, respectively. This solution is directly given as

$$n_e = n_e(0) / (1 + \alpha n_e(0) x/v_f) \quad ,$$

so that the intensity I is represented as follows.

$$I / I(0) = 1 / (1 + \alpha n_e(0) x/v_f)^2 \quad , \qquad (2-2)$$

where I(0) is the intensity at x=0 . In eq.(2-2) it is worthy to note that the decay mode depends on the initial electron density. Thus to produce and controll the steady state flowing afterglow, the mechanism of electron release as well as ion release from the discharge source must be estimated, and the relation between the discharge current

and the electron density near the discharge source is also investigated experimentally.

2-2 Electron Release from the Discharge Source

As shown in Fig.2-1 the electrodes are arranged to apply the electric field perpendicular to the flow axis so that the domain of the ionization source is clarified. In this configuration, estimation of electron release from the restraint of the electric field of the source is important in order to investigate how decrease in intensity near the discharge source is affected by the electric field distortion owing to the flow.

Assuming that there is no loss except for that of the charged particles flowing out into the downstream, the mechanism of electron release and the flow directional electric field are estimated analytically using the quasi-one dimensional approximation.

If the ionization process is the electron collisional one, the fundamental equations can be written as:

$$f\, n_e - \mathrm{div}\, \vec{u}_e n_e = 0 , \qquad (2\text{-}3)$$

$$f\, n_e - \mathrm{div}\, \vec{u}_+ n_+ = 0 , \qquad (2\text{-}4)$$

$$\vec{u}_e = \vec{v}_f - \mu_e \vec{E} \quad , \quad \vec{u}_+ = \vec{v}_f + \mu_+ \vec{E} , \qquad (2\text{-}5)$$

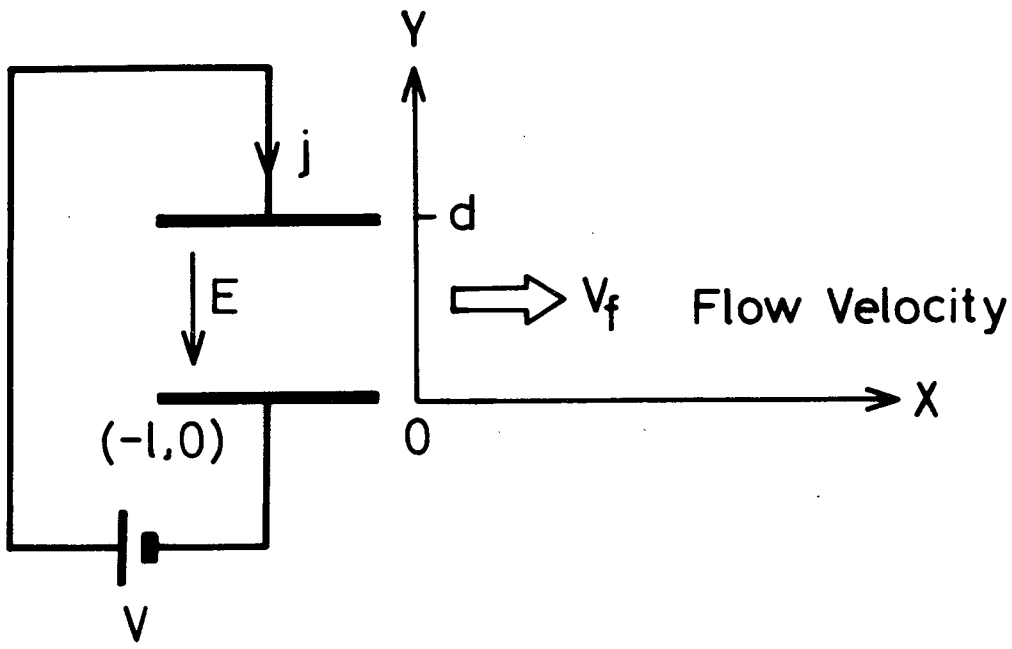

Fig.2-1 Discharge electrodes arranged to apply the electric field perpendicular to the flow axis.

$$\text{div}\,\vec{E} = (e/\varepsilon_0)(n_+ - n_e) = -\nabla^2\Phi\ , \qquad (2\text{-}6)$$

where f is the ionization frequency which is intimately related to Townsend's first ionization coefficient $\bar{s}$, as follows.

$$f = \bar{s}\,|u_e| \ . \qquad (2\text{-}7)$$

And with the suffixes of e and + denoting electrons and ions respectively, μ, n and u represent their mobilities, densities and drift velocities, respectively.

From the difference between eqs.(2-3) and (2-4), the following equation can be obtained using eq.(2-6).

$$\text{div}\left\{ (\mu_+ n_+ + \mu_e n_e)\vec{E} + (\varepsilon_0/e)\vec{v}_f \text{div}\,\vec{E} \right\}$$

$$= \text{div}\,\vec{J}/e = 0 \ . \qquad (2\text{-}8)$$

Introducing a new function Ψ defined by the following equations:

for $x > -\tilde{l}$

$$e(\partial\Psi/\partial y) = J_x \ , \quad e(\partial\Psi/\partial x) = -J_y$$

and for $x < -\tilde{l}$

$$\Psi = 0 \ ,$$

the eq.(2-8) can be rewritten as:

$$-(\mu_+ n_+ + \mu_e n_e)\,\Phi_x - (\varepsilon_0/e)v_f\nabla^2\Phi = \Psi_y \quad , \qquad (2\text{-}9)$$

$$-(\mu_+ n_+ + \mu_e n_e)\,\Phi_y = -\Psi_x \quad . \qquad (2\text{-}10)$$

Here, it is found that $e\Psi_x$ and $e\Psi_y$ represent the electric current through the unit area in the y-direction and the x-direction, respectively.

Using eqs.(2-9) and (2-10), eqs.(2-3) and (2-4) are represented with Φ and Ψ as follows.

$$-\Phi_x\Psi_x - (\varepsilon_0/e)v_f\Phi_y\nabla^2\Phi = \Phi_y\Psi_y \quad , \qquad (2\text{-}11)$$

$$\frac{\partial}{\partial x}\left[-\nabla^2\Phi\left\{\Phi_x - v_f\left(\frac{1}{\mu_+} - \frac{1}{\mu_e}\right) - \frac{v_f^2}{\mu_+\mu_e\Phi_x}\right\} + \frac{ev_f\Psi_y}{\varepsilon_0\mu_+\mu_e\Phi_x} + \bar{s}\Phi_x\Phi_y + \bar{s}\frac{e\Psi}{\varepsilon_0\mu_+}\right] + \frac{\partial}{\partial y}\left[-\Phi_y\nabla^2\Phi + \bar{s}(\Phi_y - \Phi_x)/2\right] = 0 \qquad (2\text{-}12)$$

When the width of the discharge electrode as shown in Fig.2-1 is denoted by W, the discharge current can be described as follows.

$$dj_+ = \text{grad}\,\Phi\cdot\vec{u}_+ en_+ Wdxdy/V,\quad dj_e = \text{grad}\Phi\cdot\vec{u}_e en_e Wdxdy/V \quad , \qquad (2\text{-}13)$$

where $\vec{u}_+$: $(v_f - \mu_+\Phi_x\ ,\ -\mu_+\Phi_y)$,

$\vec{u}_e$: $(v_f + \mu_e\Phi_x\ ,\ \mu_e\Phi_y)$

and V is the terminal voltage between the electrodes.

By rearranging eq.(2-13) as follows, it can be solved as a line integral along the boundary line.

$$dj/W = (dj_+ - dj_e)/W = (e/V)(\Psi_y\Phi_x - \Psi_x\Phi_y)dxdy$$

and then,

$$j/W = (e/V) \oint_C (\Psi_y\Phi dy + \Psi_x\Phi dx) . \qquad (2\text{-}14)$$

It is very complicated to obtain the solution directly from calculating eqs.(2-11), (2-12) and (2-14), and a numerical solution is not necessary for the purpose. As to make a situation clear, it is important to solve it analitically using a proper approximation as follows.

$$\Phi_y = -E = V/d = \text{const.} \quad (E < 0 \text{ in Fig.2-1 })$$

where d is the distance between the discharge electrodes .

The x component of the velocities of charged particles dose not contribute to the convective discharge current in this electrode configuration and out of the electrode no electric current is collected in the plasma flow so that $\Psi_y = 0$.

From eq.(2-11), Ψ is obtained as,

$$\Psi = (\varepsilon_0/e)v_f E \ln \Phi_x/\Phi_x(\tilde{-1}) \quad , \qquad (2\text{-}15)$$

where $\tilde{l}$ is the length of the discharge electrode.

By use of eq.(2-14) the boundary condition can be written as

$$\Psi(0) = - j/(eW) , \tag{2-16}$$

so that $\Phi_x(0)$ can be related to $\Phi_x(-\tilde{l})$ as follows.

$$\Phi_x(0) = \Phi_x(-\tilde{l})\exp\left(- \frac{j}{\varepsilon_0 v_f EW}\right)$$

$$= \Phi_x(-\tilde{l})\exp\left(- \frac{j}{\varepsilon_0 v_f EF}\tilde{l}\right) , \tag{2-17}$$

where F is the area of the discharge electrode and the sign of j is identified with that of E .

Since $n_+(-\tilde{l}) = n_e(-\tilde{l}) = 0$, $\Phi_{xx}(-\tilde{l}) = 0$.

In the discharge region, $-\tilde{l} < x < 0$, the following relationship can be obtained from eq.(2-12) .

$$\mu_+\mu_e\Phi_{xx}\Phi_x/v_f - (\mu_e - \mu_+)\Phi_{xx} - (\Phi_{xx}/\Phi_x)/v_f$$

$$+ \mu_+\mu_e\bar{s}E(\Phi_x - \Phi_x(-\tilde{l}))/v_f - \mu_e\bar{s}E \ln(\Phi_x/\Phi_x(-\tilde{l})) = 0. \tag{2-18}$$

Taking eq.(2-17) into consideration, Φ_x may be written for $x \geq 0$ as follows.

$$\mu_+\mu_e(\Phi_x^2 - \Phi_x^2(0))/2v_f - (\mu_e - \mu_+)(\Phi_x - \Phi_x(0))$$

$$- v_f \ln(\Phi_x/\Phi_x(0)) = (j/\varepsilon_0 FE)x \qquad (2\text{-}19)$$

where the production terms in eq.(2-12) are neglected i.e. $\bar{s} = 0$. With the continuity of the charged particle density at the distance 0, $\Phi_x(-\tilde{l})$ can be obtained from eqs.(2-18) and (2-19) as :

$$\Phi_x(-\tilde{l}) = \frac{v_f j}{\mu_+ \varepsilon_0 FE}\left(\frac{1}{\mu_e \bar{s} E} + \frac{\tilde{l}}{v_f}\right)\left(1 - \exp\left(-\frac{j\,\tilde{l}}{\varepsilon_0 v_f FE}\right)\right)^{-1}. \qquad (2\text{-}20)$$

From eq.(2-20), the self-sustaining condition in the flow may be found as follows: $\tilde{l}/v_f > -1/\mu_e \bar{s} E$ that is, $f > v_f/\tilde{l}$. Equation(2-19) is approximatelly written as

$$\Phi_x = \Phi_x(0)\exp(-jx/\varepsilon_0 v_f FE) \ . \qquad (2\text{-}21)$$

$$(x > 0)$$

This relationship agrees with that obtained by assuming eq.(2-8) as the function of x only. Equation(2-8) can be rewritten as

$$\mathrm{div}\,\vec{J} = \mathrm{div}\left\{\sigma_c \vec{E} + e\vec{v_f}(n_+ - n_e)\right\} = 0,$$

where $\sigma_c = e(n_+\mu_+ + n_e\mu_e)$.

If the spatial dependence of the conductivity σ_c is not taken into consideration, the above equation can be represented as

$$v_f \frac{\partial(n_+ - n_e)}{\partial x} + (\sigma_c/\varepsilon_0)(n_+ - n_e) = 0.$$

Then the solution is obtained as

$$n_+ - n_e = C \exp(- \frac{\sigma_c}{\varepsilon_0 v_f} x) ,$$

so that Φ_x is proportional to $\exp(- \sigma_c x/\varepsilon_0 v_f)$. This relationship is found to be identical to eq.(2-21) with defining σ_c equal to j/FE.[2)]

From eqs.(2-6), (2-9) and (2-19), n_e and n_+ can be obtained as:

$$n_e = \frac{j}{eFE} \frac{v_f}{\mu_e(v_f/\mu_e + \Phi_x)(\mu_+ + \mu_e)} , \qquad (2\text{-}22)$$

$$n_+ = \frac{j}{eFE} \frac{v_f}{\mu_+(v_f/\mu_+ - \Phi_x)(\mu_+ + \mu_e)} . \qquad (2\text{-}23)$$

From eqs.(2-20), (2-22) and (2-23), it is found that at first massive ions transferred downstream by collisions with flowing neutral atoms are released from the electric field of the discharge source much easier than electrons and consequently by the produced Coulomb force in the flow direction electrons are also released from the electric field to become the plasma flow. This interpretation is supported by the rela-

tion(2-20) in which v_f/μ_+ is the electric field on EGD effect.[3)]

Under the typical experimental conditions where $j = 6\times10^{-3}$ A, $v_f = 100\ ms^{-1}$, $F = 2\times10^{-5}\ m^2$ and $E = 5\times10^4\ Vm^{-1}$, the value of the reciprocal characteristic length $j/(\varepsilon_0 v_f FE)$ is very large that is about $7\times10^6\ m^{-1}$ so that the flow directional electric field at the outlet of the discharge source, $-\Phi_x(0)$, becomes very small and decreases very rapidly. Consequently the effect of this electric field can be neglected in the present case.

In the glow discharge region in which the terminal voltage is almost constant, it is found that the number density of electrons released from the discharge source is proportional to the discharge current.

2-3 Experimental Apparatus

A steady mercury atomic flow is made in Rankine cycle and its block diagram is shown in Fig.2-2. Liquid mercury in a boiler is vaporized by indirect heating and the mercury vapor is further superheated before a buffer to stabilize pressure and come through a de-Laval nozzle. Thus a steady uniform flow can be obtained. In the superheater, the heat input is provided enough to avoid the formation of mercury molecules as well as condensation. In the extremity of the test sec-

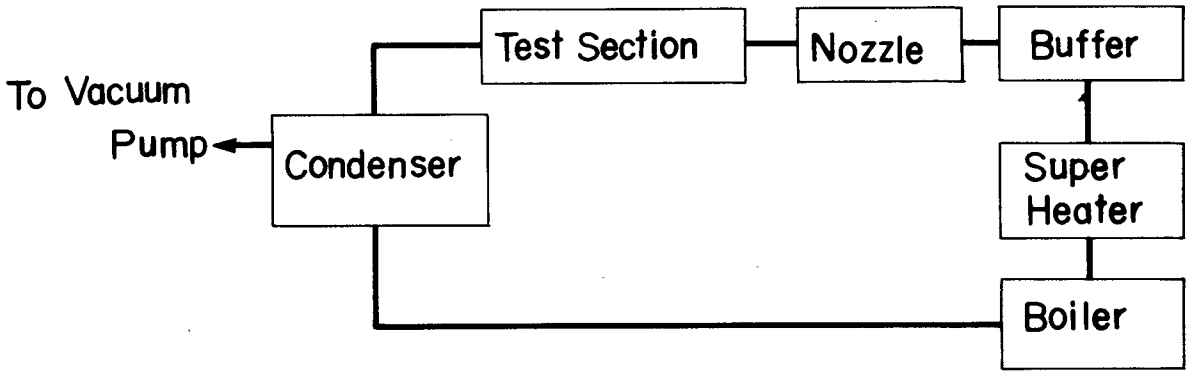

Fig.2-2 Block diagram of the flow system.

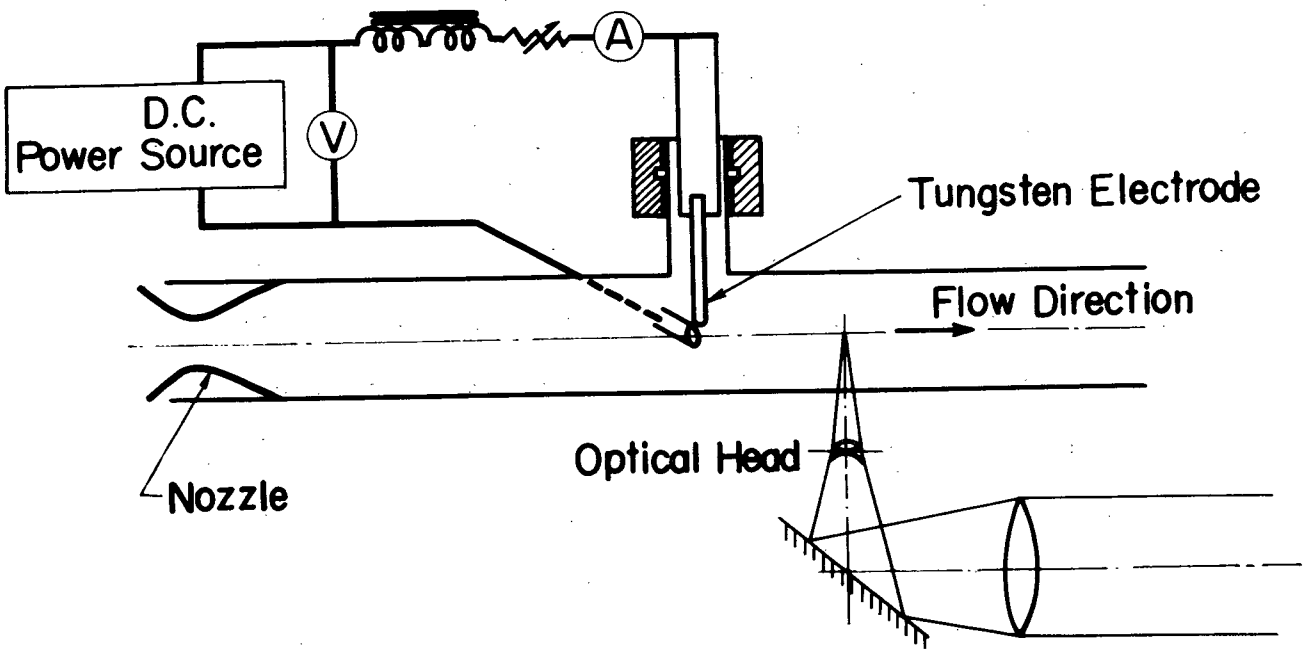

Fig.2-3 The arrangements of the discharge electrodes and the optical head.

tion, the mercury atomic flow is condensed by the water-cooled condenser and turned to the boiler by gravitation. The test section consists of a transparent quartz tube with a diameter of 3 cm, and the length of the tube is taken to be 100 cm so that d.c. field is not affected by the encompassing metals such as the boiler and the superheater. In order to stabilize the d.c. discharge, a transformer with dropping characteristics is provided in the d.c. power source and stabilization coils are also connected with the external circuit. The electrodes are tungsten rods 5 mm in diameter. The discharge electrodes are so arranged not to be affected in intensity along the flow downstream by the d.c. field.(Fig.2- 3)

The density and temperature of electrons released from the discharge electrode is measured by the triple probe method.[4] The radiation emitted from mercury excited atoms is measured spectroscopically through the optical head of the retrofocus type. For the relative intensity measurements in the wavelength range of 2500 - 6000 Å, the entire detection system has been calibrated against a standard tungsten ribbon lamp.[5] The accuracy of the relative intensity measurents may be estimated to be equivalent to that of the probe method. The deviation for the constants calculated from the experimental results is within several percents all over operation.

The detailed interpretations on the measurements mentioned above will be described in Chapter 3.

2-4 Experimental Results and Discussions

The electron density and temperature are measured with a triple probe at about 1 cm from the electrode. When the optical measurements are carried out, the probe is removed from the test section.

Figure 2-4(a) shows the relation between the discharge current and the electron density and temperature at a static pressure of 0.65 mmHg and a flow velocity of 130 ms^{-1}. The electron density is found to increase linearly with the discharge current under the constant electron temperature condition where the applied voltage is almost kept constant. Figure 2-5(a) shows also the similar relation at a static pressure of 2.0 mmHg. The electron temperature are about 2 eV at 0.65 mmHg and about 1.5 eV at 2.0 mmHg, respectively.

The line intensities at 1 cm from the discharge electrode are also found to increase linearly with the discharge current that is, with the electron density as shown in Figs. 2-4(b) and 2-5(b). In such a region, where the line intensities increase linearly with the electron density and the electron temperature is still high enough to excite the mercury atoms, the recombination process can be neglected.

The density of the atoms n_i at the i-th excited level except 6^3P_1 state can be described as

(a)

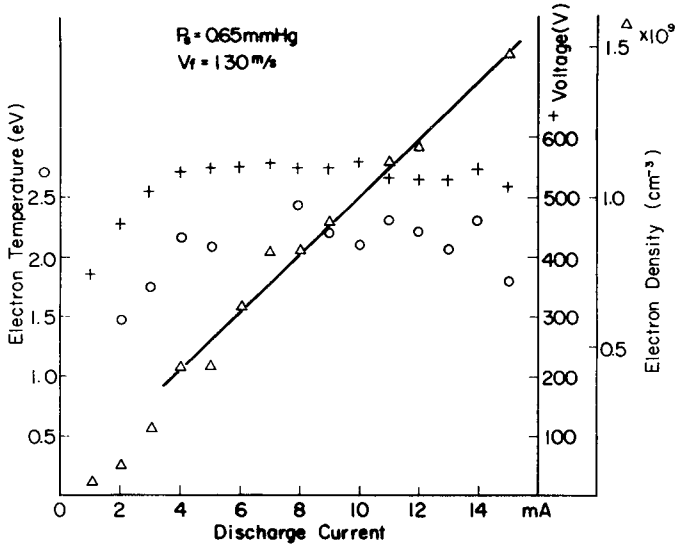

(b)

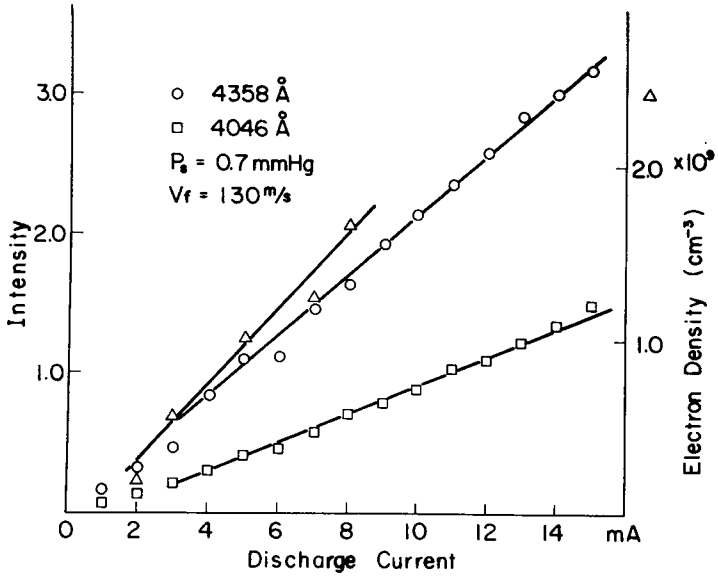

Fig.2-4(a) and Fig.2-4(b) Electron density and temperature, and relative line intensities vs discharge current at the distance about 1 cm from the electrode. (p_s = 0.65 mmHg)

(a)

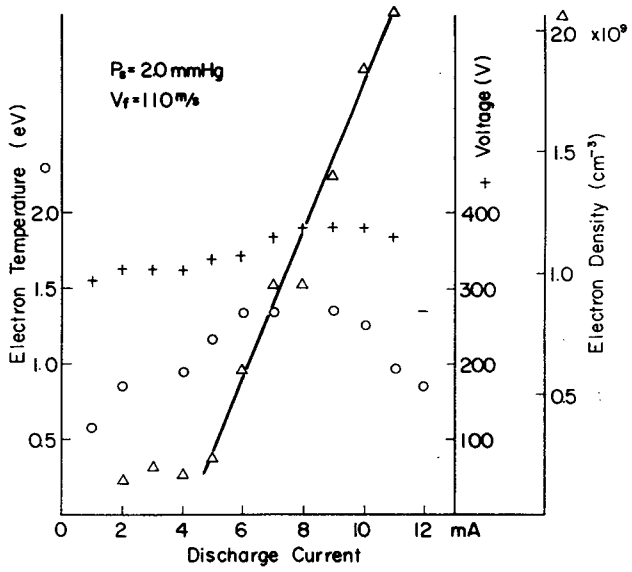

(b)

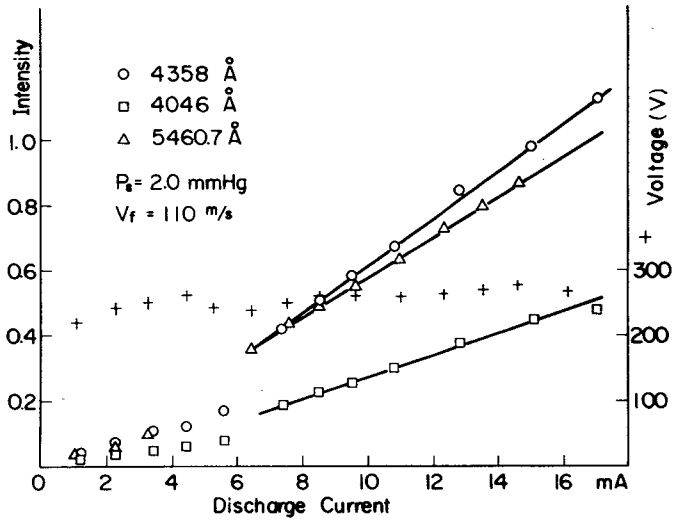

Fig.2-5(a) and Fig.2-5(b) Electron density and temperature, and relative line intensities vs discharge current at the distance about 1 cm from the electrode.

(p_s = 2. mmHg)

$$\frac{dn_i}{dt} = \sum_m \langle v\sigma \rangle_{mi} n_e n_m - \sum_m \langle v\sigma \rangle_{im} n_e n_i - \sum_k \langle v\sigma \rangle_{ik} n_e n_i$$

$$+ \sum_k \langle v\sigma \rangle_{ki} n_e n_k - \sum_m A_{im} n_i \quad (m < i < k) \qquad (2\text{-}24)$$

where $\langle v\sigma \rangle_{mi} n_e$, $\langle v\sigma \rangle_{ik} n_e$ are the transition probabilities for collisional excitation by electrons, $\langle v\sigma \rangle_{im} n_e$, $\langle v\sigma \rangle_{ki} n_e$ are the probabilities of the inverse process, that is, the second kind collisions and A_{im} is the probability of the radiative transition.

Since the radiative transition probability of the measured line is very large in comparison with $(v_f/n_i)\partial n_i/\partial x$, and the discharge is steady, eq.(2-24) can be written as

$$n_i = (K_i / \sum_m A_{im}) n_e \qquad (2\text{-}25)$$

where

$$K_i = \frac{\sum_m \langle v\sigma \rangle_{mi} n_m + \sum_k \langle v\sigma \rangle_{ki} n_k}{1 + (\sum_k \langle v\sigma \rangle_{ik} + \sum_m \langle v\sigma \rangle_{im}) n_e / \sum_m A_{im}} .$$

Then the intensity I_{im} becomes

$$I_{im} = (A_{im} / \sum_m A_{im}) h\nu_{im} K_i n_e . \qquad (2\text{-}26)$$

In active thin plasma, the excitations from the ground levels are dominant so that the term for the ground level is

much larger than the terms for the other excited levels in the numerator of K_i, which approximates to $\langle v\sigma \rangle_{0i} n_o$. Therefore the intensity I_{im} emitted from the level i which has large transition probability is proportional to $A_{im} h\nu_{im} / \sum_m A_{im}$. From Figs.2-4(b) and 2-5(b), ratios of the transition probabilities for the lines emitted from 7^3S_1 states, 4046.6, 4358.3 and 5460.7 Å, can be given as follows.

$$A_{4046.6} : A_{4358.3} : A_{5460.7} = 0.44 : 1.0 : 1.1 .$$

These ratios are found to agree well to those of the values from NBS Table[6] that are 0.42 : 1.0 : 1.0 .

Thus the line intensity emitted from highly excited levels is found to be regarded as that of the spontaneous radiation.

2-5 Concluding Remarks

For the mechanism of electron release from the discharge electrode it is interpreted that massive ions transferred downstream by collisions with flowing neutral atoms are released from the electric field of the discharge source much easier than electrons at first, and consequently by the produced Coulomb force in the flow direction electrons are also released from the discharge source to become the plasma flow.

It is verified from the quasi-one dimensional approximation that the produced flow directional electric field de-

creases rapidly and is not affected in the measured intensity decrease.

The electron density near the discharge source is found to increase linearly with the discharge current in the glow discharge region. It is indicated to be controlled by the electron excitation, which is supported by the fact that the line intensity of radiation emitted from highly excited levels increases with the electron density.

In this experimental condition, the line intensity of radiation emitted from highly excited levels is found to be proportional to the spontaneous radiation emitted from excited atoms, because the ratios of the transition probabilities estimated from the relative intensity measurements agree well with those of the values from NBS Table.

References

1) A.von Engel : Ionized Gases (Clarendon Press. Oxford, 1965)

2) M.Nishikawa,Y.Fujii-e and T.Suita : J.Phys.Soc.Japan 30(1971) 528.

3) O.M.Stuetzer : Phys. of Fluids 5(1962) 534.

4) S.L.Chen and T.Sekiguch : J.appl.Phys. 36(1965) 2363.

5) R.Stair,W.E.Schneider and J.K.Jakson : Appl.Optics 2(1963) 1151.

6) C.H.Corliss and W.R.Bozman : Experimental Transition Probabilities for Spectral Lines of Seventy Elements (Washington N.B.S. 1962) P.152.

Chapter 3.

Intensity Distribution near the Discharge Source*

In a flowing mercury afterglow with d.c. discharge source, rapid decrease in intensity of Hg lines near the source is investigated. Both the axial intensity distribution along the flow downstream and the radial one are interpreted in connection with the diffusion of electrons to the wall and the electron attachment. The effective diffusion coefficient is found to be $D_{\beta,\gamma} = 2.7\times10^{3}/p \ \ cm^{2}s^{-1}$, which is close to the ambipolar diffusion coefficient under the experimental conditions i.e. $n_e = 5\times10^{8} \ \ cm^{-3}$ and $T_e = 2 \ \ eV$.

As for the resonance line ($6^3P_1 - 6^1S_0$), slow decrease in intensity as compared with decrease in intensity of lines emitted from the higher levels is taken to be due to the radiative imprisonment and in consequence the absorption coefficient of this line is obtained as $1.2\times10^{-13}n_o \ \ cm^{-1}$ and the quenching probability of the state 6^3P_1 due to the collisions with mercury atoms as $\langle v\sigma\rangle_{10}n_o = 1.1\times10^{-13}n_o \ \ s^{-1}$.

3-1 Introduction

It has been reported that the intensity of the spectral emission from a pulsed mercury discharge exhibited a compli-

---

*The main part of this chapter was published in Journal of the Physical Society of Japan,Vol.30, No.2, P.528-536, February, 1971.

cated decay on the whole, i.e. an initial rapid decay followed by a decrease with slow decay constnt[1,2], and it was assumed that the main processes governing the initial decay were spontaneous radiative decay of the mercury states excited by electrons and the slow rate of decay was probably controlled by dissociative recombination of molecular mercury.[1]

When d.c. discharge was kept in a steady mercury gas flow, the distribution of the intensity of certain mercury lines along the flow from the discharge source also exhibited the same profile as mentioned above: rapid decrease near the discharge source followed by slow decrease somewhat distant from the source.[3] The first region in which the intensity decrease rapidly is interpreted as the spontaneous emission of the excited mercury atoms and the electrons in this region are still active.

In most of the experiments of the flowing afterglow, the radio frequency discharge is excited and there are a few of the reports in which decrease in intensity of mercury lines near the source has been discussed.

In this chapter it is investigated how decrease in intensity of mercury lines is related to decrease in the number density of charged particles under non-thermal equilibrium condition near the d.c. discharge source.

Decrase in the number density of electrons is assumed to be due to the diffusion and the attachment as a linear volume loss. The observed intensities of mercury lines are interpreted in Section 3-3 for intensity of radiation emitted from highly excited levels and that of the resonance line.

3-2 Experimental Apparatus and Procedure

A steady mercury vapor flow is made in Rankine cycle described in the previous chapter, in which the arrangement of the discharge electrodes in the inlet of the test section is also mentioned. The radiation emitted from the test section is focused on the slit set in front of the spectrograph through the optical head of the retrofocus type. Intensities of more than two of the emitted lines are measured simultaneously with an Ebert type spectrograph equipped with 1p21 photomultipliers. In measuring the intensity distribution along the flow, the signals from the photomultipliers are amplified by a logarithmic amplifier and are fed to a recorder. The optical head is scanned downstream at a rate of 10 cm/min.

On the other hand, the measurement of the radial intensity distribution is performed by scanning the image across a diameter by a transverse slit, and the true distribution is calculated by Pearce's method.[4] A slit position is con-

verted to the electric signal by a potentiometer, which is fed to X-axis and the intensity at the position to Y-axis of the X-Y recorder. The flow velocity is obtained by the time of flight method; the time interval in which the slug of the ionized gas made by a pulsed discharge arrives at a certain position is measured with the probe and the optical head. These measured values agreed well with each other and it was verified that the flow velocity is constant over the distance of at least 50 cm downstream from the discharge electrode. As an example, the results of the time of flight method measured by the probe are shown in Fig.3-1.

The measurements of the electron temperature and density are carried out by the probe method, mainly with the triple probe. When the optical measurements are carried out, the probe is removed from the test section.

The block diagram of the experimental arrangement is shown in Fig.3-2.

In the wavelength range of 2500 - 6000 Å, it is examined spectrographically that the emitted lines from the test section exhibited those from excited mercury atoms only, except the continuous band fluorescence which is the near ultra violet region centered at about 3350 Å and is treated in Chapter 5.

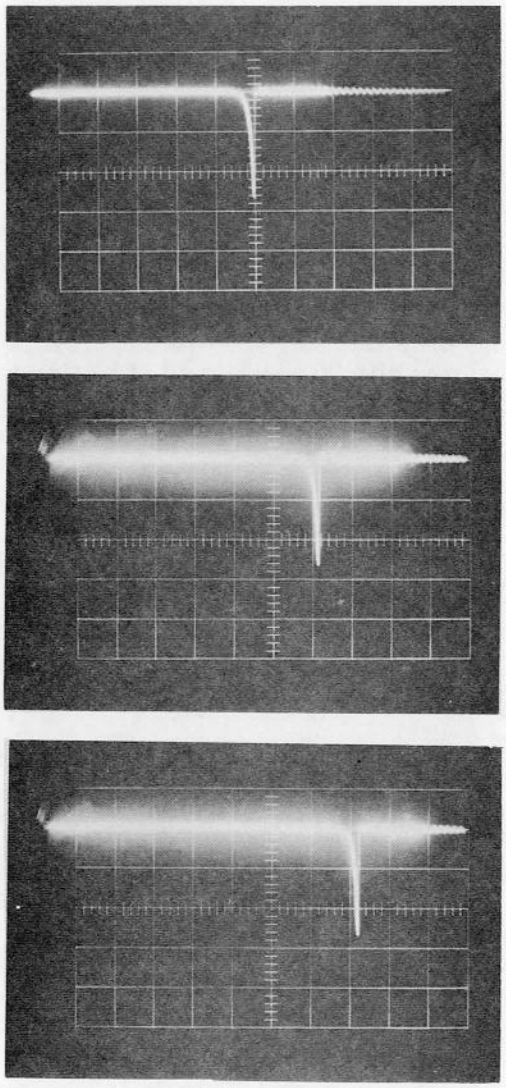

x_1: a certain position at the distance about 27 cm from the discharge electrode.

$x_2 = (x_1 + 6)$ cm

$x_3 = (x_2 + 6)$ cm

0.5 ms/div.

Fig.3-1 The time interval in which the slug of the ionized gas made by a pulsed discharge arrives at the position: x_1, x_2, x_3. From this measurement it is found that the time interval is 0.55 ms per 6 cm i.e. v_f = 110 ms^{-1}. (p_s = 2. mmHg)

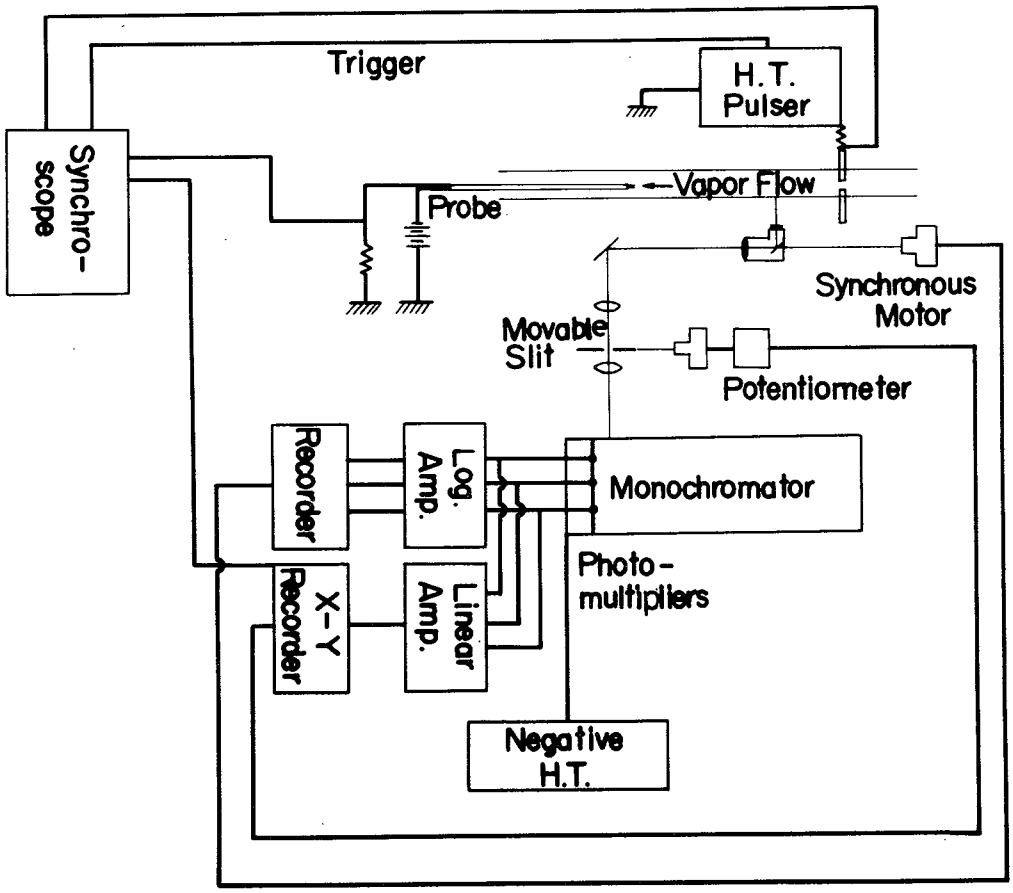

Fig.3-2 Schematic diagram of apparatus for the measurements of radiation intensities and flow velocity.

3-3 Axial Intensity Distribution

The typical intensity distribution of the atomic mercury lines along the flow downstream are shown in Figs.3-3 and 3-4. In these experiments, the static pressures are 0.78 mmHg (120 °C) and 1.8 mmHg (140 °C) respectively, and the flow velocities are 135 ms^{-1} in both cases. On the whole, the intensities of the atomic lines exhibit rapid decrease near the source followed by slow decrease. These intensity distribution along the flow direction are similar in profile to the decays of the intensities in the pulsed mercury afterglow.[1,2] Near the source, the intensity of the resonance line, 2536 Å, decreases slowly in comparison with that of the line emitted from the higher level; the latter characteristic length is one third or fourth as small as that of the resonance line. Among the higher levels, however, the higher level give a little longer characteristic length as shown in Figs.3-3 and 3-4 : the transition from 7^3S_1: 4046.6, 4358.6, 5460.7 Å, and the transition from 7^3D_2: 2652.0 Å.

The electron density is measured with the probe in the flow direction and is also found to decrease rapidly near the source as shown in Fig.3-5.

In Chapter 2 the atomic line intensities are indicated to increase linearly with the electron density near the source. Thus the rapid decrease in intensity is found to be control-

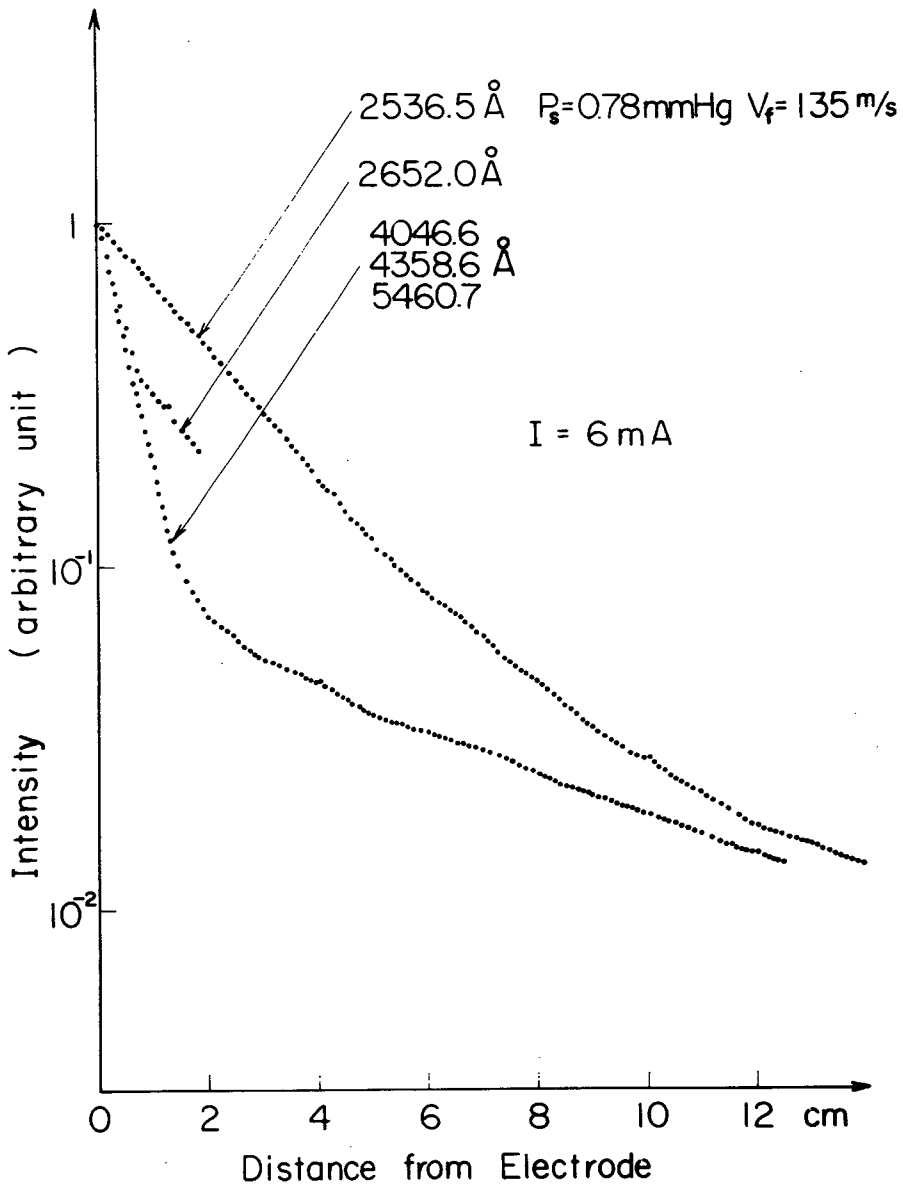

Fig.3-3 Line intensity decreases along the flow direction at the pressure 0.78 mmHg.

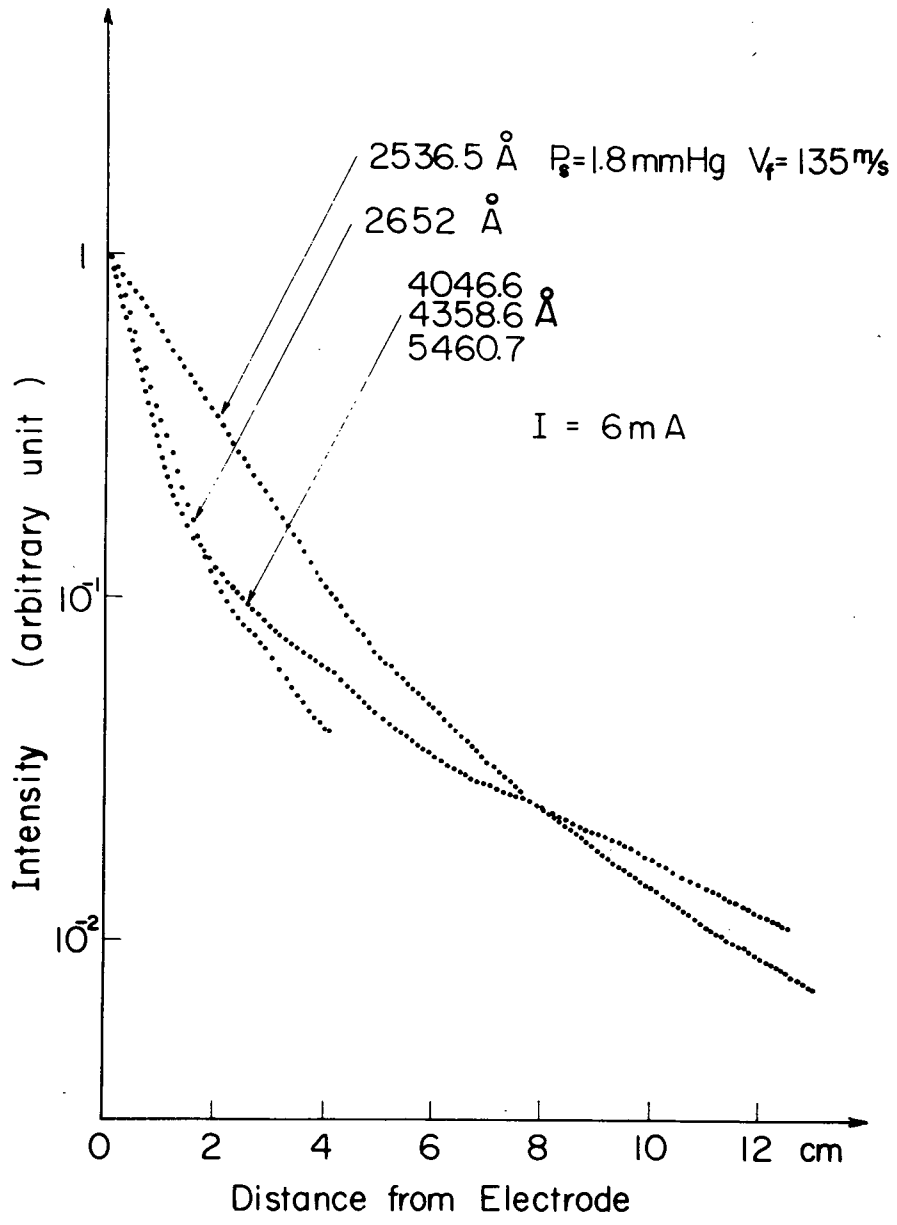

Fig.3-4 Line intensity decreases along the flow direction at the pressure 1.8 mmHg.

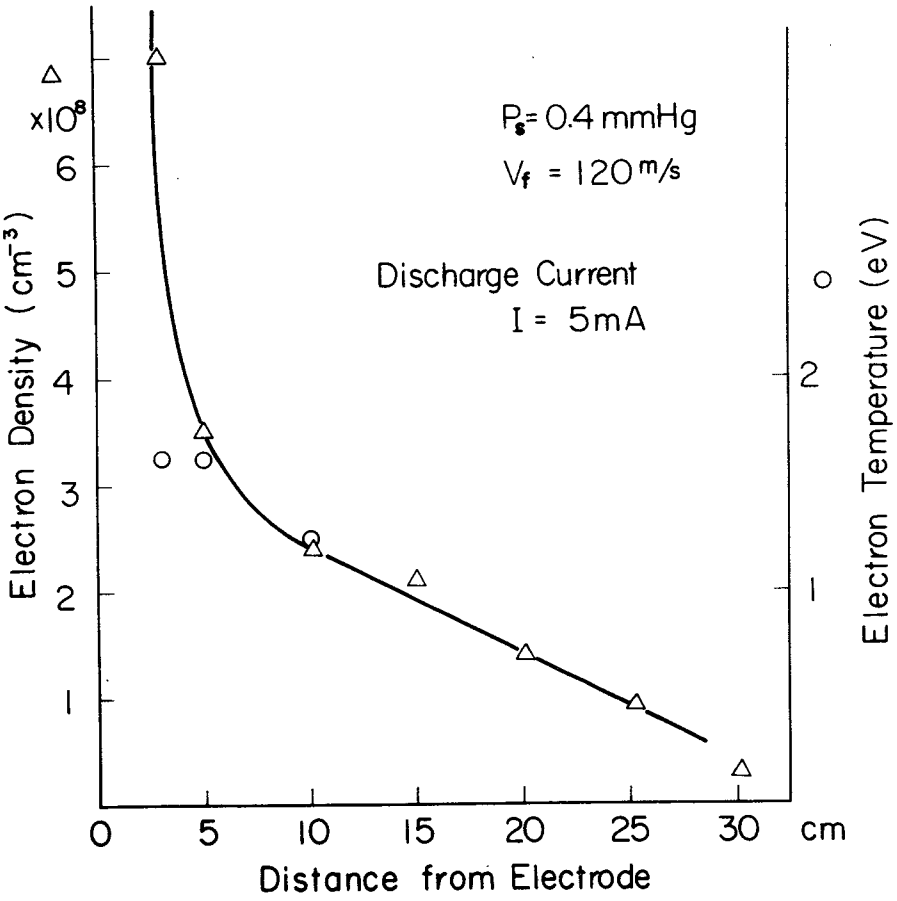

Fig.3-5 Electron density decrease along the flow direction.

led by the electron density distribution which is similar to the intensity distribution.

Then it is important to take the electron density decrease into consideration. The charged particles contained in a cylindrical tube diffuse toward the wall, and in consequence the space charge field $\vec{E}_s$ will, in general, draw the ions toward the wall and repel the electrons. The particle flux can be written as follows.

$$\Gamma_e = - D_e \nabla n_e - \mu_e \vec{E}_s n_e \quad , \tag{3- 1}$$

$$\Gamma_+ = - D_+ \nabla n_+ + \mu_+ \vec{E}_s n_+ \quad , \tag{3- 2}$$

$$\Gamma_- = - D_- \nabla n_- - \mu_- \vec{E}_s n_- \quad , \tag{3- 3}$$

where the suffixes of e, + and - represent electrons, ions and negative ions respectively, and μ is the mobility.

In the steady state, $\Gamma_e = \Gamma_+ - \Gamma_-$ and the situation has been treated mathematically to lead the relation for the electron flux.

$$\Gamma_e = - \frac{(\mu_e D_+ + \mu_+ D_e) + (\mu_- D_e - \mu_e D_-)}{\mu_e + \mu_+ \gamma + \mu_- \beta} \nabla n_e$$

$$= - D_{\beta,\gamma} \nabla n_e \quad , \tag{3- 4}$$

where $\beta = n_-/n_e$ and $\gamma = n_+/n_e$.

The expression for $D_{\beta,\gamma}$ reduces to D_e in the free diffusion limit when $\gamma = D_e/D_+$ and $\beta = 0$, and reduces to D_a in the ambipolar limit when $\gamma = 1$ and $\beta = 0$.

Under the condition where $D_e/\mu_e \gg D_+/\mu_+$ and $D_e/\mu_e \gg D_-/\mu_-$ i.e. $T_e \gg T_+$, $\mu_e \gg \mu_+$ and $\mu_e \gg \mu_-$, $D_{\beta\gamma}$ becomes approximately

$$D_{\beta,\gamma} = (\mu_+/\mu_e)D_e(\beta + \gamma) = D_a(\beta + \gamma) \qquad (3-5)$$

where D_a is the ambipolar diffusion coefficient.

Because the presence of the negative ions distorts the space charge field, the effective diffusion coefficient $D_{\beta,\gamma}$ generally falls in between the ambipolar and the free diffusion coefficient. Under a certain limit for weakly ionized gas, it becomes considerably large, approching to the free diffusion limit.[6] In active plasma, the recombination process can be neglected and the electron attachment is assumed as a linear volume loss.

Assuming the cross section of the electron attachment as η/v_e cm^2 where η and v_e are the electron attachment coefficient and the velocity of electron,[7] the electron density is represented as follows.

$$v_f \frac{\partial n_e}{\partial x} = -(D_{\beta,\gamma}/\Lambda_0^2)n_e - \eta n_o n_e \qquad (3-6)$$

where Λ_0 is the first root of $J_o(a/\Lambda_0) = 0$, that is, $\Lambda_0 = a/2.4048$, a is the radius of the cylinder and n_o is the density of neutral atoms.

Assuming a parabolic viscous flow for the neutral mercury atoms:

$$v_f(r) = v_{f_0}(1 - r^2/a^2) , \qquad (3-7)$$

eq.(3-6) is rewritten as follows.[8)]

$$v_{f_0}\frac{\partial n_e}{\partial x} = -(D_{\beta,\gamma}/\Lambda^2)n_e - 1.258\eta n_o n_e \qquad (3-8)$$

where $\Lambda = a/2.709$ and v_{f_0} is the flow velocity on the axis.

The reciprocal characteristic length of decrease in intensity δ_e is given from eqs.(2-26) and (3-8).

$$-\delta_e = \frac{1}{I_{im}}\frac{\partial I_{im}}{\partial x} = -\frac{1}{v_{f_0}}(\frac{D_{\beta,\gamma}}{\Lambda^2} + 1.258\eta n_o). \qquad (3-9)$$

The density of neutral mercury atoms is proportional to the measured static pressure p_s and to the reciprocal saturation temperature T_s^{-1}. Therefore the density can be expressed to be proportional to the normalized pressure p as follows.

$$p = (p_s/T_s)T_{s1} ,$$

where T_{s1} is the saturation temperature at the vapor pressure

1 mmHg. Making use of this normalized pressure, eq.(3-9) is given as

$$\delta_e v_{f_0} p = (D_{\beta,\gamma}/\Lambda^2)p + 3.04\times10^{16}\eta p^2 . \qquad (3\text{-}10)$$

Figure 3-6 shows the relation between $\delta_e v_{f_0} p$ and the discharge current. In general $\delta_e v_{f_0} p$ is found to be independent of the discharge current, however, for the transition from the level near the ionization level the fluctuation of δ_e tends to increase a little with the discharge current.

As shown in Fig.3-7, $\delta_e v_f p$ is found to depend linearly on p^2. Using eq.(3-10), $D_{\beta,\gamma}$ and η can be calculated and these results are shown in Table 3-1.

On an average, the value of η becomes 1.6×10^{-13} $cm^3 s^{-1}$, and in comparison with the value calculated by P.Dandurand[9] this value is about eight times large, but assuming that the cross section of the electron attachment is equal to η/v_e, this cross section agrees to that calculated by H.S.W.Massey at 4 eV.[7] The effective diffusion coefficient was found to be about one hundredth as small as the free diffusion coefficient in this experimental condition.

Decrease in intensity of the resonance line will be undermentioned.

The slow decrease in intensity of the resonance line in

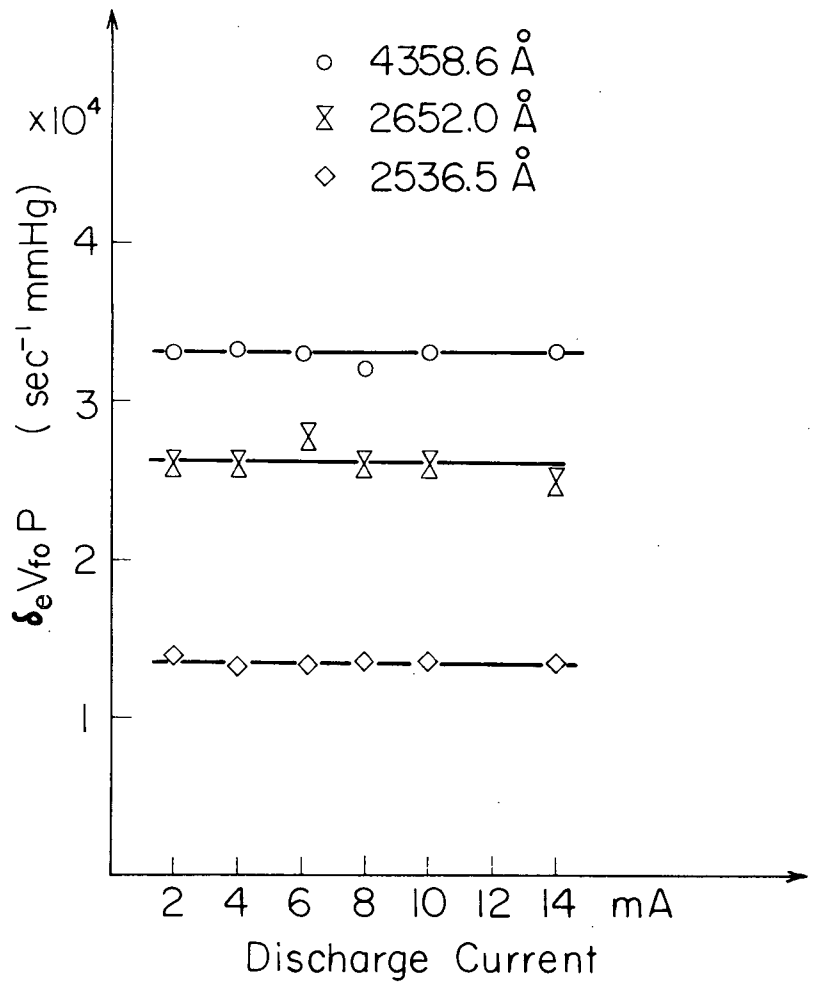

Fig.3-6 The reciprocal characteristic lengths of intensity decreases vs discharge current.

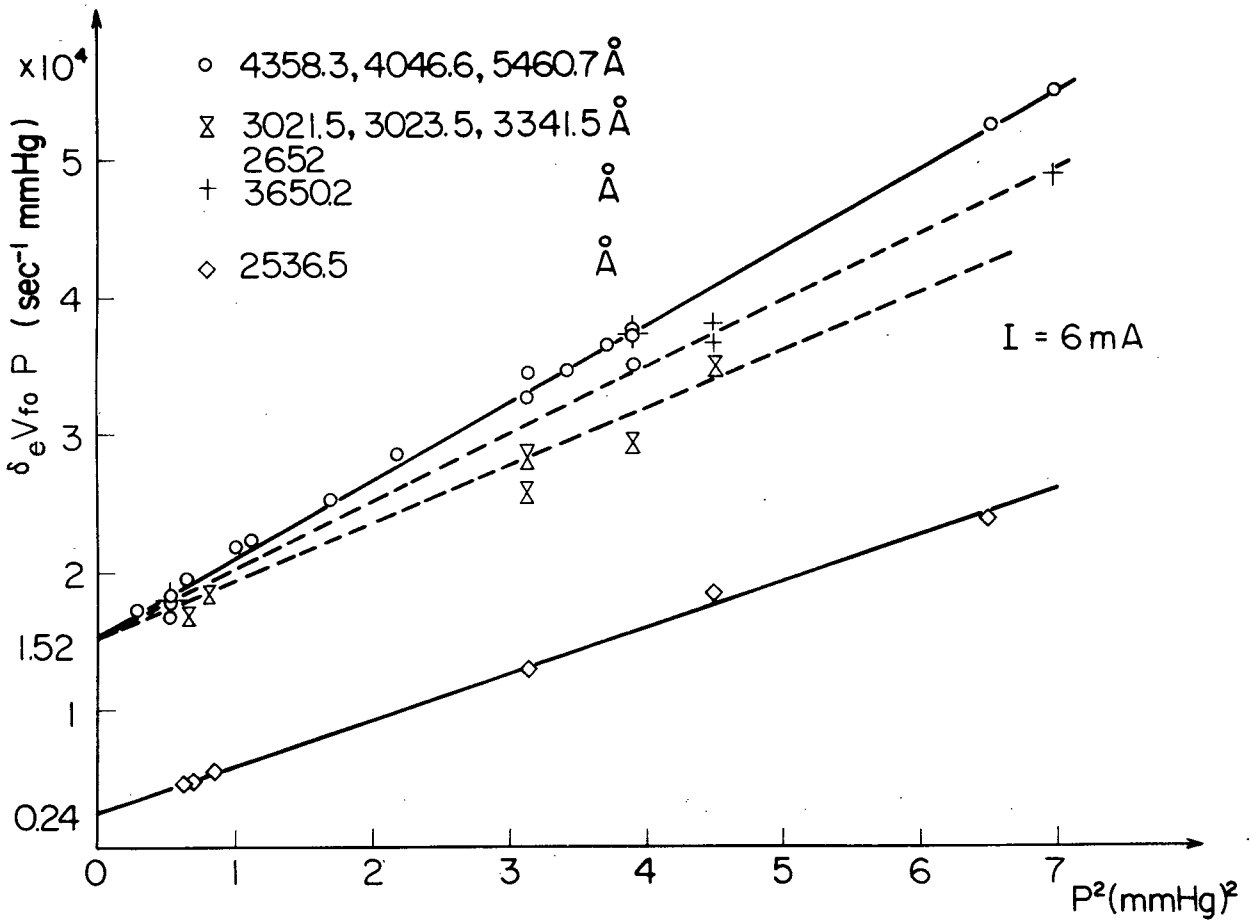

Fig.3-7 $\delta_e v_{fo} p$ for various line intensity decreases as a function of the square of the normalized static pressure.

Table 3-1 Effective diffusion coefficient $D_{\beta,\gamma}$ and electron attachment coefficient η.

The upper state of the observed line	η ($cm^3 s^{-1}$)	$D_{\beta,\gamma}p$ ($cm^2 s^{-1} mmHg$)
7^3S_1	1.8×10^{-13}	4.7×10^3
6^3D_3	1.6×10^{-13}	2.7×10^3 *
$7^3D_{3,2}$, 8^3S_1	1.4×10^{-13}	2.4×10^3 **

* The value with the correction for the restricted discharge source.

** Calculated from the half breadth of the radial intensity distribution.

Table 3-2 Absorption coefficient of the resonance radiation and quenching cross section of $Hg(6^3P_1)$

Absorption coefficient (cm^{-1})	Quenching cross section of $Hg(6^3P_1)$ ($Å^2$)
$k_o = 1.2\times10^{-13} n_o$	0.038
$1.31\times10^{-13} n_o$ *	

* From Zemansky's data.[11)]

comparison with that of lines emitted from the higher levels may be taken to be due to the radiative imprisonment.

It may be appropriate to consider that the decrease in intensity of the resonance line in this region is controlled by the resonance absorption and the atomic collision as a linear volume loss,

$$Hg(6^3P_1) + Hg \longrightarrow Hg(6^3P_0) + Hg. \qquad (3\text{-}11)$$

If the quenching probability of the resonance level is represented as $\langle v\sigma \rangle_{10} n_o$, the decrease in intensity of the resonance radiation is written as

$$v_{fo} \frac{\partial n_r}{\partial x} = - (D_r/\Lambda^2) n_r - 1.258 \langle v\sigma \rangle_{10} n_o n_r , \qquad (3\text{-}12)$$

where n_r and D_r are the density of excited atoms in the resonance level 6^3P_1 and the diffusion coefficient of the radiation diffusing through gas atmosphere respectively.
According to C.Kenty, the diffusion coefficient D_r is given by[10)]

$$D_r = \frac{\sqrt{2}\Lambda}{3\sqrt{\pi} k_o \tau} \left\{ \sqrt{2}\, F(\sqrt{1n\ k_o\Lambda}) - F(\sqrt{21n\ k_o\Lambda}) \right\} , \qquad (3\text{-}13)$$

where $F(t) = \exp(-t^2) \int_o^t \exp(x^2) dx$,

τ is the life time of the state 6^3P_1,

k_o the absorption coefficient at the center of the line,

and Λ the thickness of the layer of gas.

Using eq.(3-12), the reciprocal characteristic length of the resonance radiation δ_r is represented by

$$\delta_r v_{f_0} p = (D_r/\Lambda^2)p + 3.04\times10^{16}\langle v\sigma\rangle_{10}p^2 \qquad (3\text{-}14)$$

From Fig.3-7, $\delta_r v_{f_0} p$ depends linearly on p^2 so that $(D_r/\Lambda^2)p$ is found to be 0.24×10^4 s^{-1}mmHg.

Substituting $\tau = 1.1\times10^{-7}$ s and $\Lambda = 0.57$ cm into eq.(3-13), k_o is obtained as

$$k_o = 2.86\times10^3\ p \quad cm^{-1}$$

or rewriting p to n_o

$$k_o = 1.2\times10^{-13}n_o \quad cm^{-1}.$$

This relationship agrees well with that given by M.W.Zemansky, that is, $k_o = 1.3\times10^{-13}n_o$ cm^{-1}. [11]

Then, the quenching probability of the state 6^3P_1 by mercury atoms can be given as $\langle v\sigma\rangle_{10}n_o = 1.1\times10^{-13}n_o$ s^{-1}, so that at about 400°K, an average quenching cross section can be yielded as $\langle\sigma\rangle_{10} = 0.038$ Å^2 when the relative motion of the particles is taken into consideration. This value is about one order smaller than the quenching cross section of the state 6^3P_1 by nitrogen molecules by E.W.Samson.[12] These results are tabulated in Table 3-2.

3-4 Radial Intensity Distribution

To clarify the charged particle diffusion to the wall as mentioned in the previous section 3-3, it is important to measure the radial distribution of the excited atoms.

The apparent radial intensity distribution I(y) is measured by means of scanning across the image focused in front of the slit of the spectrograph. Assuming that the source has a cylindrical symmetry, the relationship between the observed distribution I(y) and the true n(r) is given by

$$I(y) = 2\int_{r=y}^{a} \frac{n(r)r}{\sqrt{r^2 - y^2}}\, dr \quad .$$

In order to get the true intensity distribution, the inverse transform of the Abel's integral is carried out by the Pearce's method.[4)]

The true radial distributions near the source are shown in Fig.3-8. These profiles are similar to those of the diffusions in the free space. And in our case, the effect that the discharge occurs on the restricted region has to be taken into consideration.

If the active region as the source of charged particles is represented by a radius b from the center axis, the radial distribution can be described as follows.

For $0 \leq r \leq b$,

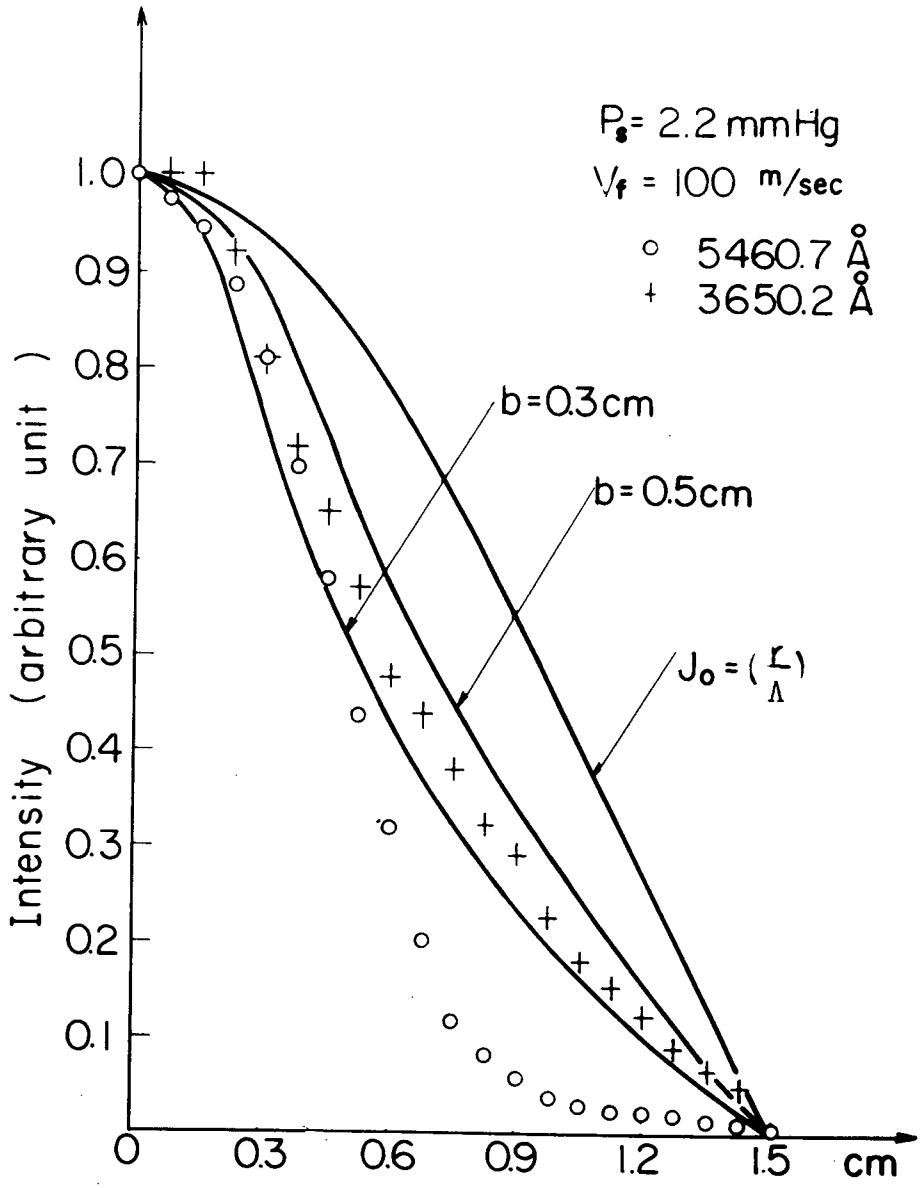

Fig.3-8 Radial intensity distribution.

The solid lines show analytic solution of the radial distribution which restricts an active region within a certain radius b, and the plots show the inverted radial intensity distributions.

$$n_e/n_e(0) = J_o(\, r/\Lambda_c \,) \qquad (3\text{-}15)$$

and for $b \leq r \leq a$

$$n_e/n_e(0) = (b/\Lambda_c) J_1(b/\Lambda_c) \ln(a/r) \qquad (3\text{-}16)$$

where the corrected diffusion length Λ_c must satisfy the following equation,

$$\ln(a/b) = \frac{J_o(b/\Lambda_c)}{(b/\Lambda_c) J_1(b/\Lambda_c)} \qquad (3\text{-}17)$$

and J_o and J_1 are the zero-th and the first order Bessel's function respectively. The relationship(3-17) is shown in Fig.3-9. The solid lines in Fig.3-8 show the cases when $b = 0.3$ and $b = 0.5$ where the corrected diffusion lengths are 0.292 and 0.424 respectively. (Fig.3-9)

Through the experiments, the discharge electrodes are set up at the interval of 1 cm. ($2b = 1$ cm) The diffusion coefficient corrected for this effect is also shown in Table 3-1.

The parameter b represents the diffusing rate of the active region as the ionized gas moves to the flow downstream, and defines the half breadth of the radial intensity distribution.

In the region near the source where rapid decrease in intensity is observed, the half breadths of the radial intensity distributions as a function of the distance from the electrode are shown in Fig.3-10, which represents the process of

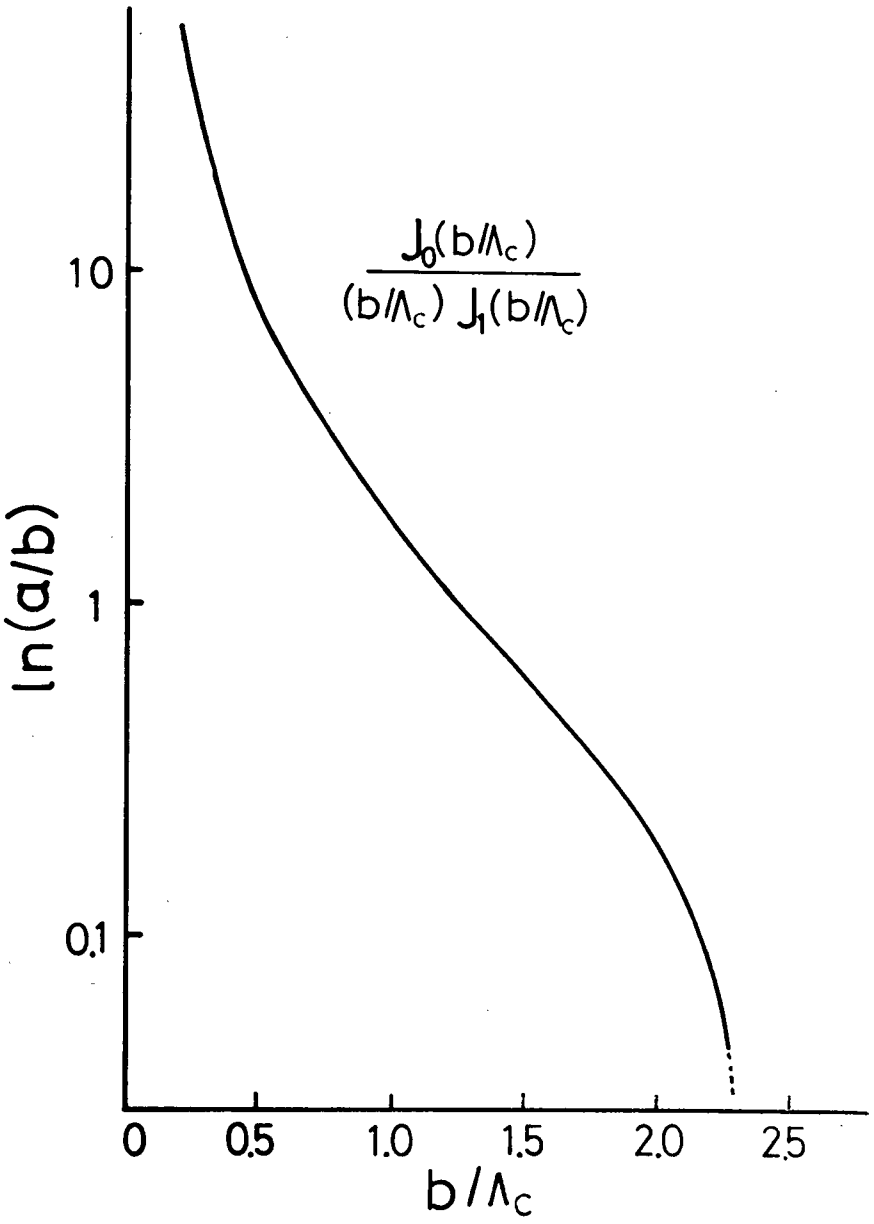

Fig.3-9 Relation between ln(b/a) and b/Λ_c.

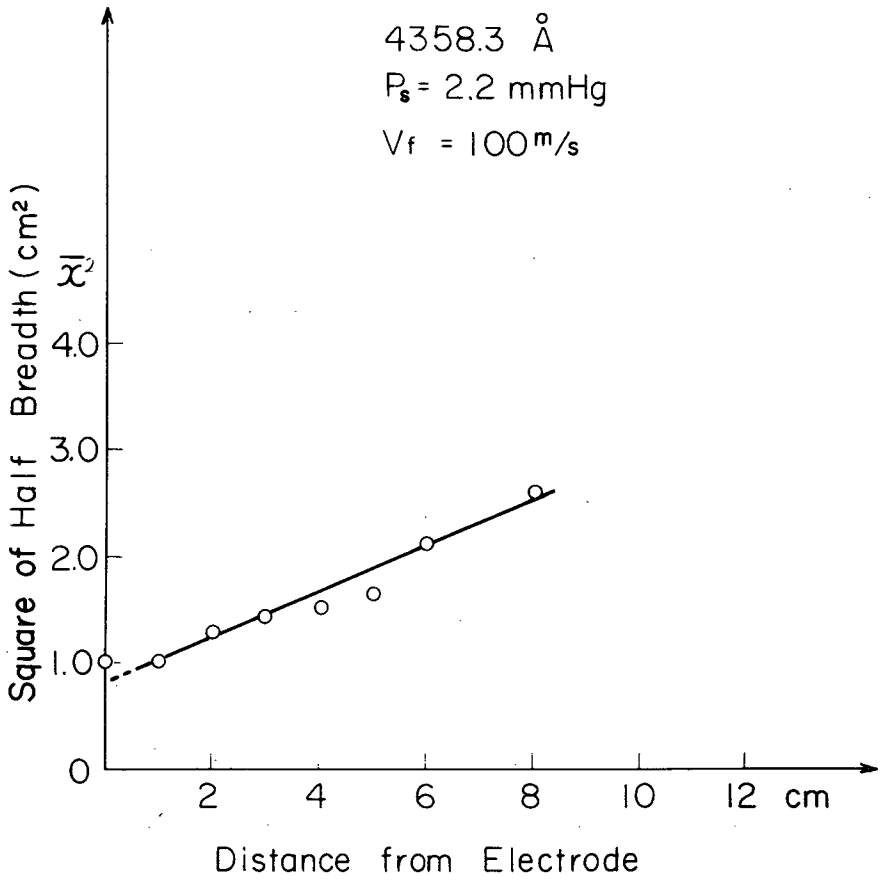

Fig.3-10 Relation between half breadth of the radial intensity distribution and distance from the discharge electrode.

the diffusion toward the wall.

Using eqs.(3-16) and (3-17), the half breadth is defined as follows under the condition that $b/a < 0.56$ or $\chi^2 < 1.26a^2$.

$$\chi = 2a \exp\left\{ -(1/2)\ln(a/b)/J_0(b/\Lambda_c) \right\}. \qquad (3\text{-}18)$$

Then taking the notation $\overline{\chi_0^2}$ for square of the effective diameter of the discharge source, the relationship between $\overline{\chi^2}$ and the distance from the electrode may be approximately described as

$$\overline{\chi^2} - \overline{\chi_0^2} = 2 D_{\beta,\gamma} x / v_{f_0} . \qquad (3\text{-}19)$$

From this relationship, it can be calculated that

$$D_{\beta,\gamma} p = 2.4 \times 10^3 \quad \mathrm{cm^2 s^{-1} mmHg}.$$

This value agrees well with that of the corrected diffusion coefficient with a restricted active region, which is given in Table 3-1.

3-5 Discussions and Concluding Remarks

In the preionized gas flow, the intensities decreasing rapidly near the source are measured and interpreted. In this region, it is found that the plasma introduced into the flow is considerably active and decrease in intensity of

radiation emitted from the levels higher than the resonance level is ascribed to the diffusion and to the electron attachment as a linear volume loss of the electrons. It is estimated that the recombination process is masked by them.

As mentioned in Chapter 2, the statement above is supported by the fact that the intensity of radiation near the source increases linearly with the electron density and electron temperature is high enough to excite atoms and not to be associated with the recombination process. The diffusion coefficient calculated from the experimental results is found to be about 4-5 times as large as the ambipolar diffusion coefficient measured previously in the positive column.[13)]

This value can be interpreted as the transition from free to ambipolar diffusion under the experimental condition and as the increment of the diffusion coefficient due to the negative ion produced by electron attachment.

The limit where the transition from free to ambipolar diffusion is remarkable in mercury atoms is calculated by means of constant ratio approximation[6)] and it can be found that the free diffusion predominates in the condition as follows:

$$T_e = D_e/\mu_e > 3.5\times10^{-7} n_e$$

where T_e and n_e present the electron temperature in eV and

the electron density per cubic centimeters respectively. Under the present experimental conditions with $n_e = 5 \times 10^8$ cm^{-3} and $T_e = 2$ eV, the effective diffusion coefficient calculated by constant ratio approximation is almost equal to D_a, however, that calculated by accurate calculation[6] will be estimated about 1.5 times as large as D_a. Since in nonequilibrium ionization, the ambipolar diffusion coefficient is proportional to the electron temperature, the corrected effective diffusion coefficient introduced in this analysis can probably be estimated to be near the ambipolar diffusion coefficient at 2 eV.

The decrease in intensity of the resonance radiation masks the rapid decrease in intensity related by the electron diffusion and the electron attachment. This decrease is interpreted as imprisonment of radiation. The absorption coefficient calculated from the experimental results agrees well with that given by M.W.Zemansky. The collision process as the linear volume loss that the resonance states are quenched by collisions with mercury atoms and the cross section is obtained as 0.38 $Å^2$, taking the relative motion of both atoms into consideration.

References

1) R.Anderson and E.Steep : J.Opt.Soc.Amer. 53(1963) 1139.

2) E.Steep and R.Anderson : J.Opt.Soc.Amer. 55(1965) 31.

3) M.Nishikawa,Y.Fujii-e and T.Suita : Japan J.appl.Phys. 7(1968) 442.

4) W.J.Pearce : Optical Spectrometric Measurements of High Temperatures ed P.J.Dickerman (Chicago Univ. Press. Chicago, 1961) P.123.

5) S.L.Chen and T.Sekiguch : J.appl.Phys. 36(1965) 2362.

6) W.P.Allis and D.J.Rose : Phys.Rev. 93(1954) 84.

7) H.S.W.Massey and R.A.Smith : Proc.Roy.Soc. A 155(1936) 442.

8) J.R.Sellars,M.Tribus and J.S.Klein : Trans.ASME (1956) 441.

9) P.Dandurand and R.B.Holt : Phys.Rev. 82(1951) 868.

10) C.Kenty : Phys.Rev. 42(1932) 823.

11) A.C.G.Mitchell and M.W.Zemansky : Resonance Radiation and Excited Atoms (Cambridge Univ. Press. 1961) P.233.

12) E.W.Samson : Phys.Rev. 40(1932) 940.

13) W.L.Granowski : Der electrische Strom im Gas (I.Akad.Verlag. Berlin, 1955)

Chapter 4.

Electron Attachment near the Discharge Source*

The electron attachment process near the discharge source described in Chapter 3 may be interpreted as the production process of the short lived negative ion attributed by U.Fano and J.W.Cooper on the experimental ground that the maximum of the metastable atom density is found in this region and the negative ions are not found downstream far from this region. If this process can be regarded, the dissociative rate constant of the short lived negative ions converted to the metastable atoms and electrons may be estimated to be about 2×10^4 s^{-1} experimentally.

4-1 Introduction

Lately the fine structure of the optical excitation functions has been found by means of monoenergetic electron beams in a low energy range.[1,2] However, a similar method is invalid for investigating excitation functions of metastable levels, since the radiative transitions from these levels are forbidden by the selection rules. So the transmission of monoenergetic electrons through various gases and vapors

---

*Part of the contents is presented in Journal of the Physical Society of Japan, Vol.31, No.3, P. 910-918, September, 1971.

are measured and a large number of resonances in the transmission current have been observed by J.A.Simpson and collaborators.[3] Those resonances are attributed to the reversible formation of a negative ion according to the reaction scheme:

$$e + A \longrightarrow A^- \longrightarrow e + A .$$

By U.Fano and J.W.Cooper[4] it was shown that when many levels of A^- belong to a single configuration, the upper ones among them may lie above the inelastic threshold of the reaction: $e + A \longrightarrow e + A^*$, so that the reaction $e + A \longrightarrow A^- \longrightarrow e + A^*$ is energetically possible. The excitation functions of mercury radiative levels were investigated but on the other hand those of the metastable states $6^3P_{0,2}$ of mercury have not been investigated accurately at the present time. A.I.Korotkov measured the excitation function for the $6^3P_0 - 6^1S_0$ transition by an electrical method based on recording the kinetic energy of electrons which were subjected to inelastic collisions of the second kind with metastable mercury atoms. Then, using the Klein and Rosseland relationship[5] the excitation function was established for inelastic collisions of the first kind, which corresponds to the $6^1S_0 - 6^3P_0$ transition. It was found that the excitation function has two fine structure maxima. For the interpretation of the first maximum, it is suggested that the possibility of

the electron attachment given by U.Fano and J.W.Cooper is not excluded.[6]

In this chapter, the electron attchment process given by them is explained in the section 4-2 and the applicability of this process to the experiment is interpreted on the bases of the experimental results in the section 4-3.

4-2 Short-lived Negative Ions

A large number of resonances in the transmission of monoenergetic electron beams through mercury vapor have been observed by C.E.Kuyatt,J.A.Simpson and S.R.Mielczarek.[3] The three resonances observed in the electron energy from 4 to 5 eV are shown in Fig.4-1. Assuming the presence of the short-lived negative ions, the levels of Hg^- at 4.07, 4.29 and 4.89 eV are identified spectroscopically as follows:[4]

$$4.07\ \text{eV} \qquad 6s6p^2\ {}^4P_{1/2}\ ,$$

$$4.29\ \text{eV} \qquad 6s6p^2\ {}^4P_{3/2}\ ,$$

$$4.89\ \text{eV} \qquad 6s6p^2\ {}^4P_{5/2}\ .$$

The ${}^4P_{5/2}$ resonance lies above the ${}^3P_0$ mercury metastable state threshold and practically coincides with the ${}^3P_1$ threshold so that the following reaction is energetically possible.

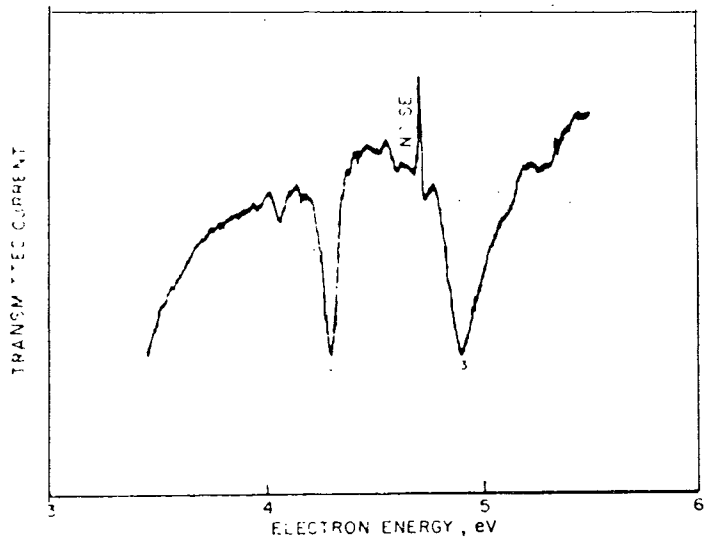

Fig.4-1 Resonances in transmission in Hg. (from Ref.3)

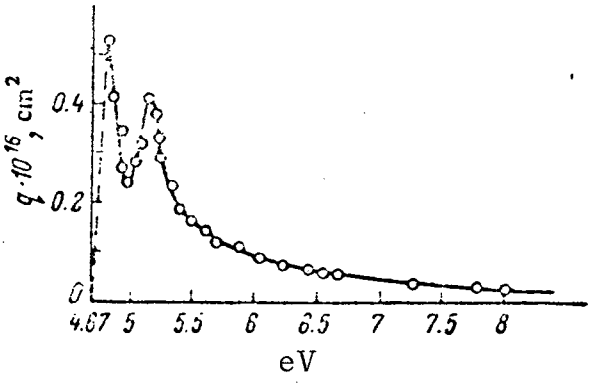

Fig.4-2 Dependence of the effective cross section on electron velocity. (from Ref.5)

$$e + Hg \longrightarrow Hg^{-}(^{4}P_{5/2}) \longrightarrow e + Hg^{*}(^{3}P_{0}) \qquad (4-1)$$

The excitation functions of the metastable state $6^{3}P_{0}$ were measured by K.I.Korotkov, and was found to have two fine structure maxima. Figure 4-2 reproduces tracing of dependence of the effective cross section on electron velocity from Ref. 5. The presence of the first maximum located near the excitation threshold may be interpreted as being due to the reaction(4-1).

When the cross section of negative ion formation in the reaction(4-1) is denoted by σ_a, the dependence of this electron attachment coefficient η on the electron temperature T_e can be represented as:

$$\eta = \langle v_e \sigma_a \rangle = \sqrt{2/m_e} \int_0^\infty \sqrt{U} \sigma_a(U) F(T_e, U) dU \ , \qquad (4-2)$$

where U and $F(T_e,U)$ are the electron kinetic energy and the Maxwell energy distribution at T_e, respectively.
Denoting the center of the resonance and the resonance width by U_o and ΔU respectively, the cross section $\sigma_a(U)$ may be approximated from Fig.4-1 as follows:

for $U_o - \Delta U/2 \leq U \leq U_o + \Delta U/2$,

$$\sigma_a = \text{const.}$$

and for $U < U_o - \Delta U/2$ or $U > U_o + \Delta U/2$,

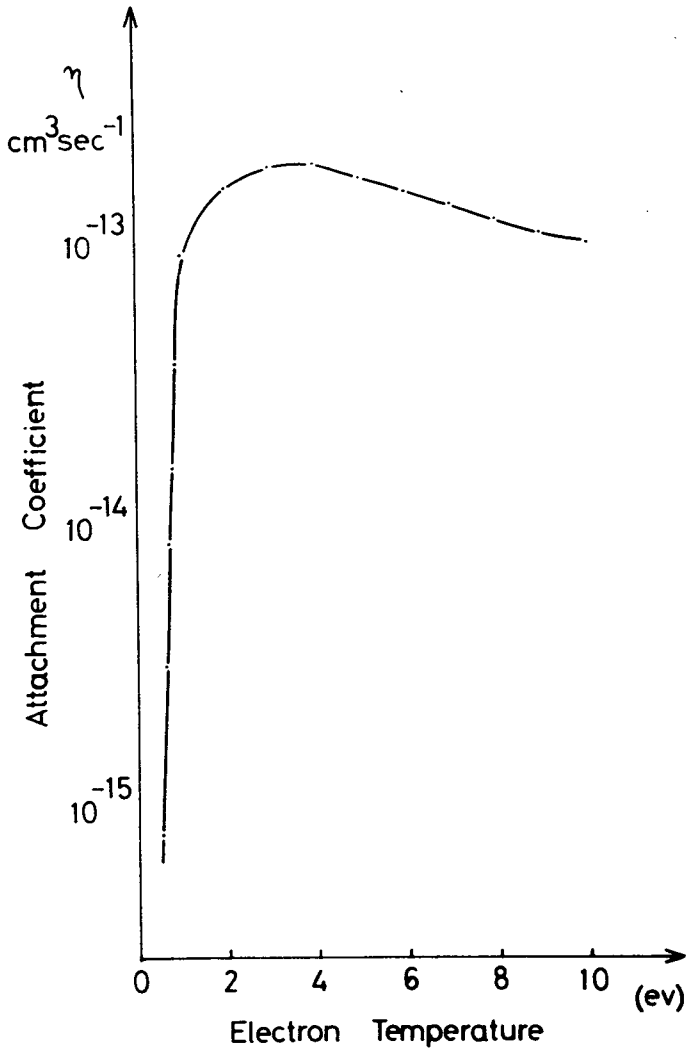

Fig.4-3 Dependence of the electron attachment coefficient η on the electron temperature T_e.

$$\sigma_a = 0 .$$

When U_o = 4.9 eV, ΔU = 0.4 eV and $\eta(T_e = 2\ eV) = 1.6 \times 10^{-13}$ $cm^{-3}s^{-1}$ from the result in Chapter 3, the dependence of η on T_e is shown in Fig.4-3.

It is found that the electron attachment of the reaction (4-1) may not be taken into consideration at the electron temperature lower than about 0.5 eV from Fig.4-3.

Thus the applicability of the electron attachment process (4-1) to the present experiment is discussed as follows.

4-3 Experimental Verification

As shown in Fig.4-4(a), it was found that decrease in intensity of mercury lines was rapid near the discharge source followed by slow somewhat distant from the source.
The reciprocal characteristic length of rapid decrease in intensity δ_e was found to be represented as[7)]

$$\delta_e = (D_{ae}/\Lambda^2 + \eta n_o)/v_f = (1.52/p + 0.487p) \times 10^4 / v_f \quad cm^{-1}, \tag{4-3}$$

where D_{ae}, Λ, ηn_o, v_f and p are the ambipolar diffusion coefficient in $cm^2 s^{-1}$, the diffusion length of the radial component in cm, the electron attachment probability in s^{-1}, the flow velocity in cm s^{-1} and the static pressure in mmHg, respectively.

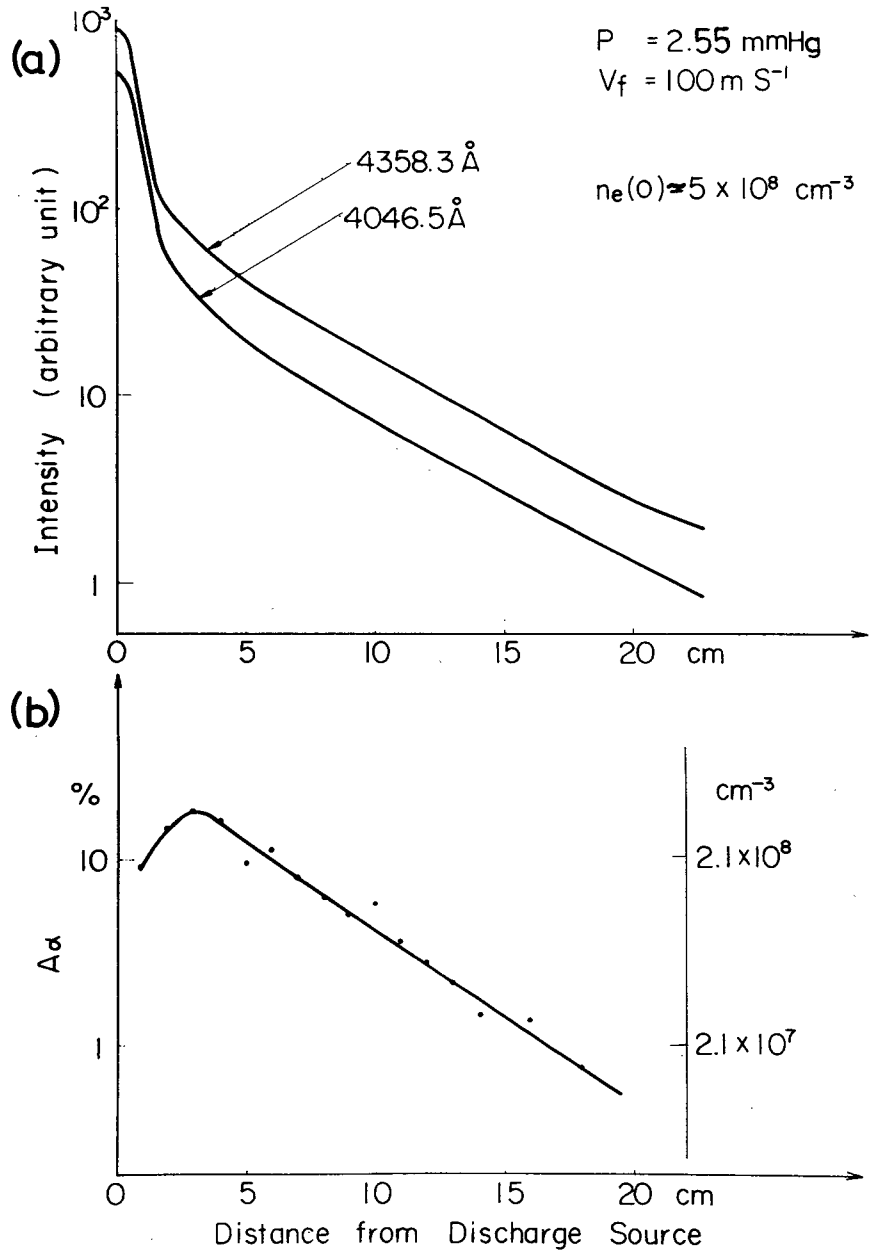

Fig.4-4(a) Decrease in intensity along the flow downstream.

Fig.4-4(b) Density variation of metastable atom along the flow downstream. The density is calculated from absorption on the assumption that $\Delta\nu_e/\Delta\nu_a = 1$.

If the electron attachment coefficient η is applicable to the region where the intensity distribution decreases slowly, negative ions become dominant so that the slow decrease in intensity somewhat distant from the discharge source will have to be interpreted as the recombination between positive and negative ions. In order to examine which is predominant in this region, electron or negative ion, the relation between current and voltage induced by MHD effect is measured in the arrangement as shown in Fig.4-5. The experimental conditions and results are shown in Table 4-1.

In the MHD channel with the parallel electrodes, the current can be expressed as follows.[8)]

$$I_L = (S/d)\frac{e\,n\,(e\tau/m)}{1 + (e\tau/m)^2B^2}(v_fBd - V) \quad , \qquad (4-4)$$

where m is the mass of charged particle,

n the density of charged particle,

and τ the mean free time.

Since n is about 5×10^8 cm^{-3} in this case, the value $(e/m)\tau$ is calculated at about 4.5 in MKSA system of units from the relationship(4-4) and the value agrees with that for electrons at the electron temperature from 0.1 to 0.2 eV, i.e. $(e/m_e)\tau_e \sim 10/p$ in MKSA system of units.[9)]

Consequently, it is found that the charged particles in this

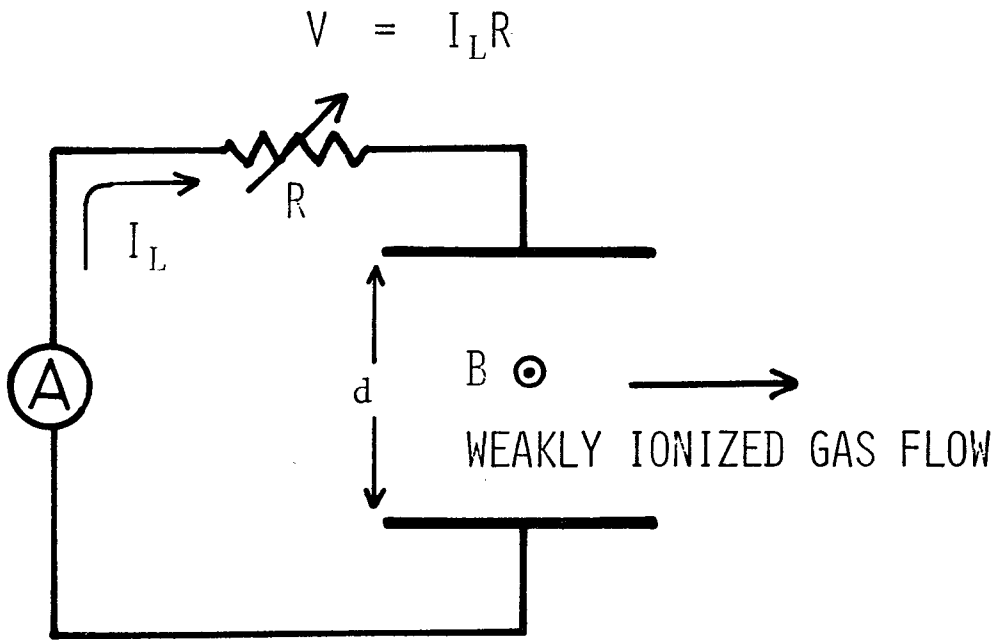

Fig.4-5 Measurement of current and voltage induced by MHD effect using the continuous electrodes.

Table 4-1 Relation between current and voltage induced by MHD effect. (at about 15 cm from the discharge source)

Terminal voltage V (mV)	Current I_L (μA)
2	7.5
70	7.1
630	4.2

Experimental condition

Discharge current	8 mA (400 V)
Magnetic flux density	B=0.46 Weber/m^2
Gap of electrodes	d=2.3 cm
Area of electrode	S=1.5cm x 8cm
Flow velocity	v_f=130 m/s
Static pressure	p=2.2 mmHg

region where the intensity decreases slowly are almost electrons and positive ions.

As for production of short-lived negative ions near the discharge source where the electron temperature is high (~2 eV), an electron attachment process by energy resonance can be considered. The short-lived negative ion may be separated into the metastable atom $Hg(6^3P_0)$ and electron with slow velocity as shown in the reaction(4-1).

The other production process for the metastable atom can be also considered as follows:

$$Hg(6^3P_1) + Hg \longrightarrow Hg(6^3P_0) + Hg. \qquad (4-5)$$

The density of the resonance state atom $Hg(6^3P_1)$ was found to decrease exponentially near the discharge source. Its diffusion loss and the loss due to the reaction(4-5) is described in Chapter 3 and can be represented as

$$D_r/\Lambda^2 + \langle v\sigma \rangle_{10} n_o = (0.24/p + 0.34p)\times 10^4 \ \ s^{-1}, \qquad (4-6)$$

where D_r, Λ and $\langle v\sigma \rangle_{10} n_o$ are the diffusion coefficient of the radiation diffusing through gas atmosphere, the diffusion length of the radial component and the quenching probability as shown in the reaction(4-5), respectively.

Assuming that the probability of electron excitation from the

ground state to 6^3P_1 state is almost equal to that of electron excitation from the ground state to 6^3P_0 state,[9] the ratio of the density of the resonance state atom to that of the metastable atom at the outlet of the discharge source, $n_r(0)/m_o(0)$, may be approximately in inverse proportion with their loss probabilities.

If the reciprocal characteristic length of slow decrease in the metastable atom density is denoted by δ_m, the loss probability of the metastable atom can be represented as $v_f\delta_m$. Consequently $n_r(0)/m_o(0)$ is estimated to be about 0.2 at the pressure 2.55 mmHg. From the statement mentioned above, it is found that the peak value as shown in Fig.4-4(b) cannot be interpreted as only the production of the metastable atom by the reaction(4-5) because the density of the resonance state atom decreases more rapidly than that of the metastable atom, and $n_r(0)$ is estimated to be smaller than $m_o(0)$.

Since the metastable atom density was found to be comparable with the electron density as shown in Figs.4-4(a) and (b), a peak in the density variation of the metastable atom as shown in Fig.4-4(b) is possible to be interpreted by the reaction(4-1).

Since the reciprocal characteristic length of decrease in the active electron density was found to be δ_e as shown in

the relation(4-3), the number density of atoms excited from the ground state to the metastable state by electrons per unit time can be written as

$$f_{em} n_e(0) \exp(-\delta_e x) \ , \qquad (4-7)$$

where f_{em} is the frequency of excitation from the ground state to the metastable state. Near the discharge source the electron temperature is still high so that the recombination process can be neglected.

Denoting that m_o, n_-, n_e and n_o are the densities of metastable atoms, negative ions, electrons and atoms,respectively and the corresponding diffusion coefficients are D_m, D_{a-} and D_{ae}, the rate equations involving the reaction(4-1) near the source can be approximately written as :

$$v_f \frac{\partial m_o}{\partial x} = - \frac{D_m}{\Lambda^2} m_o - \nu_m m_o + \nu_- n_- + f_{em} n_e(0) \exp(-\delta_e x) , \qquad (4-8)$$

$$v_f \frac{\partial n_-}{\partial x} = - \frac{D_{a-}}{\Lambda^2} n_- + \eta n_o n_e - \nu_- n_- \ , \qquad (4-9)$$

$$v_f \frac{\partial n_e}{\partial x} = - v_f \delta_e n_e + \nu_- n_- \ , \qquad (4-10)$$

where ν_- and ν_m are the dissociative rate constant in the reaction(4-1) and the quenching rate of metastable atom, re-

spectively. Taking the initial conditions: $n_e(x=0) = n_e(0)$, $n_-(x=0) = 0$, $m_o(x=0) = m_o(0) = f_{em} n_e(0)/(v_f \delta_m)$, at the outlet of the discharge source, the solutions for these equations are represented as:

$$m_o = \left\{ m_o(0) \frac{\delta_e}{\delta_e - \delta_m} + \frac{\nu_- K (\varepsilon_1 - \varepsilon_2)}{v_f (\varepsilon_2 - \delta_m)(\varepsilon_1 - \delta_m)} \right\} \exp(-\delta_m x) - \frac{\nu_- K}{v_f} \left\{ \frac{\exp(-\varepsilon_2 x)}{\varepsilon_2 - \delta_m} - \frac{\exp(-\varepsilon_1 x)}{\varepsilon_1 - \delta_m} \right\} - \frac{m_o(0)\delta_m}{\delta_e - \delta_m} \exp(-\delta_e x) , \quad (4\text{-}11)$$

$$n_- = K \left\{ \exp(-\varepsilon_2 x) - \exp(-\varepsilon_1 x) \right\} , \quad (4\text{-}12)$$

$$n_e = \frac{n_e(0)}{\varepsilon_1 - \varepsilon_2} \left\{ (\delta_e - \varepsilon_2)\exp(-\varepsilon_1 x) + (\varepsilon_1 - \delta_e)\exp(-\varepsilon_2 x) \right\} , \quad (4\text{-}13)$$

where $\delta_m = (D_m/\Lambda^2 + \nu_m)/v_f$,

$\delta_- = (D_{a-}/\Lambda^2 + \nu_-)/v_f$,

$\delta_e = (D_{ae}/\Lambda^2 + \eta n_o)/v_f$,

$$\varepsilon_1 = \frac{1}{2} \left\{ \delta_e + \delta_- + \sqrt{(\delta_e - \delta_-)^2 + 4\eta n_o \nu_-/v_f^2} \right\} ,$$

$$\varepsilon_2 = \frac{1}{2} \left\{ \delta_e + \delta_- - \sqrt{(\delta_e \quad \delta_-)^2 + 4\eta n_o \nu_-/v_f^2} \right\} ,$$

and $$K = \frac{v_f (\varepsilon_1 - \delta_e)(\delta_e - \varepsilon_2)}{\nu_- (\varepsilon_1 - \varepsilon_2)} n_e(0) .$$

When $1 \gg \exp(-\delta_e \tilde{x})$, $1 \gg \exp -(\varepsilon_1 - \varepsilon_2)\tilde{x}$, $\varepsilon_1 \gg \varepsilon_2$, $\varepsilon_1 \gg \delta_m$ and $\delta_e \gg \delta_m$, the peak value of the metastable atom density $m_o(\tilde{x})$ can be written as

$$m_o(\tilde{x}) \simeq \nu_- K \exp(-\varepsilon_2 \tilde{x})/(v_f \delta_m) \ , \tag{4-14}$$

where $\tilde{x}$ is the axial distance at the peak point, and using eq.(4-14) the following relationship will be approximately satisfied at $\tilde{x}$.

$$\left\{\exp\left[(\varepsilon_2 - \delta_m)\tilde{x}\right] - 1\right\}/(\varepsilon_2 - \delta_m) \simeq \left\{1 - \frac{m_o(0)}{m_o(\tilde{x})} \exp(-\delta_m \tilde{x})\right\}/\delta_m \ . \tag{4-15}$$

Here the right hand side of eq.(4-15) is determined from the results as shown in Fig.4-4(b) i.e. $\delta_m = 0.22\ cm^{-1}$ and $m_o(0)/m_o(\tilde{x}) \simeq 0.5$ at $\tilde{x} \simeq 3$ cm, so that ε_2 is estimated to be $0.32\ cm^{-1}$ graphically.

Since the diffusion coefficient of negative ions D_{a-} is very small,[10] ν_- is represented as

$$\nu_- = \frac{v_f \varepsilon_2 (D_{ae}/\Lambda^2 + \eta n_o - v_f \varepsilon_2)}{D_{ae}/\Lambda^2 - v_f \varepsilon_2} \ . \tag{4-16}$$

Using the relationship(4-3), ν_- is estimated to be about $2 \times 10^4\ s^{-1}$ from eq.(4-16).

In the region where intensity distribution decreases slowly

somewhat distant from the discharge source, the density of negative ions becomes very small because the rate of electron attachment by energy resonance is expected to become smaller with thermalization of electrons as shown in Fig.4-3. Consequently the effect of these negative ions need not be taken into consideration somewhat distant from the discharge source.

4-4 Concluding Remarks

In Chapter 3 rapid decrease in intensity is related to the electron diffusion and the electron attachment as a linear volume loss because $\delta_e v_f p$ depends linearly on p^2. However, in the region where axial intensity distribution decreases slowly somewhat distant from the discharge source, electrons are found to be predominant by estimating the value $(e/m)\tau$ from measurements of current and voltage induced in MHD channel. The metastable atom density exhibits the maximum density at about 3 cm from the discharge source at the pressure $p = 2.55$ mmHg. These experimental results may be explained consistently by taking the reaction(4-1) into consideration.

Assuming the electron attachment process shown by U.Fano and J.W.Cooper, the dissociative rate constant of the short-lived negative ions is estimated to be about 2×10^4 s^{-1}. So in the region somewhat distant from the discharge source,

the effect of these negative ions is found not to be taken into consideration.

References

1) S.E.Frish : Optical Spectra of Atoms (State Publishers of Physical-Mathematical Literature, Moscow, 1963)

2) I.P.Zapesochnyi and O.B.Shpenik : Sov.Phys.-Dokl. 10(1965) 140.

3) C.E.Kuyatt,J.A.Simpson and S.R.Mielczarek : Phys.Rev. A 385(1965) 138.

4) U.Fano and J.W.Cooper : Phys.Rev. A 400(1965) 138.

5) A.I.Korotkov : Opt. and Spectros. 28(1970) 347.

6) O.Klein and M.Rosseland : Z.Physik 4(1921) 46.

7) M.Nishikawa,Y.Fujii-e and T.Suita : J.Phys.Soc.Japan 30(1971) 528.

8) G.W.Sutton and A.Sherman : Engineering Magnetohydrodynamics (McGraw-Hill Book Company 1965)

9) A.von Engel : Ionized Gases (Clarendon Press, Oxford 1965)

10) J.B.Hasted : Physics of Atomic Collision (London Butterworths 1964) P.23.

Chapter 5.

Decrease in Metastable Atom Density Distant* from the Discharge Source

In spectroscopic measurement, the continuous band fluorescence which is in the near ultraviolet region centered at about 3350 Å was found. This fluorescence is known to be the spontaneous radiation emitted from the metastable molecules $Hg_2(^3O_u^-)$, which are produced by collisions between the metastable atoms $Hg(6^3P_0)$ and the ground state atoms $Hg(6^1S_0)$. This conversion frequency from metastable atoms to metastable diatomic molecules is found to be $8.3\times10^2 p \ \ s^{-1}$ and the diffusion coefficient of metastable atoms is estimated to be $82/p \ \ cm^2s^{-1}$ when the radial dependence of flow velocity is not taken into consideration. Assuming a parabolic viscous flow, those values are $6.6\times10^2 p \ \ s^{-1}$ and $64/p \ \ cm^2s^{-1}$ respectively. This diffusion coefficient is agreeable to that obtained by A.O.McCoubrey.

5-1 Introduction

The resonance radiation which is the radiation emitted from the levels nearest of the ground state is reabsorbed by

---

*Part of the contents is presented in Journal of the Physical Society of Japan, Vol.31, No.3, P. 910-918, September, 1971.

ground state atoms in circumference and is imprisoned as a result.[1] The study of resonance radiation and related problems is a powerful means of obtaining information concerning the interaction of light and matter. By a resonance lamp, only the resonance levels can be produced for the initial condition so that the spectra connected with atoms and their structure have been investigated for various gases.[2] In those investigations, the metastable atoms $Hg(6^3P_0)$ produced by collisions of resonance state atoms and ground state atoms have been observed in mercury vapor.[3,4]

Thus the density variation of the long-lived metastable atoms, resolved on time, has been investigated in large numbers as proceeding to the study of resonance radiation and related problems.[5]

The continuous band fluorescence which is in the near ultraviolet region centered at about 3350 Å was observed by A.O. McCoubrey. This fluorescence was interpreted as the spontaneous radiation emitted from metastable diatomic molecules $Hg(^3O_u^-)$ which are produced by collisions of metastable atoms $Hg(6^3P_0)$ and ground state atoms $Hg(6^1S_0)$.[5,6]

In this chapter, the conversion frequency from metastable atoms to metastable diatomic molecules and the diffusion coefficient of metastable atoms are investigated from decrease in the metastable atom density observed in a flowing after-

glow. These results are compared with the results obtained by the other persons mentioned above.

5-2 Experimental Method

The density of metastable atoms is determined from the absorption measurement, in which the emission spectrum λ4046.6 Å (7^3S_1-6^3P_0) emitted from a low pressure mercury lamp was used as a light source. This lamp was operated by d.c. voltage. The resonance line λ2536.5 Å (6^3P_1-6^1S_0) also emitted from the lamp has no effect on the test section, because it was almost absorbed at the lamp envelope. The light source travels in the axial direction with the optical head of the retrofocus type to measure the absorption. The measurement system and the test section are shown in Fig. 5-1. Radiation emitted from the lamp is chopped by 1000 Hz chopper and focuses into an image of the slit S_1 on the flow axis through the lense L_1. The absorbed light intensity is detected by a photomultiplier through the optical head. The signal is fed to the selective amplifier of 1000 Hz and further amplified signal is rectified to be fed to a recorder.

With I_a being the intensity measured in the case when mercury vapor flow is excited and I_{ao} being that measured in the case when unexcited, the absorption A_α is directly obtained as

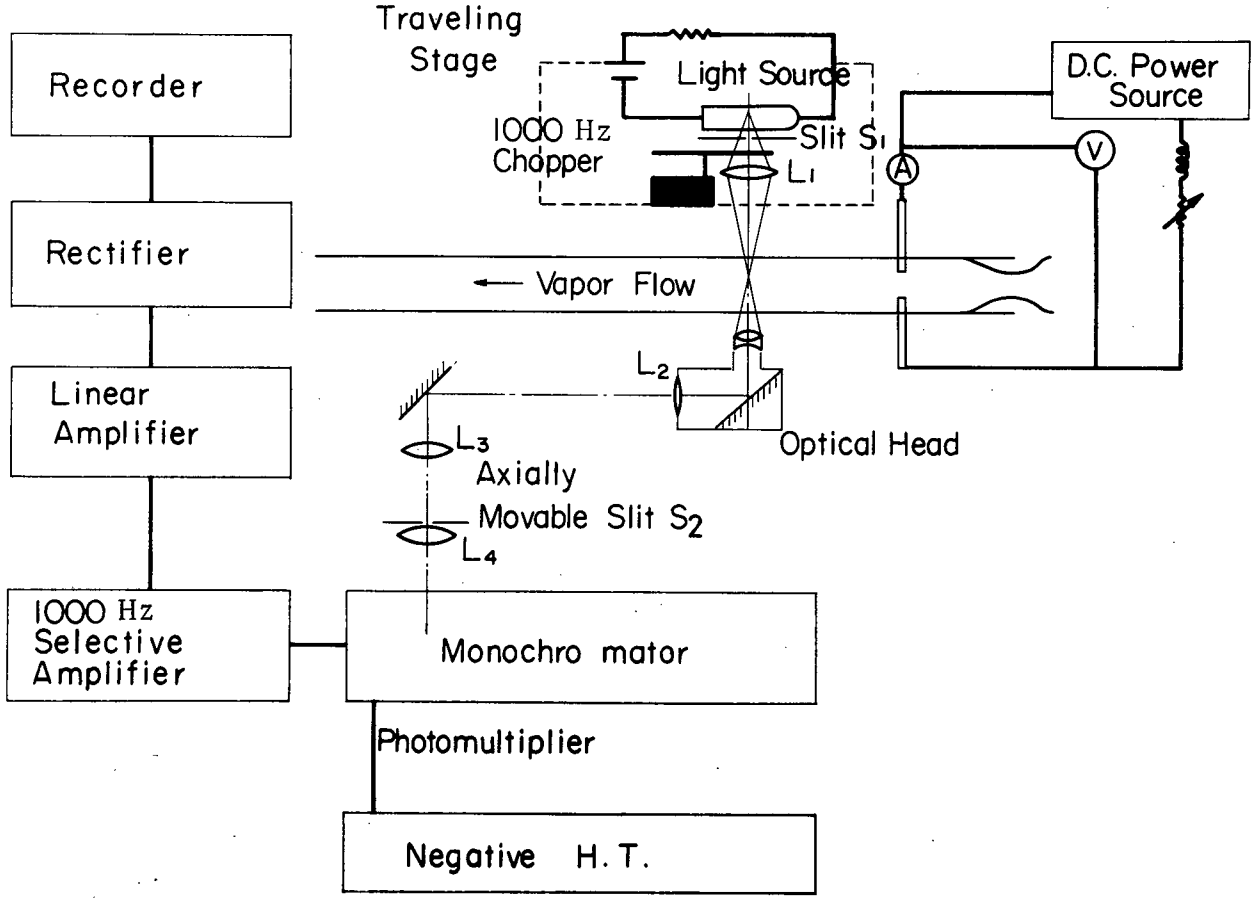

Fig.5-1 Block diagram for measurement of absorption.

$$A_\alpha = 1 - I_a/I_{ao} .$$

Using an emission line spectrum as the light source, the absorption depends on the emission and absorption line widths, and when Doppler broadening alone is present the absorption is obtained as,[2)]

$$A_\alpha = \sum_{n=1} - \frac{(-k_o L)^n}{n! \sqrt{1 + n(\Delta\nu_e/\Delta\nu_a)^2}} \qquad (5\text{-}1)$$

where $\Delta\nu_e$ and $\Delta\nu_a$ are the half widths of the emission and the absorption line respectively, L is the length of absorption path and k_o is the absorption coefficient which is represented as follows.

$$k_o = \frac{2}{\Delta\nu_o}\sqrt{\frac{\ln 2}{\pi}}\ \frac{e^2}{mc}\ \bar{f}\ m_o \qquad (5\text{-}2)$$

where $\Delta\nu_o$ is Doppler width,

$\bar{f}$ the oscillator strength of the upper level of the observed line

and m_o the metastable atom density.

In this experimental condition A_α is approximately proportional to $k_o L$, because $k_o L \ll 1$, and the line width by Doppler broadening does not change considerably so that the absorption A_α is regarded as being proportional to the density of

metastable atoms from eqs.(5-1) and (5-2).

5-3 Experimental Results and Discussions

In the region where the electron temperature is relatively low ($\sim$0.1 eV) somewhat distant from the discharge source, the electron attachment by energy resonance need not be taken into consideration as mentioned in Chapter 4 so that the third and the fourth term on the right side of eq.(4-8) can be neglected, and the density of metastable atoms is found to decrease exponentially as shown in Figs.4-3(b) and 5-2. Figure 5-2 shows that a slope of the density decrease on semi-logarithmic plots depends on the flow velocity at a similar static pressure and is proper to decrease as the flow velocity increases. This reciprocal characteristic length δ_m was found to be independent of the discharge current. Pressure dependence of δ_m is shown in Fig.5-3, in which $\delta_m v_f p$ is found to increase linearly with p^2.

In spectroscopic measurement, the continuous band fluorescence which is in the near ultraviolet region centered at about 3350 Å was found (Fig.5-4). It is postulated that the following reactions may occur in a mercury vapor flow.[5)]

$$Hg(6^3P_0) + Hg \longrightarrow Hg_2(^3O_u^-)$$

$$Hg_2(^3O_u^-) \longrightarrow 2\,Hg + h\nu\ (3350\ \text{Å}). \qquad (5\text{-}3)$$

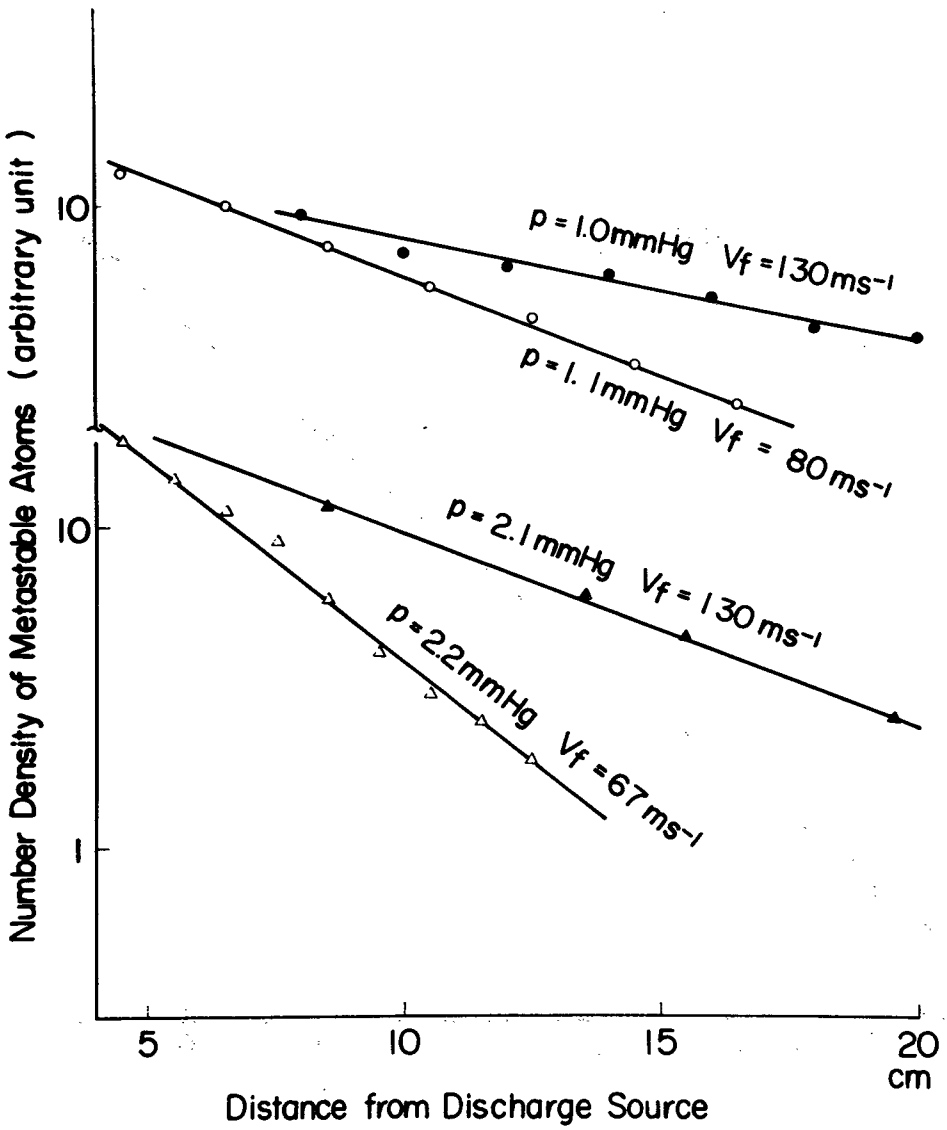

Fig.5-2 Decrease in the metastable atom density. Slope of the density decrease depends on the flow velocity.

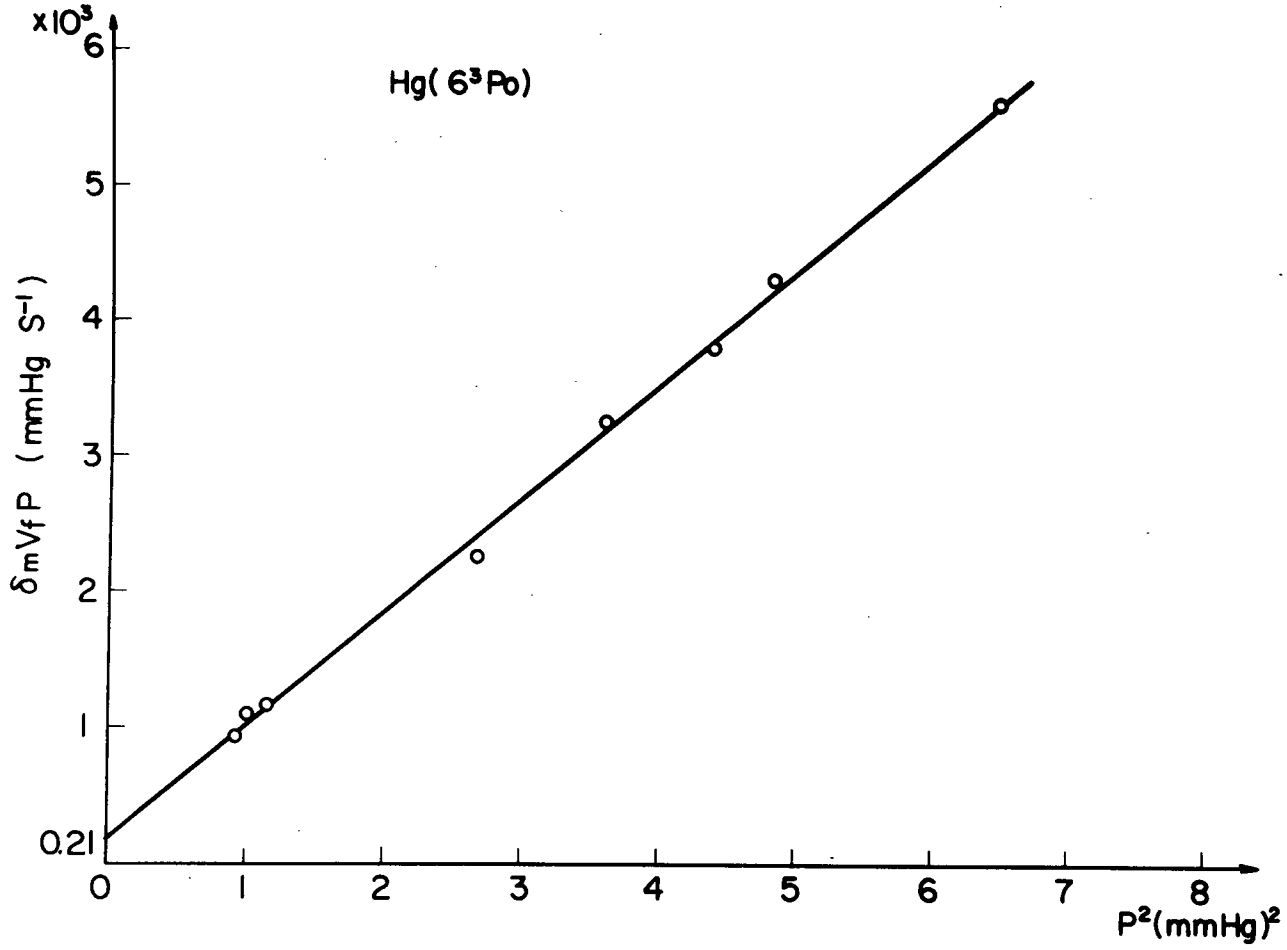

Fig.5-3 Relation between $\delta_m v_f p$ and p^2.

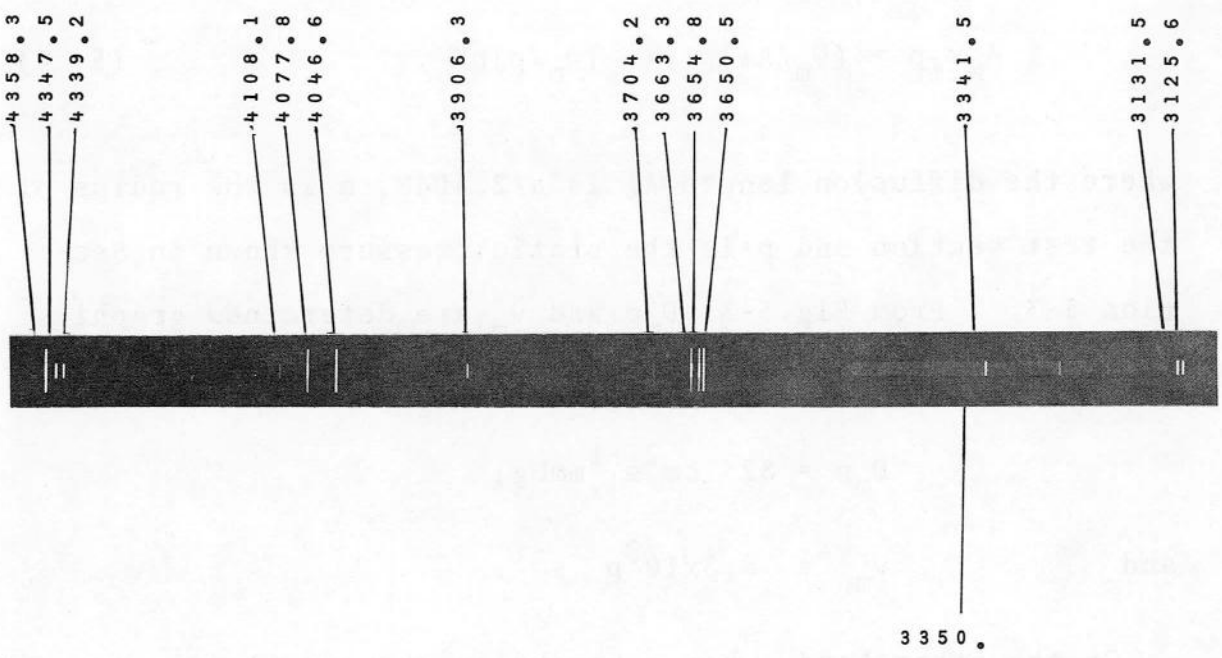

(band fluorescence)

Fig.5-4 The band fluorescence of mercury vapor at the pressure about 2 mmHg.

If the rate at which metastable atoms are converted to metastable diatomic molecules is denoted by ν_m, $\delta_m v_f p$ is described as follows when the radial dependence of the flow velocity is not taken into consideration.

$$\delta_m v_f p = (D_m/\Lambda_0^2)p + (\nu_m/p)p^2 , \qquad (5-4)$$

where the diffusion length Λ_0 is a/2.4048, a is the radius of the test section and p is the static pressure shown in Section 3-3. From Fig.5-3, $D_m p$ and ν_m are determined graphically as follows,

$$D_m p = 82 \quad cm^2 s^{-1} mmHg,$$

and

$$\nu_m = 8.3 \times 10^2 p \quad s^{-1}.$$

On the other hand, when a parabolic viscous flow is assumed as eq.(3-7), eq.(5-4) can be rewritten as

$$\delta_m v_f p = (D_m/\Lambda^2) + 1.258(\nu_m/p)p^2 , \qquad (5-5)$$

where Λ = a/2.709 . In this case $D_m p$ and ν_m are obtained as:

$$D_m p = 64 \quad cm^2 s^{-1} mmHg,$$

$$\nu_m = 6.6 \times 10^2 p \quad s^{-1}.$$

The diffusion coefficient $D_m = 64/p \ cm^2 s^{-1}$ at 380 - 400 °K in the case when a parabolic viscous flow is assumed agrees well with that measured by A.O.McCoubrey whose value is 87/p at 473 °K,[5] since the diffusion coefficient is proportional to $T^{3/2}$.[8] By H.Coulliette, the density of metastable atoms was measured and the diffusion coefficient corrected to the temperature 380 °K is $D_m = 1.52 \times 10^{18}/n_o \ cm^2 s^{-1}$, that is 63/p $cm^2 s^{-1}$, whose value agrees with the present result.

The conversion process from metastable atoms to metastable diatomic molecules is considered to occur by the two body collision in this experiment, on the other hand A.O.McCoubrey found the process by the three body collidion which occurs at the rate $\nu_m = 10^{-30} n_o^2 \ s^{-1}$ that is $\nu_m = 5.8 \times 10^2 p^2 \ s^{-1}$, in the condition where mercury vapor at the pressure less than about 1.5 mmHg was superheated from 70 °C to 100 °C above the saturation temperature, however, the value agrees with that shown in this experiment at about 1 mmHg.

5-4 Concluding Remarks

From exponential decrease in the metastable atom density somewhat distant from the discharge source, the diffusion coefficient and the rate constant at which metastable atoms are converted to metastable diatomic molecules by collisions with ground state atoms are estimated to be $D_m = 82/p \ cm^2 s^{-1}$

and $\nu_m = 8.3 \times 10^2 p \ \ s^{-1}$, respectively when the radial dependence of the flow velocity is not taken into consideration.

On the other hand assuming a parabolic viscous flow, those values are $D_m = 64/p \ \ cm^2 s^{-1}$ and $\nu_m = 6.6 \times 10^2 p \ \ s^{-1}$, respectively. This diffusion coefficient is agreeable to the results obtained by A.O.McCoubrey and H.Coulliette.

The conversion rate by the three body collision was estimated to be $\nu_m = 5.8 \times 10^2 p^2 \ \ s^{-1}$ at the pressure range from 0.5 to 1.5 mmHg by A.O.McCoubrey, however, in the present experiment the conversion process is found to occur by the two body collision at the rate $\nu_m = 6.6 \times 10^2 p \ \ s^{-1}$, whose value agrees well with the result obtained by him at about 1 mmHg. In the condition of his experiment, mercury gas was superheated from 70 °C to 100 °C, on the other hand, in the present case mercury gas is almost near the saturation temperature.

References

1) T.Holstein : Phys.Rev. 72(1947) 1212.

2) A.C.G.Mitchell and M.W.Zemansky : Resonance Radiation and Excited Atoms (Cambridge Univ. Press 1961)

3) L.Rayleigh : Proc.Roy.Soc. A 137(1932) 101.

4) M.Nishikawa,Y.Fujii-e and T.Suita : J.Phys.Soc.Japan 30(1971) 528.

5) A.O.McCoubrey : Phys.Rev. 93(1954) 1249.

6) G.Herzberg : Spectra of Diatomic Molecules (D. Van Nostrand Company,Inc., New York, 1950)

7) H.Coulliette : Phys.Rev. 32(1928) 636.

8) A.von Engel : Ionized Gases (Clarendon Press, Oxford 1965)

Chapter 6.

Intensity Distribution Distant from the Discharge Source*

Slow decrease in intensity of mercury atomic lines somewhat distant from the discharge source is found to be controlled by the dissociative recombination process.

From a slope of this decrease on semi-logarithmic plots, it is found that conversion from atomic mercury ions to molecular ions occurs at the rate of $150p^2 \ \ s^{-1}$ and the ambipolar diffusion coefficient for atomic ions in mercury atoms is estimated to be $160/p \ \ cm^2s^{-1}$.

The ambipolar diffusion coefficient for molecular mercury ions and the dissociative recombination coefficient are estimated to be $620/p \ \ cm^2s^{-1}$ and $3.7\times10^{-7} \ \ cm^3s^{-1}$ respectively from the dependence of the reciprocal characteristic length on the electron density.

6-1 Introduction

Hitherto, measurements of the electron density and the intensity of emitted radiation or absorption in the afterglow by a pulsed discharge have been one of the approches to yield informations concerning the collision processes involving

---

*The main part of this chapter was published in Journal of the Physical Society of Japan, Vol.31, No.3, P. 910-918, September, 1971.

electrons, ions and excited atoms. Possible recombination processes which are important loss processes of the charged particles in gases have been already reviewed by H.S.W. Massey.[1)]

In a mercury afterglow, F.L.Mohler found a recombination coefficient of 2.3×10^{-10} $cm^3 s^{-1}$, using the probe method at 0.27 mmHg pressure for 2000 °K electrons.[2)] On the other hand, at the pressure from 0.08 to 0.5 mmHg this coefficient was estimated to be 5×10^{-9} $cm^3 s^{-1}$ using the microwave technique by P.Dandurand and R.B.Holt.[3)]

Thereafter, atomic collision processes occurring in mercury vapor added with helium to bring the electrons into thermal equilibrium quickly with the gas were determined from microwave measurements by M.A.Biondi.[4)] He found that at the pressure over 1 mmHg, the electron decay curve showed increasing evidence of recombination, and from the results the recombination coefficient was obtained to be 5.5×10^{-7} $cm^3 s^{-1}$. This large value was explained from the dissociative recombination process.[5)] As mentioned above, several constants in mercury ionized gas have been already investigated by many persons, however, these values are different in the various experimental conditions.

In this experiment at the static pressure from 0.5 to 3.5 mmHg a stable mercury vapor flow near the saturation temper-

ature is excited by d.c. discharge. In this steady flowing mercury afterglow, intensity distribution of certain mercury lines along the flow from the discharge source exhibited rapid decrease near the source followed by slow decrease somewhat distant from the source.[6] The rapid decrease in intensity near the source was interpreted in connection with the electron ambipolar diffusion to the wall and the electron attachment in Chapter 3.

In this chapter, atomic collision processes involving ions are investigated in a flowing mercury afterglow somewhat distant from the discharge source.

6-2 Axial Intensity Distribution

Intensity distribution decreases slowly somewhat distant from the discharge source as shown in Figs.4-3(a) and 6-1. The slow decrease in intensity may be expected to be controlled by recombination process.

It was found that a slope of the intensity decrease on semi-logarithmic prots did not vary with the discharge current, which is proportional to the electron density in glow discharge, at the low pressure from about 0.5 to 2 mmHg, however, with pressure increase it varied complicately and its current dependence became clearer at the pressure more than 2.7 mmHg as shown in Fig.6-2.

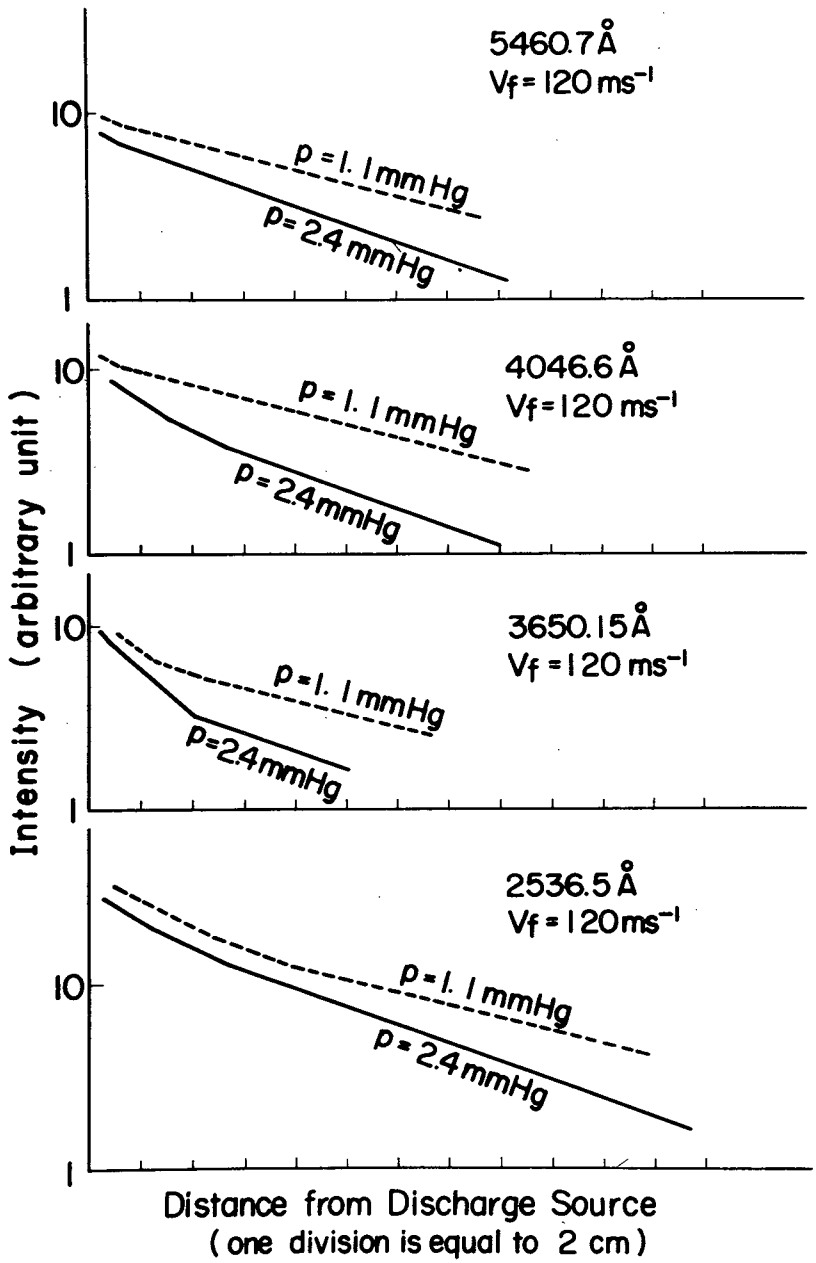

Fig.6-1 Decrease in intensity of Hg lines somewhat distant from the discharge source.

In this region, the following reactions[4] are considered.

$$Hg^+ + 2\,Hg \longrightarrow Hg_2^+ + Hg\,, \qquad (6\text{-}1)$$

$$Hg_2^+ + e \longrightarrow Hg^* + Hg\,, \qquad (6\text{-}2)$$

where * indicates an excited atom.

At the low pressure where a slope of the intensity decrease on semi-logarithmic plots is independent of the discharge current, the decrease in intensity may be controlled by the reaction(6-1), for the reason that the ambipolar diffusion coefficient of molecular mercury ion may be expected to be larger than that of atomic ion because the mobility of molecular ion is larger than that of atomic ion in atomic gas.[7] The statement can be interpreted as the result of charge exchange which occurs most frequently when ions move through the same neutral gas.[8] Consequently the mobility of ions in the same neutral gas is expected to become small apparently due to the charge exchange. On the other hand, with pressure increase the reaction(6-2) is dominant and the decrease in intensity will become to depend on the discharge current.

The dissociative recombination coefficient is theoretically found to be about 100 times larger than the radiative recombination coefficient,[9] which is neglected in this case, so that the rate equations of these reactions can be written

as follows.

$$v_f(\partial n_+/\partial x) = -(D_{a+}/\Lambda^2)n_+ - \nu n_+ \quad , \qquad (6-3)$$

$$v_f(\partial n_{2+}/\partial x) = -(D_{a2+}/\Lambda^2)n_{2+} + \nu n_+ - \alpha_{2+} n_{2+} n_e \quad , \qquad (6-4)$$

$$v_f(\partial n_e/\partial x) = -(D_{ae}/\Lambda^2)n_e - \alpha_{2+} n_{2+} n_e \quad , \qquad (6-5)$$

where $D_{a+} = (\mu_+/\mu_e)D_e + D_+$,

$D_{a2+} = (\mu_{2+}/\mu_e)D_e + D_{2+}$,

and $D_{ae} = (n_+/n_e)D_{a+} + (n_{2+}/n_e)D_{a2+}$

on the assumption that $T_e > T_+ = T_{2+}$, $1 \gg (\mu_+/\mu_e)(n_+/n_e)$ and $1 \gg (\mu_{2+}/\mu_e)(n_{2+}/n_e)$.

With the suffixes e, + and 2+ representing electrons, atomic ions and molecular ions respectively, n, D_a, D, μ, ν and α_{2+} are their densities, ambipolar diffusion coefficients, diffusion coefficients, mobilities, the conversion frequency from atomic ions to molecular ions and the dissociative recombination, respectively. The diffusion length is denoted by Λ which may be proper to be represented in the most simple form a/2.4048 in the case when the radial dependence of the flow velocity is not taken into consideration .

Here the electron ambipolar diffusion coefficient D_{ae} is func-

tion of n_+ and n_{2+}, it is too difficult to solve these equations involving eq.(6-5), however, it may be good approximation to assume that $n_e = n_+ + n_{2+}$ instead of eq.(6-5).

At low pressure where a slope of the intensity decrease on semi-logarithmic plots is independent of the discharge current, assumed that $n_+ \gg n_{2+}$, n_e is approximated to be n_+ and consequently the solutions of these equations can be approximately represented as:

$$n_+ = n_+(0)\ \exp(-\delta_+ x)\ , \qquad (6\text{-}6)$$

$$n_{2+} = n_{2+}(0)\ \exp(-\delta_{2+} x) + \frac{\nu n_+(0)}{v_f(\delta_{2+} - \delta_+)} \left\{ \exp(-\delta_+ x) - \exp(-\delta_{2+} x) \right\}, \qquad (6\text{-}7)$$

where $\delta_+ = (D_{a+}/\Lambda^2 + \nu)/v_f$,

and $\delta_{2+} = (D_{a2+}/\Lambda^2 + \alpha_{2+} n_+(0))/v_f$.

For molecular ion production, only the production mechanism obeying to the reaction(6-1) is considered in the present case so that the initial value of molecular ion density can be taken as $n_{2+}(0) = n_+(0)/(v_f \delta_{2+})$ which is calculated from the condition that $\partial n_{2+}/\partial x \,\big|_{x=0} = 0$.

Since the observed intensity I is proportional to $\alpha_{2+} n_{2+} n_e$ or $\alpha_{2+} n_{2+}(n_+ + n_{2+})$, the reciprocal characteristic length ζ

is represented as:

$$\zeta = -I^{-1}(\partial I/\partial x)$$

$$= \delta_+ \frac{1 - \exp\{-(\delta_{2+} - \delta_+)x\}}{1 - (\delta_+/\delta_{2+})\exp\{-(\delta_{2+} - \delta_+)x\}}$$

$$+ \delta_+ \frac{1 - \dfrac{\nu}{v_f(\delta_{2+} - \delta_+) + \nu} \exp\{-(\delta_{2+} - \delta_+)x\}}{1 - \dfrac{\nu}{v_f(\delta_{2+} - \delta_+) + \nu} \dfrac{\delta_+}{\delta_{2+}} \exp\{-(\delta_{2+} - \delta_+)x\}} . \quad (6-8)$$

Since $\delta_{2+} > \delta_+$ in the low pressure range, ζ is approximately obtained as $\zeta = 2\delta_+$ at the position distant from the source where the intensity decreases exponentially, so that $\zeta v_f p$ can be written as:

$$\zeta v_f p = 2 (D_{a+} p/\Lambda^2 + \nu p) . \quad (6-9)$$

As shown in Fig.6-2, $\zeta v_f p$ is found to depend linearly on p^3. Using eq.(6-9), the ambipolar diffusion coefficient and the conversion frequency from atomic ions to molecular ions can be graphically obtained as

$$D_{a+} = 1.6\times10^2/p \quad cm^2 s^{-1}$$

and $$\nu = 1.5\times10^2 p^2 \quad s^{-1}$$ respectively.

This conversion frequency ν is in comparable order with $100p^2$

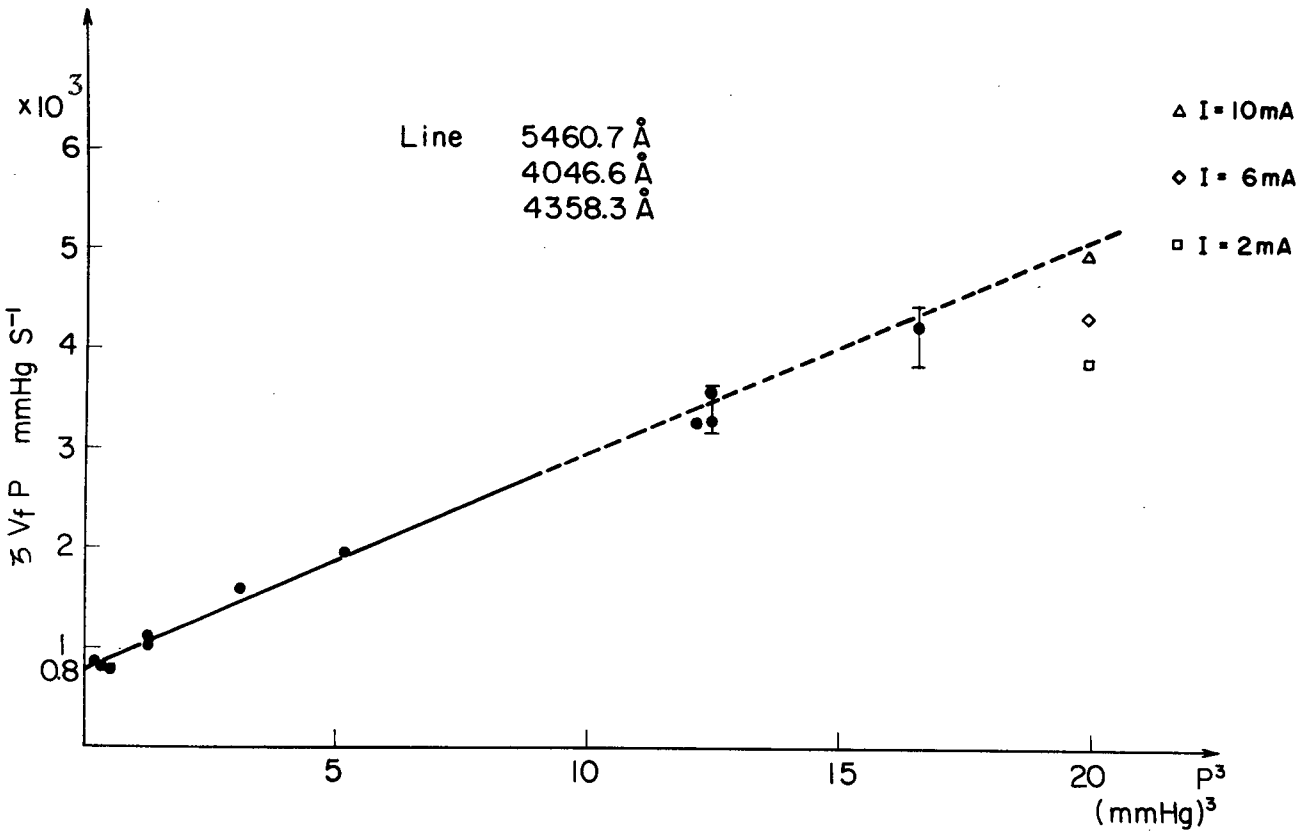

Fig.6-2 Dependence of $\zeta v_f p$ on p^3.

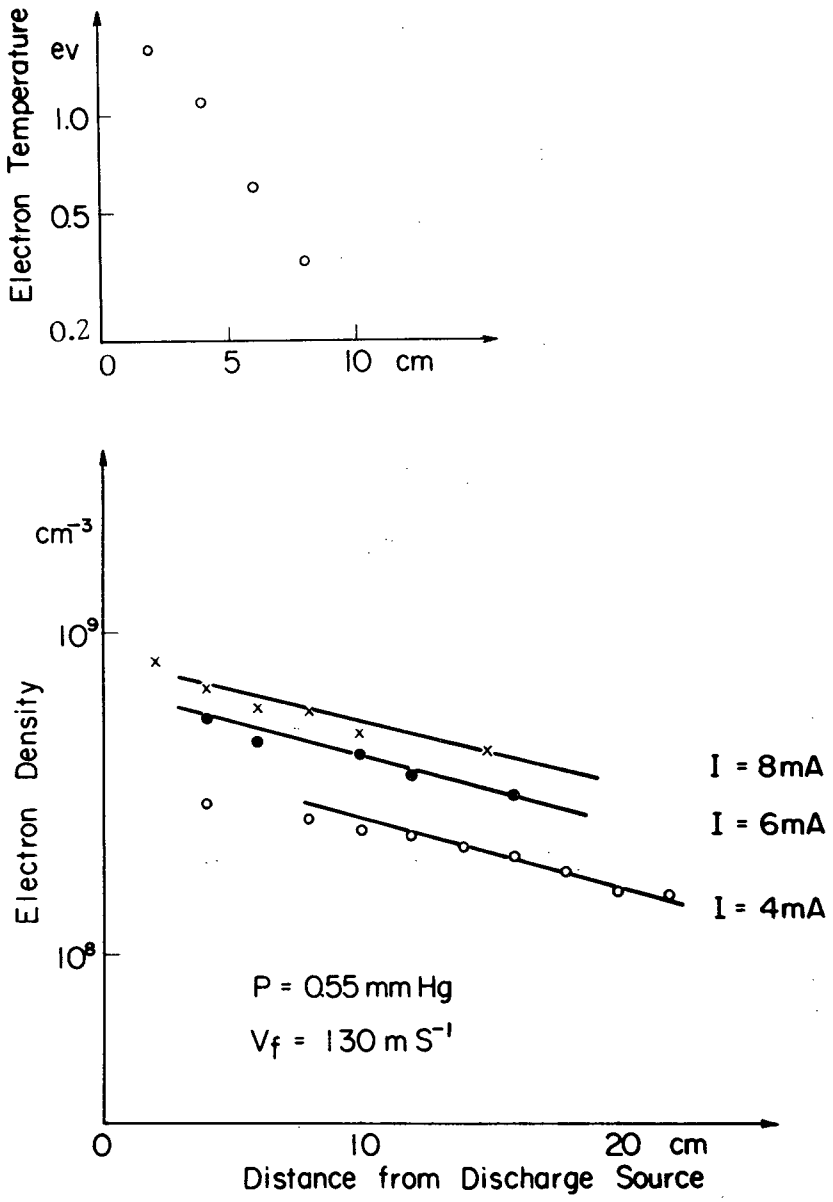

Fig.6-3 Decrease in the electron density somewhat distant from the discharge source, and decrease in the electron temperature.

estimated by M.A.Biondi.[4)]

The electron density distribution along the flow axis at the pressure 0.55 mmHg is shown in Fig.6-3.
Denote the reciprocal characteristic length of the decrease in electron density somewhat distant from the discharge source by ζ_e, $\zeta_e v_f p$ is about half of $\zeta v_f p$ in value. This result supports that the recombination process is dominant in this region.

As pressure increases, atomic ions are almost converted to molecular ions so that the reaction(6-2) is predominant and the rate equation can be described as:

$$v_f \frac{\partial n_{2+}}{\partial x} = - \frac{D_{a2+}}{\Lambda^2} n_{2+} - \alpha_{2+} n_{2+}^2 \quad . \tag{6-10}$$

And ζ in this case can be calculated as follows:

$$\zeta = - I^{-1}(\partial I/\partial x)$$

$$= \frac{2(D_{a2+}/\Lambda^2 + \alpha_{2+} n_{2+}(0))/v_f}{1 + \frac{\alpha_{2+} n_{2+}(0)}{D_{a2+}/\Lambda^2}\left\{1 - \exp\left(- \frac{D_{a2+}}{v_f \Lambda^2} x\right)\right\}} \quad . \tag{6-11}$$

When $D_{a2+}x/(v_f\Lambda^2) \ll 1$ and $\alpha_{2+}n_{2+}(0)x/v_f \ll 1$, ζ is approximately described as $\zeta = 2(D_{a2+}/\Lambda^2 + \alpha_{2+}n_{2+}(0))/v_f$ that is

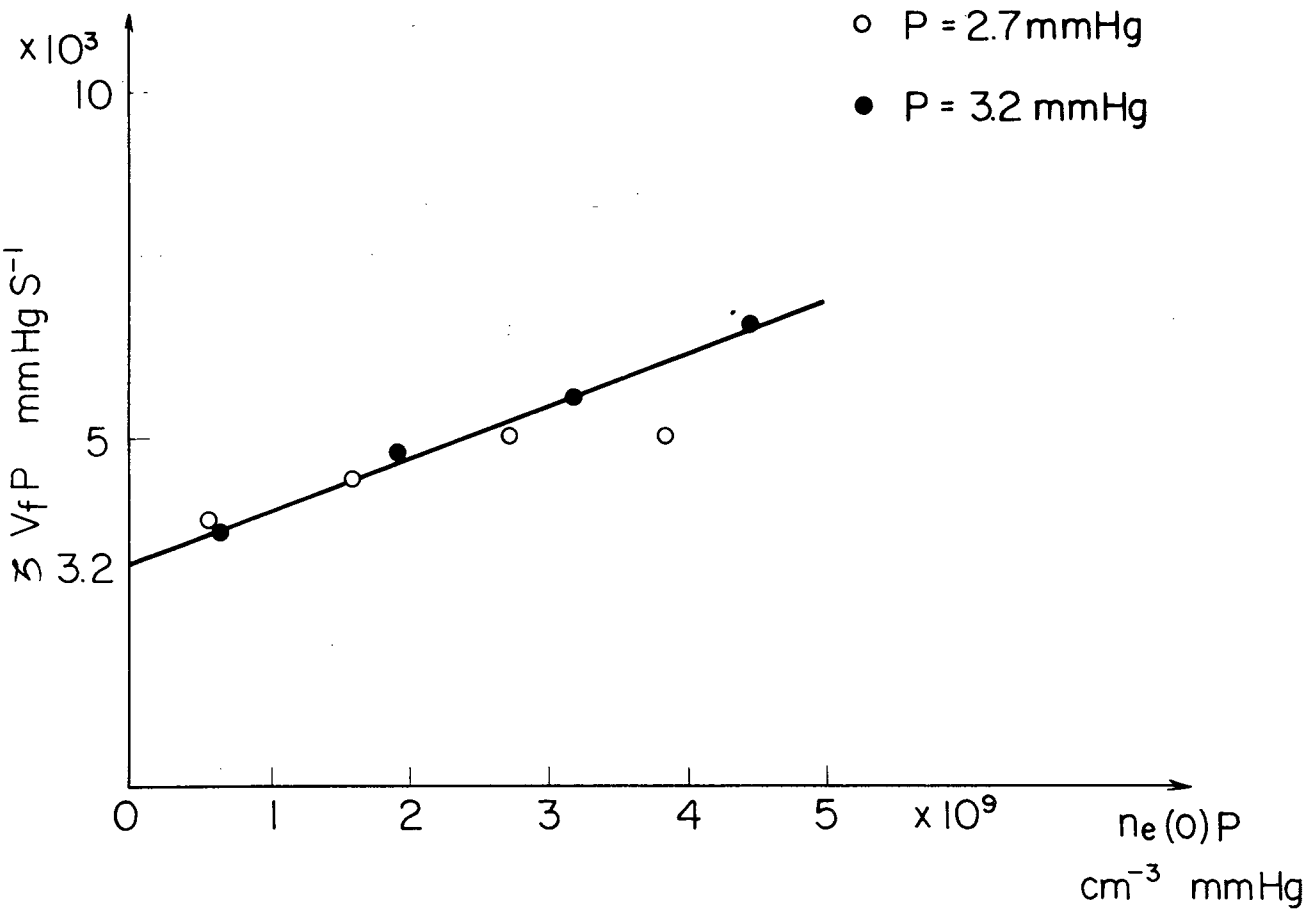

Fig.6-4 Dependence of $\zeta v_f p$ on $n_e(0)p$.

$$\zeta v_f p = 2(D_{a2+} p/\Lambda^2 + \alpha_{2+} n_{2+}(0) p) , \qquad (6\text{-}12)$$

so that the reciprocal characteristic length becomes to depend on the initial ion density as shown in Fig.6-4. In this case it was found from the triple probe measurement that the initial electron density increased with the discharge current at the rate of 10^8 $cm^{-3}mA^{-1}$ on the average at the position about 2 cm from the discharge source downstream. From the relation(6-12) and Fig.6-4, the ambipolar diffusion coefficient for molecular ions and the dissociative recombination coefficient are obtained as follows:

$$D_{a2+} = 6.2\times10^2/p \quad cm^2s^{-1},$$
$$\alpha_{2+} = 3.7\times10^{-7} \quad cm^3s^{-1}.$$

This recombination coefficient is about 1.5 times smaller than the value 5.5×10^{-7} cm^3s^{-1} measured by M.A.Biondi. The ratio of the ambipolar diffusion coefficient for molecular ions to that for atomic ions shows somewhat large value as $D_{a2+}/D_{a+} = 3.9$.

6-3 Radial Intensity Distribution

In the recombination region, the radial intensity distributions were calculated by Pearce's method[10] from the intensity measurements by scanning across the image. Those results are shown in Fig.6-5. The profile is found to be flat

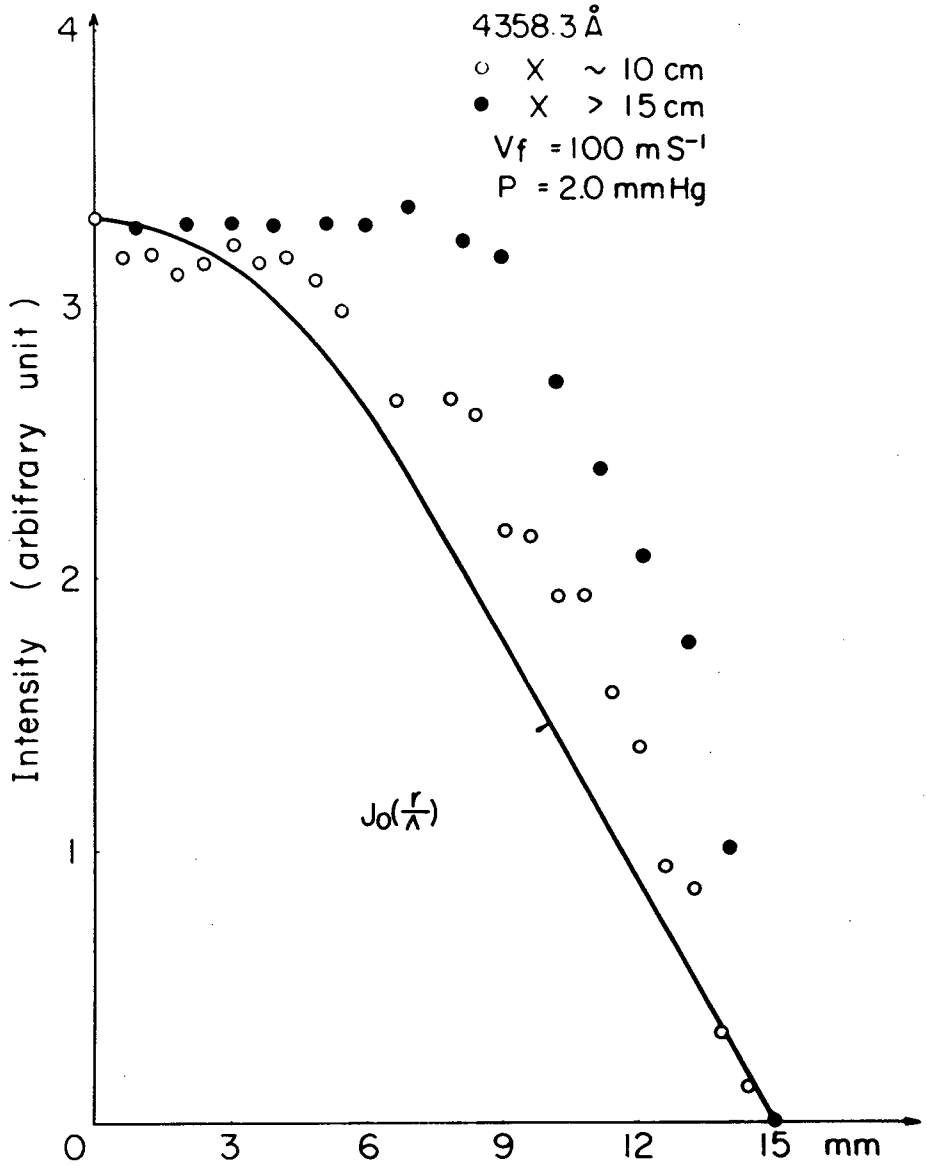

Fig.6-5 Radial intensity distribution.

The plots show the inverted radial intensity distribution by Pearce's method.

in comparison with the zeroth Bessel function and to become flatter along the flow downstream. Since the observed intensity is proportional to $\alpha_{2+}n_{2+}n_e$, the radial distribution of molecular ions will be expected to be flatter than the profile.

In the condition where $T_e \gg T_g$, the ratio of the ambipolar diffusion coefficients is proportional to that of the electron temperatures so that the electron temperature T_e in this region can be roughly estimated to be T_e = 0.12 eV by the result of the previous chapter in which $D_{ae} = 2.7\times10^3/p$ cm^2s^{-1} at the electron temperature about 2 eV.[11] This electron temperature is relatively high in comparison with that in the afterglow reported by M.A.Biondi.[4] From the radial intensity distribution as shown in Fig.6-5, it may be expected that electrons with high energy diffuse against the ambipolar space charge field to the boundary layer or the wall which is a large energy damper and are thermalized to recombine with molecular ions.

6-4 Concluding Remarks

Slow intensity decrease somewhat distant from the source is related to the dissociative recombination process. At the low pressure from 0.5 to 2 mmHg, the reciprocal characteristic length ζ was independent of the charge current. From this pressure range, the ambipolar diffusion coefficient for

atomic ions and the conversion frequency at which atomic ions are converted to molecular ions are obtained as $D_{a+} = 1.6 \times 10^2/p$ $cm^2 s^{-1}$ and $\nu = 1.5 \times 10^2 p^2$ s^{-1}, respectively. The conversion frequency is in comparable order of $100p^2$ estimated by M.A. Biondi. The current dependence of ζ became clearer at the pressure than 2.7 mmHg. From this dependence, the ambipolar diffusion coefficient for molecular ions and the dissociative recombination coefficient are estimated to be $D_{a2+} = 6.2 \times 10^2/p$ $cm^2 s^{-1}$ and $\alpha_{2+} = 3.7 \times 10^{-7}$ $cm^3 s^{-1}$, respectively. This recombination coefficient is about 1.5 times smaller than that measured by M.A.Biondi. From the deta of the ambipolar diffusion coefficient, the electron temperature in this region is estimated to be about 0.12 eV, whose value is relatively high in comparison with the electron temperature in the afterglow reported by M.A.Biondi. It may be expected that electrons with high energy diffuse to the boundary layer near the wall which may be a large energy damper, and are thermalized to recombine with molecular ions. This interpretation will be supported by the radial intensity distribution as shown in Fig.6-5.

References

1) H.S.W.Massey : Phil.Mag.,Suppl. 1(1952) 395.

2) F.L.Mohler : J.Reseach Natl.Bur.Standards 19(1937) 559.

3) P.Dandurand and R.B.Holt : Phys.Rev. 82(1951) 868.

4) M.A.Biondi : Phys.Rev. 90(1953) 730.

5) M.A.Biondi and T.Holstein : Phys.Rev. 82(1951) 962.

6) M.Nishikawa, Y.Fujii-e and T.Suita : Japan J.appl.Phys. 7(1968) 442.

7) J.A.Hornbeck : Phys.Rev. 84(1951) 615.

8) W.DE Groot and F.M.Penning : Handb.Phys. 23/1, Springer, Berlin, 1933.

9) C.B.Collins : Phys.Rev. 140(1965) 1850.

10) W.J.Pearce : Optical Spectrometric Measurements of High Temperature, P.J.Dickerman, editor,(Chicago Univ.Press. Chicago, 1961) P.123.

11) M.Nishikawa, Y.Fujii-e and T.Suita : J.Phys.Soc. of Japan 30(1971) 528.

Chapter 7.

Depopulation of Excited Mercury Atoms by Collisions with Hydrogen Molecules

Using the steady state flowing afterglow method, hydrogen molecules are introduced, in their ground states, into the mercury afterglow plasma in which the dissociative recombination process is predominant, and the depopulation of the excited mercury states by collisions with hydrogen molecules are investigated. The quenching of the radiation emitted from 7^3S_1 or 6^3D state is explained by assuming that after the dissociative recombination the dissociated atom in the excited state whose transition probability is smaller than that of 7^3S_1 or 6^3D state is depopulated by collisions with hydrogen molecules.

Slow decrease in intensity of Hg lines can be interpreted by the two cascade transitions' model in the dissociative recombination region. This model may make sure of the results in Chapter 6.

The resonance state 6^3P_1 and the metastable state 6^3P_0 are also quenched and these quenching cross sections are estimated to be $\bar{\sigma}_{q1} = 6.6$ Å^2 and $\bar{\sigma}_{qo} = 0.25$ Å^2 respectively.

The main part of this chapter was published in Japanese Journal of Applied Physics, Vol. 10, No. 7, P.827-834, July, 1971.

7-1 Introduction

There have been many studies of quenching properties of various gases, but all of them have used optical methods for exciting atoms.[1] Recently with the development of lasers, the studies of relaxation mechanisms in excited laser levels have been discussed in large number of papers, and the destruction of excited states in discharge plasma containing molecular impurities is of great interest in connection with the problem of creating a medium with a negative absorption coefficient, that is a laser action.[2,3]

In mercury gas, for instance, it appears that a means for providing rapid depletion of the lower P states is necessary for the population inversion to occur, since the electron cross sections for excitation of the upper states are reasonably large.[4] On the ground that hydrogen molecules de-excite the population of the resonance state 6^3P_1 or the metastable state 6^3P_0, the behavior of mercury discharge plasma containing the hydrogen molecular impurity also has been investigated in connection with the popuration inversion.[5] However, it will be difficult to isolate and evaluate the role of quenching by the impurities in the discharge because the impurities change the electrokinetic characteristics of the discharge.

The steady state flowing afterglow method replaces time

resolution with spatial resolution[6,7] so that the hydrogen molecular reactant can be introduced, in its ground state, into the afterglow plasma where the dissociative recombination process is predominant.[8,9,10]

In this chapter, using the steady state flowing afterglow method, quenching of the radiation emitted from the state with large radiative transition probability and depopulation of the metastable atom due to hydrogen molecule introduction into the afterglow plasma are investigated, and cascade transitions from the upper states to the state with large radiative transition probabilities are discussed in the recombination region.

7-2 Experimental Apparatus

The steady state mercury vapor flow is made in Rankine cycle and its block diagram is shown in Fig.7-1. The mercury vapor flow accelerated by a de-Laval nozzle passes through the test section consisting of a transparent quartz tube with a diameter of 3 cm and a length of 100 cm. The d.c. discharge is excited before the test section to attain a steady state flowing mercury afterglow. Into the afterglow region where the dissociative recombination is predominant,[8,9,10] the hydrogen molecular gas is introduced through a slender tube with a diameter of 1 mm. The flow rate of hydrogen

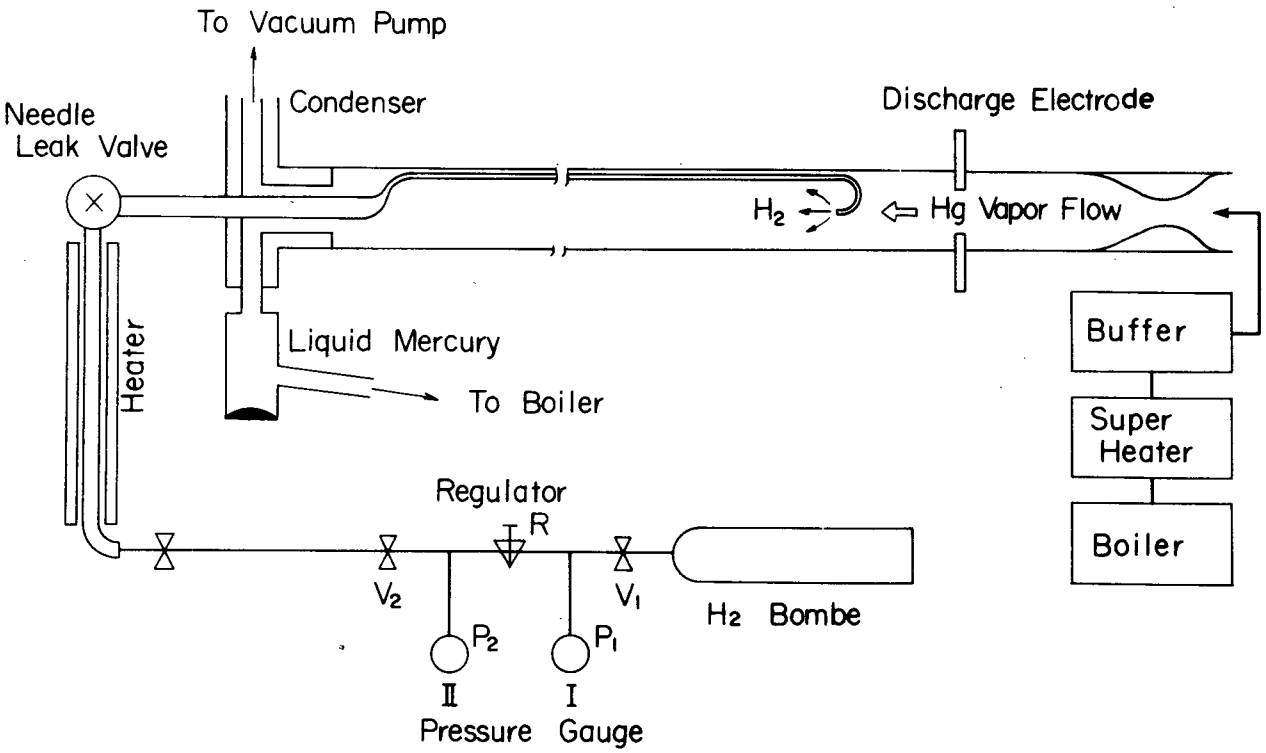

Fig.7-1 Schematic diagram of the flow system.

molecule is controlled by a calibrated variable leak valve and the pressure at the inlet of this valve was kept constant (1.2 atm), monitored by the pressure gauge II. The flow rate of hydrogen molecule was calculated from the fixed volume between the valve V_1 and the regulator R, and the time interval required for a certain pressure drop (from 90 atm to 80 atm) in the volume after the valve V_1 is shut. During this measurement the change of the pressure P_2 was not found at all. The "as received" hydrogen molecular gas with purity better than four nine was used.

In the test section, hydrogen molecules will ultimately diffuse to a uniform radial concentration so that, as far as the flow rate of hydrogen molecule $\dot{N}$ is not so large, the number density of hydrogen molecule M may be given as

$$M = \dot{N} / \pi a^2 v_f \qquad cm^{-3},$$

where a and v_f are the radius of the test section and the flow velocity of the mercury vapor respectively. The flow velocity is measured by the time of flight method, and the radiation emitted from excited mercury atoms in the test section passes through the optical head of the retrofocus type, which is able to scan along the flow axis, and is analized spectroscopically. Details of the apparatus and the method

of measurement are described in the previous chapter 3.

The metastable atom density is determined from the absorption measurement, in which the emission line λ4046.6 Å (7^3S_1 -6^3P_0) from a low pressure mercury lamp operated by d.c. voltage was used as the light source. The resonance line λ2536.5 Å (6^3P_1-6^1S_0) also emitted from the lamp had no effect on the test section, because it was almost absorbed at the lamp envelop. The light source travels in the axial direction with the optical head to measure the absorption. The method of this measurement is shown in the previous section 5-2.

The relative intensities emitted from the test section are calibrated by the tungsten ribbon standard lamp.[11)]

7-3 Two Cascade Transitions' Model in Dissociative Recombination Region

As shown in Fig.7-2, the axial intensity distribution of the mercury line, λ4358.3 Å, was found to exhibit rapid decrease near the discharge source followed by slow decrease somewhat distant from the source. The initial rapid decrease was discussed previouly[12)] and the slowly decreasing part somewhat distant from the source was interpreted as the region where the dissociative recombination is predominant.[8,9,10)] Hydrogen molecules were introduced into this region. The conditions upstream from the position of the entry port of

hydrogen molecule were not found to change, as can be seen from the curves for the case with and without hydrogen molecules.

In Figs.7-2, 7-3 and 7-4, intensities of the line λ4358.3 Å emitted from 7^3S_1 state, of the line λ3650.15 Å emitted from 6^3D_3 state and of the resonance line λ2536.5 Å emitted from 6^3P_1 state are shown for each case with and without hydrogen introduction. These figures show that intensities were reduced by the introduction of hydrogen molecules and this intensity reduction was also found to depend on the partial pressure of hydrogen molecule as shown in Fig.7-4. Thus the collision between an excited mercury atom and a hydrogen molecule prevents the excited atom from radiating.

The quenching Q is defined as

$$Q(x,M) = \frac{\text{Intensity of radiation with } H_2 \text{ at } x}{\text{Intensity of radiation without } H_2 \text{ at } x}, \quad (7-1)$$

where x is the axial distance from the discharge source.

As shown in Figs.7-2, 7-3 and 7-4, the quenching Q of the lines, λ4358.3 Å, λ3650.15 Å and λ2536.5 Å, were found to become independent of the position x beyond about 9 cm downstream, where the recombination process could be assumed to be predominant. The relations between the average values of the quenching Q in this region for each line and the hydrogen

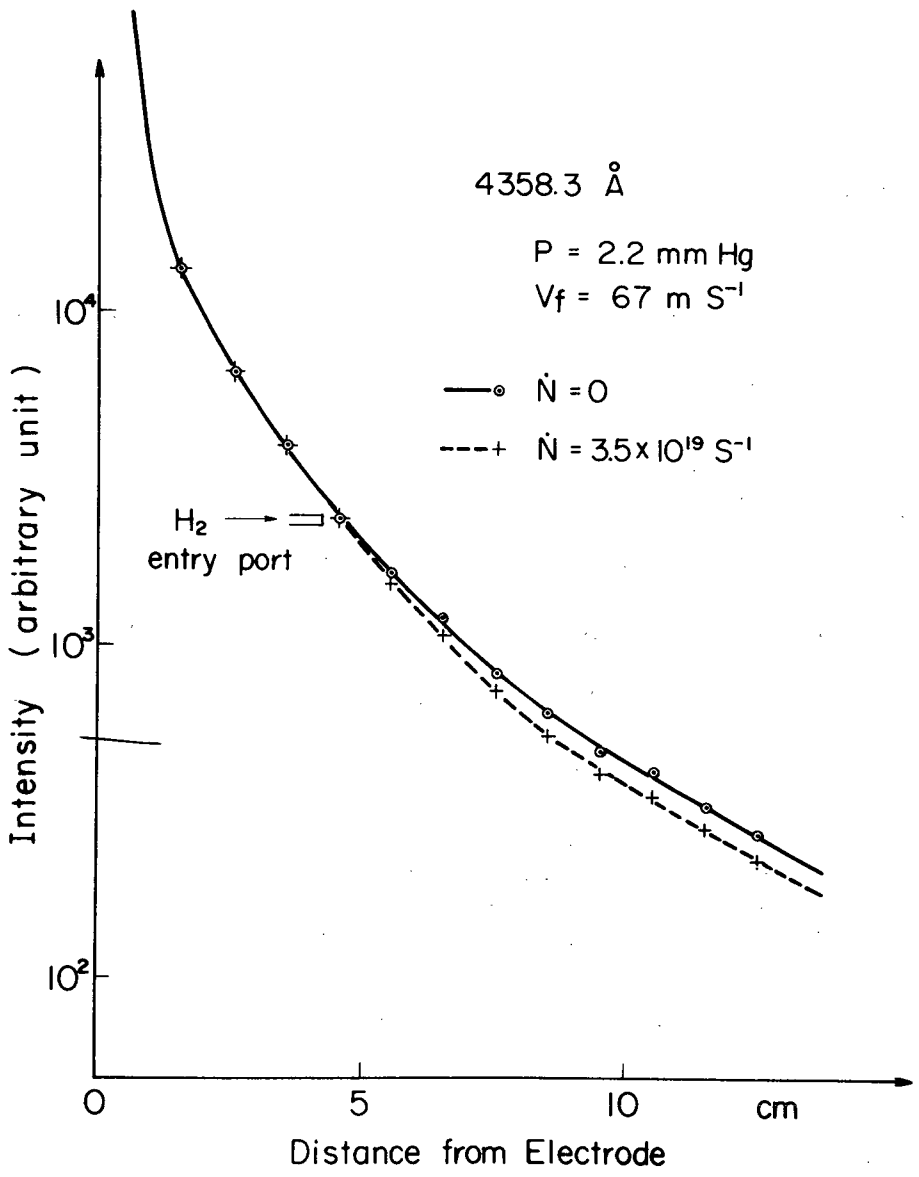

Fig.7-2 Decrease in intensity of the line λ4358.3 Å with and without hydrogen molecule.

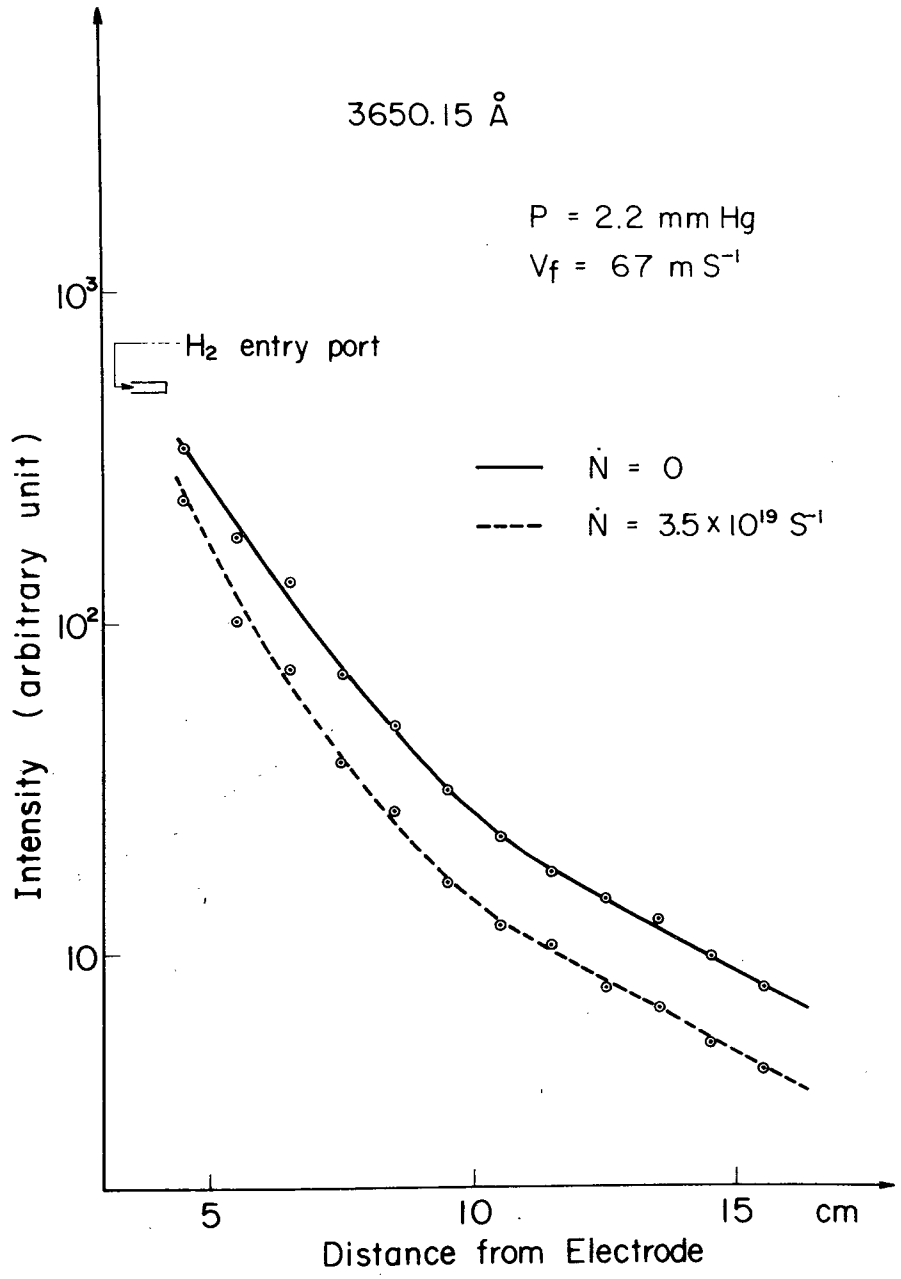

Fig.7-3 Decrease in intensity of the line λ3650.15 Å with and without hydrogen molecule.

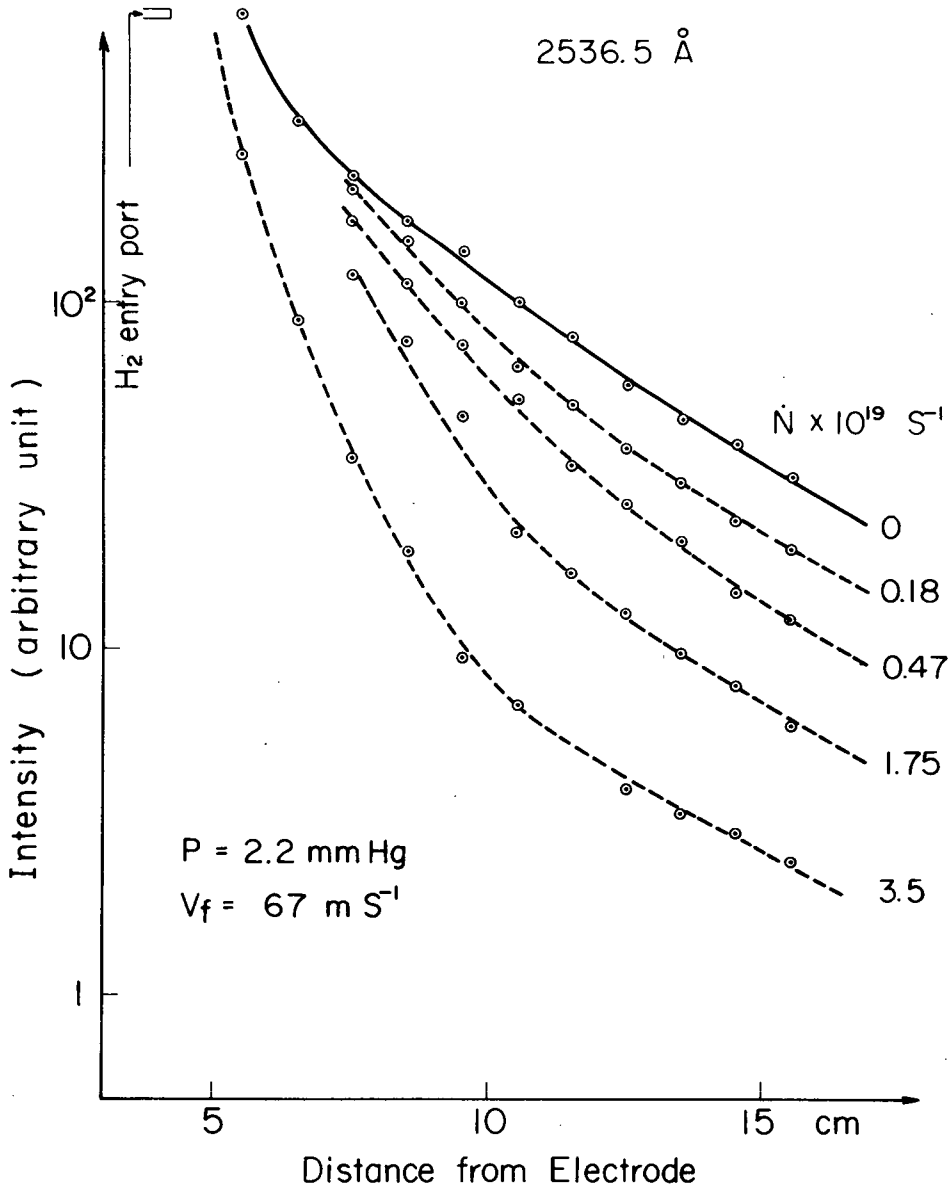

Fig.7-4 Decrease in intensity of the resonance line for various flow rates of hydrogen molecule.

molecule density M are shown in Table 7-1. The density decrease of the metastable atom $Hg(6^3P_0)$ with a long life time is shown for each flow rate $\dot{N}$ in Figs.7-6(a) and 7-6(b). From these figures, it is found that the quenching Q of the metastable atom $Hg(6^3P_0)$ decreases exponentially with the distance x. This situation shows that the metastable atom production by the cascade transition from the higher levels in the recombination region has almost no effect on the decrease in metastable atom density because the metastable atom has relatively a small decay constant and moreover is produced sufficiently at the discharge source.

In the case of quenching collision process at a low partial pressure of hydrogen molecule in the above case, it is impossible to consider that the states of 7^3S_1 or 6^3D with a large radiative transition probability of A_s or A_d, which is of the order 10^9 s^{-1}, are directly quenched by collisions with hydrogen molecules, because the experimental condition satisfies the following relations:

$$A_s \gg \langle v\sigma_q \rangle M, \qquad A_d \gg \langle v\sigma_q \rangle M,$$

where v and σ_q are the relative velocity between both particles and the quenching cross section, respectively. It is also impossible to consider that the influence of hydrogen

Table 7-1 Quenching Q of the radiation emitted from 6^3P_1, 6^3D_3 and 7^3S_1 state at the pressure 2.2 mmHg.

Line	2536.5 Å		3650.15 Å		4046.6 4358.3 Å 5460.7	
M cm^{-3}	Q	1/Q - 1	Q	1/Q - 1	Q	1/Q - 1
$7.4x10^{14}$	0.077	12.	0.54	0.85	0.84	0.20
$2.8x10^{14}$	0.19	4.4	0.75	0.33	0.93	0.075
$1.0x10^{14}$	0.38	1.6	0.89	0.12	0.97	0.025
$3.8x10^{13}$	0.62	0.62	0.96	0.045	0.99	0.010

molecules is due to the non-radiative process by the three body collision i.e.

$$Hg_2^+ + e + H_2 \longrightarrow 2\,Hg(6^1S_0) + H_2^*(2p\sigma\,^3\Sigma_u^+),$$

$$H_2^*(2p\sigma\,^3\Sigma_u^+) \longrightarrow 2\,H + KE,$$

because the stabilization time of the dissociative recombination that is, the time taken for the nuclear separation is of the order of 10^{-13} s [13], and very short.

If the cascade transitions in a dissociation product from only one higher level to both states i.e. 7^3S_1 and 6^3D, are taken into consideration, the quenching Q of the radiation emitted from 7^3S_1 state would be equal to that of the radiation emitted from 6^3D state. However, the experimental results as shown in Table 7-1 indicate that Q of the radiation emitted from 7^3S_1 state differs from that of the radiation emitted from 6^3D state. Therefore, after the dissociative recombination occurs, it is assumed that the recombined neutral molecules are instantly separated into the state n^3P and the ground state or into the state n'^3F and the ground state, where n and n' are the principal quantum number larger than 6 and that larger than 5, respectively, and assumed further that the cascade transition from n^3P state to 7^3S_1 state and that from n'^3F to 6^3D take place as shown in Fig.7-5. It is possible that the excited mercury states, n^3P, n'^3F,

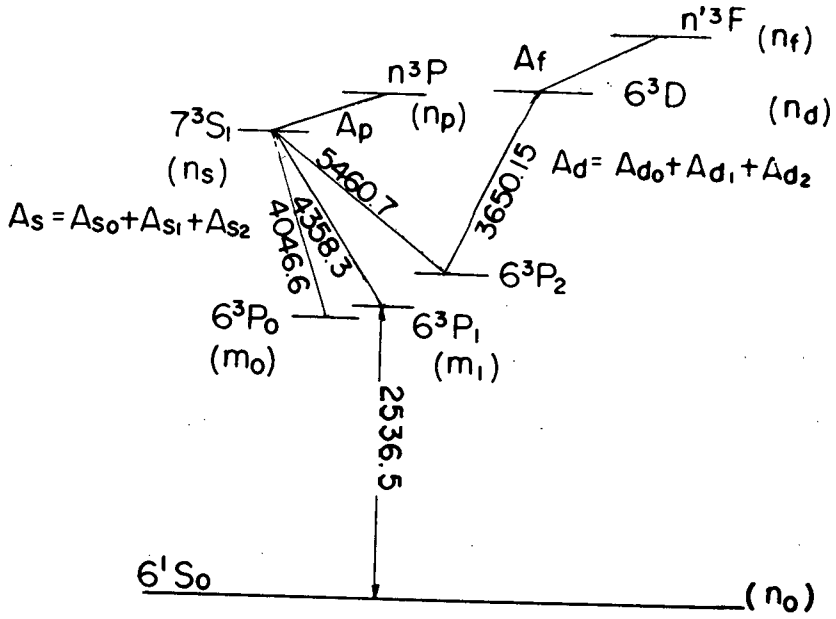

Fig.7-5 Model scheme of cascade transitions to illustrate the quenching of the radiation emitted from 7^3S_1 or 6^3D state in the dissociative recombination region.

are quenched by collisions with hydrogen molecules because the states, n^3P, n'^3F, have been estimated to have the cascade transition probabilities smaller than the states, 7^3S_1, 6^3D.[14] An energetically possible collision process can be written as,[5,15]

$$Hg(\, n^3P \text{ or } n'^3F\,) + H_2 \longrightarrow Hg(6^1S_0) + H_2^*(2p\sigma\,^3\textstyle\sum_u^+),$$

$$H_2^*(2p\sigma\,^3\textstyle\sum_u^+) \longrightarrow H + H + KE. \qquad (7\text{-}2)$$

$$(\, n \geq 7,\ n' \geq 6\,)$$

Denoting the number densities of n^3P state, n'^3F state, electron and mercury molecular ion by n_p, n_f, n_e and n_{2+} respectively, the rate equations for n_p and n_f in the recombination region can be written as:

$$v_f \frac{\partial n_p}{\partial x} = - A_p n_p - q_p M\, n_p + \alpha_p n_e n_{2+}\,, \qquad (7\text{-}3)$$

$$v_f \frac{\partial n_f}{\partial x} = - A_f n_f - q_f M\, n_f + \alpha_f n_e n_{2+}\,, \qquad (7\text{-}4)$$

where the suffixes p and f represent the state n^3P and n'^3F respectively, and A, q M and α are their cascade transition probabilities, quenching probabilities and dissociative recombination coefficients, respectively.

When $A_p \gg v_f n_p^{-1}(\partial n_p/\partial x)$ and $A_f \gg v_f n_f^{-1}(\partial n_f/\partial x)$ in the recombination region, eqs.(7-3) and (7-4) can be rewritten as:

$$n_p = \frac{\alpha_p n_e n_{2+}}{A_p + q_p M} \quad , \qquad (7\text{-}3')$$

$$n_f = \frac{\alpha_f n_e n_{2+}}{A_f + q_f M} \quad . \qquad (7\text{-}4')$$

Using eqs.(7-3') and (7-4'), the density of 7^3S_1 state, n_s and that of 6^3D state, n_d are immediately as:

$$n_s(x,M) = \frac{A_p}{A_s} \frac{\alpha_p n_e n_{2+}}{A_p + q_p M} \quad , \qquad (7\text{-}5)$$

$$n_d(x,M) = \frac{A_f}{A_d} \frac{\alpha_f n_e n_{2+}}{A_f + q_f M} \quad . \qquad (7\text{-}6)$$

Hence, the quenching Q defined by eq.(7-1) can be obtained as follows:

$$Q_s(M) = (1 + q_p M/A_p)^{-1} \quad , \qquad (7\text{-}7)$$

$$Q_d(M) = (1 + q_f M/A_f)^{-1} \quad . \qquad (7\text{-}8)$$

Rewriting these equations, the following equations are obtained: $q_p/A_p = (1/Q_s - 1)/M$, $\quad cm^3$

$q_f/A_f = (1/Q_d - 1)/M$. $\quad cm^3$

From Table 7-1, it is found that $1/Q_s - 1$ is proportional to M. The value q/A can be calculated from Table 7-1 and be obtained on the average as:

$$q_p/A_p = 2.6 \times 10^{-16} \quad cm^3 \ ,$$

$$q_f/A_f = 1.2 \times 10^{-15} \quad cm^3 .$$

The life time of the state n^3P is estimated to be of the order from 10^{-5} to 10^{-6} s,[14] so that the quenching cross section σ_{qp} is of the order from 1 to 10 $Å^2$.

From eqs.(7-5) and (7-6), α_p/α_f is obtained as:

$$\alpha_p/\alpha_f = A_s n_s(x,0)/A_d n_d(x,0) = A_s A_\lambda \acute{\lambda} I_{\acute{\lambda}}/(A_d A_{\acute{\lambda}} \lambda I_\lambda) .$$

In the recombination region, the ratio of the relative intensity of the line $\acute{\lambda}$4358.3 Å to that of the line λ3650.15 Å calibrated by the tungsten ribbon standard lamp[11] was found to be $I_{4358}/I_{-650} = 14$. From NBS Table,[16] $A_s A_\lambda \acute{\lambda}/(A_d A_{\acute{\lambda}} \lambda) = 1.6$, so that α_p/α_f is about 20.

For the lines λ3650.15 Å and $\acute{\lambda}$4046.6 Å, it was found that $I_{4046}/I_{3650} = 7.0$. Using the value of $A_s A_\lambda \acute{\lambda}/A_d A_{\acute{\lambda}} \lambda) = 3.4$ from the same table, the ratio α_p/α_f is about the same as the value mentioned above. From these results it is found that the ratio of the probability at which the recombined molecule is separated into the state n^3P and the ground state to that at which the recombined molecule is separated into the state n'^3F and the ground state after the dissociative recombination is about 20.

7-4 Quenching of the Resonance Radiation and Depopulation of the Metastable Atoms

The absorption and re-emission of the resonance radiation can be described by a diffusion quation with a diffusion coefficient D_r which was discussed by C.Kenty.[17)]

For the quenching collision processes of the resonance state, the following reactions may be taken into consideration:

$$Hg(6^3P_1) + Hg(6^1S_0) \longrightarrow Hg(6^3P_0) + Hg(6^1S_0), \quad (7\text{-}9)$$

$$Hg(6^3P_1) + H_2 \longrightarrow Hg(6^1S_0) + H + H. \quad (7\text{-}10)$$

If the quenching probability of the reaction(7-9) and that of the reaction(7-10) are denoted by $\langle v\sigma \rangle_{10} n_o$ and $q_1 M$ respectively, the rate equation for the density of atoms in the resonance state n_r is represented as:

$$v_f \frac{\partial n_r}{\partial x} = - \frac{D_r}{\Lambda^2} n_r - \langle v\sigma \rangle_{10} n_o n_r - q_1 M n_r + A_{d1} n_d + A_{s1} n_s, \quad (7\text{-}11)$$

where Λ is the diffusion length of the radial component i.e. $\Lambda = a/2.4048$ and a is the radius of the test section.

In the chapter 3 the following relation was obtained experimentally:[12)]

$$D_r/\Lambda^2 + \langle v\sigma \rangle_{10} n_o = (0.24/p + 0.34p) \times 10^4 \ s^{-1}, \quad (7\text{-}12)$$

where p is the static pressure of the mercury vapor flow in the unit of mmHg. Since $v_f n_r^{-1}(\partial n_r/\partial x) \ll D_r/\Lambda^2 + \langle v\sigma\rangle_{10} n_o$ in the recombination region, the number density of atoms in the resonance state, $n_r(x,M)$ can be represented as:

$$n_r(x,M) = \frac{A_{d1} n_d + A_{s1} n_s}{D_r/\Lambda^2 + \langle v\sigma\rangle_{10} n_o + q_1 M} \quad . \tag{7-13}$$

Using eqs.(7-1), (7-3') and (7-4'), the quenching Q_1 is obtained as follows:

$$Q_1(M) = \frac{\left(\frac{A_{s1}}{A_s}\alpha_p + \frac{A_{d1}}{A_d}\alpha_f\right)^{-1} \left\{\frac{A_{s1}}{A_s}\frac{\alpha_p}{1 + q_p M/A_p} + \frac{A_{d1}}{A_d}\frac{\alpha_f}{1 + q_f M/A_f}\right\}}{1 + q_1 M/(D_r/\Lambda^2 + \langle v\sigma\rangle_{10} n_o)} \quad . \tag{7-14}$$

Since $\alpha_p/\alpha_f \simeq 20 \gg 1$ and $A_{s1}/A_s > A_{d1}/A_d$ in the present case, the numerator of eq.(7-14) can be approximated to be Q_s. Therefore eq.(7-14) can be given as:

$$Q_1(M) = \frac{Q_s}{1 + q_1 M/(D_r/\Lambda^2 + \langle v\sigma\rangle_{10} n_o)} \quad . \tag{7-15}$$

When Q_s can be approximated by unity, q_1 may be obtained as:

$$q_1 = \langle v\sigma_{q1}\rangle = (1/Q_1 - 1)(D_r/\Lambda^2 + \langle v\sigma\rangle_{10} n_o)/M \quad . \tag{7-16}$$

From Table 7-1, the value $(1/Q_1 - 1)$ is found to be also proportional to M when $Q_s \simeq 1$. Using the relation(7-12) and eq.(7-16), q_1 is obtained on the average as:

$$q_1 = \langle v\sigma_{q1} \rangle = 1.4 \times 10^{-10} \quad cm^{-3}s^{-1} \ .$$

Defining the average cross section $\bar{\sigma}_{q1}$ as

$$\bar{\sigma}_{q1} = \langle v\sigma_{q1} \rangle / \langle v \rangle = q_1 / \langle v \rangle \ ,$$

where v is the relative velocity between a mercury atom and a hydrogen molecule, $\bar{\sigma}_{q1}$ can be given as:

$$\bar{\sigma}_{q1} = q_1 / \sqrt{(8k/\Pi)(1/m_{H_2} + 1/m_{Hg})T} \ , \qquad (7\text{-}17)$$

where k, m_{H_2}, m_{Hg} and T are the Boltzmann constant, the mass of hydrogen molecule, that of mercury atom and the saturation temperature at the static pressure of the mercury vapor flow, respectively. From eq.(7-17), $\bar{\sigma}_{q1}$ can be calculated as:

$$\bar{\sigma}_{q1} = 6.6 \ \text{Å}^2 \ .$$

This value is comparable with the value of 8.6 Å^2 obtained by M.W.Zemansky.[1)]

With the constant partial pressure of the hydrogen molecular gas, the quenching Q at the static pressure 1.1 mmHg and that at 2.2 mmHg are shown in Table 7-2.

The quenching Q of the line emitted from 6^3D_3 state: λ3650.15 Å and that of the line emitted from 7^3S_1 state: λ4046.6 Å, λ 4358.3 Å, λ5460.7 Å, are found to be independent of the static

Table 7-2 Quenching Q for the static pressure 1.1 and 2.2 mmHg.
($M = 5.7 \times 10^{14}$ cm^{-3})

Line	2536.5 Å		3650.15 Å		4046.6 4358.3 Å 5460.7	
p (mmHg)	Q_1	$1/Q_1 - 1$	Q_d	$1/Q_d - 1$	Q_s	$1/Q_s - 1$
1.1	0.072	13.	0.61	0.65	0.88	0.14
2.2	0.098	9.2	0.60	0.66	0.87	0.15

pressure of the mercury vapor flow within experimental accuracy, i.e. A_p and A_f are constant so that the radiative transitions may be predominant in the experimental condition. However, Q_1 of the resonance radiation is found to change appreciably by the static pressure. This pressure dependence can be explained from that of the radiative imprisonment of the resonance radiation, because the pressure dependence calculated from eqs.(7-12) and (7-15) agrees with the observed one.

The quenching processes of the metastable state 6^3P_0 may be also represented as follows:[15]

$$Hg(6^3P_0) + Hg(6^1S_0) \longrightarrow Hg_2(^3O_u^-) , \qquad (7\text{-}18)$$

$$Hg(6^3P_0) + H_2 \longrightarrow Hg(6^1S_0) + H + H . \qquad (7\text{-}19)$$

If the quenching probability of the reaction(7-18) and that of the reaction(7-19) are denoted by ν_m and q_oM respectively, the rate equation for the metastable atom density m_o can be written as:

$$v_f \frac{\partial m_o}{\partial x} = - \frac{D_m}{\Lambda^2} m_o - \nu_m m_o - q_o M m_o + A_{so} n_s + A_{do} n_d , \qquad (7\text{-}20)$$

where D_m is the diffusion coefficient of the metastable atom

$Hg(6^3P_0)$. Using the results obtained by A.O.McCoubrey,[18] $(D_m/\Lambda^2 + \nu_m)$ can be calculated to be of the order of 10^3 s^{-1} at the static pressure from 1 to 2 mmHg in this case. Since this value is relatively small, the treatment used above for the quenching of 6^3P_1 cannot be applied to the case of eq.(7-20). From Figs.7-6(a) and 7-6(b), it is found that the density of the metastable atom decreases exponentially along the flow axis. It is indicated that the metastable atoms which have a small decay constant are produced at the discharge source in a sufficient quantity and are not affected by cascade transitions in the recombination region, so that the production by the cascade transitions in eq.(7-20) may be neglected. Consequently m_o can be approximately calculated as:

$$m_o(x,M) = m_o(x_o) \exp\left\{-(D_m/\Lambda^2 + \nu_m + q_oM)x/v_f\right\} , \qquad (7\text{-}21)$$

where x_o is the position of the entry port of hydrogen molecule. The quenching Q_o is given as:

$$Q_o(x,M) = \exp(-q_oMx/v_f) = \exp(-\Delta\delta_m x) , \qquad (7\text{-}22)$$

where $$v_f\Delta\delta_m = q_oM . \qquad (7\text{-}22')$$

In Table 7-3, $v_f\Delta\delta_m$ for the parameter M is shown, and q_o is calculated from eq.(7-22') as:

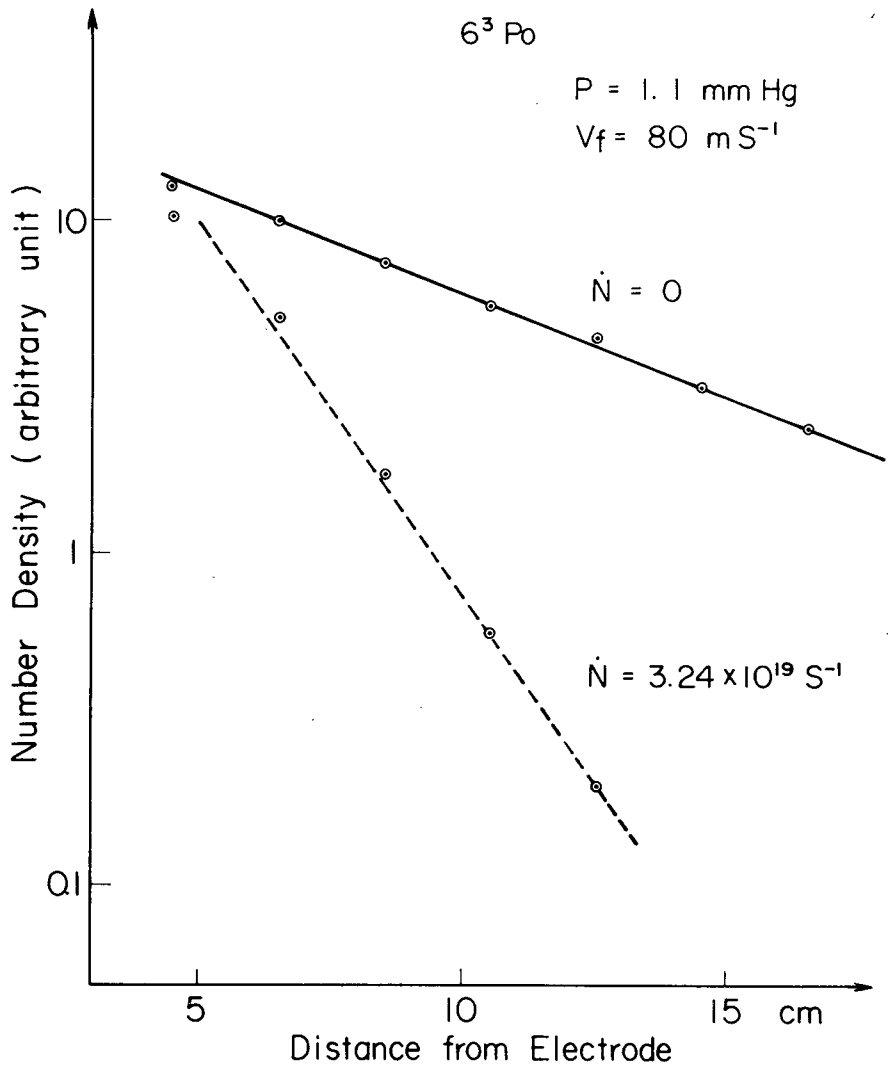

Fig.7-6(a) Decrease in the metastable atom density with and without hydrogen molecule.

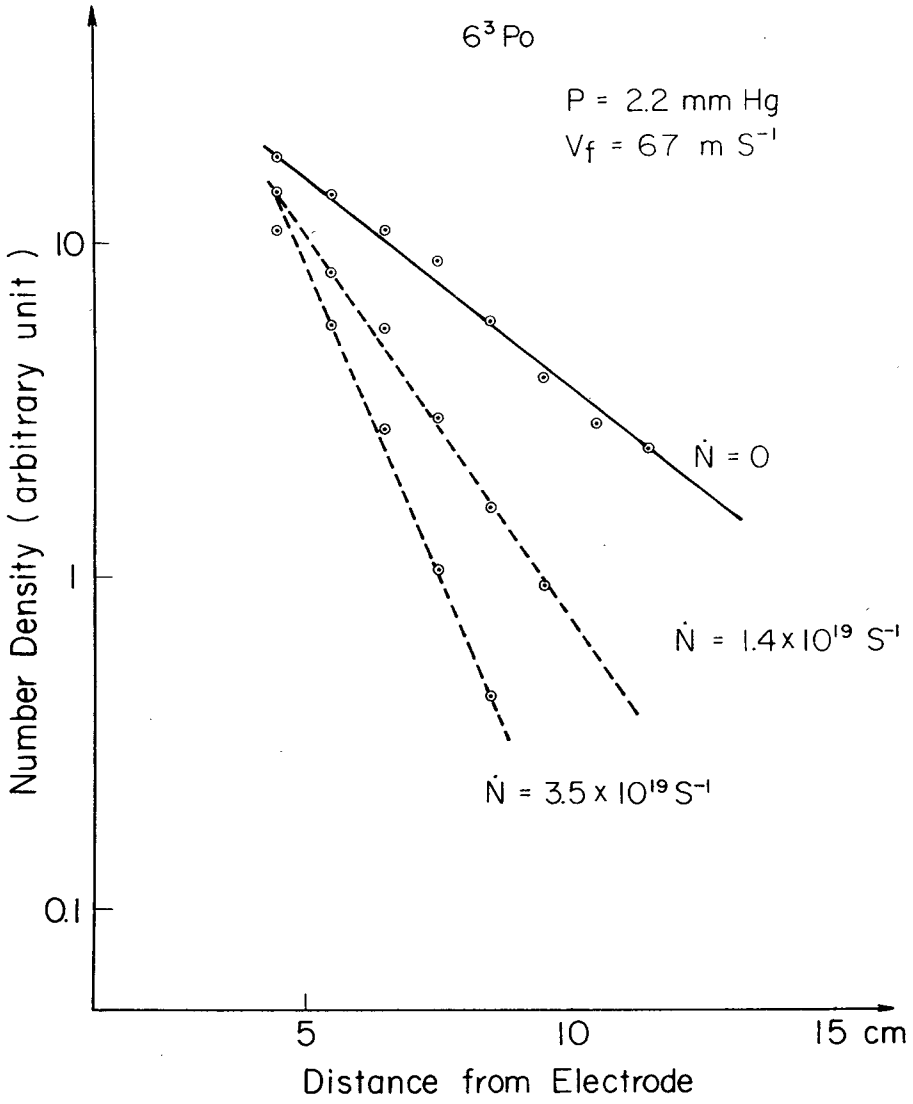

Fig.7-6(b) Decrease in the metastable atom density with and without hydrogen molecule.

Table 7-3 Relation between $v_f \Delta\delta_m$ and the hydrogen molecule density M

M (cm^{-3})	7.4×10^{14}	5.7×10^{14}	3.0×10^{14}
$v_f \Delta\delta_m$ (s^{-1})	3.8×10^{3}	3.0×10^{3}	1.6×10^{3}
$v_f \Delta\delta_m / M$ $(cm^3 s^{-1})$	5.1×10^{-12}	5.2×10^{-12}	5.2×10^{-12}

$$q_o = 5.2 \times 10^{-12} \quad cm^{-3}s^{-1}.$$

The quenching cross section of the metastable state by collisions with hydrogen molecules, $\bar{\sigma}_{qo}$ can be calculated similarly as : $\bar{\sigma}_{qo} = 0.25$ $\mathring{A}^2$.

There is few reports in which this cross section $\bar{\sigma}_{qo}$ is estimated.[19)]

7-5 Concluding Remarks

Using the steady state flowing afterglow method, time resolution is replaced with spatial resolution so that the hydrogen molecular reactant can be introduced, in its ground state, into the afterglow plasma where the dissociative recombination process is predominant. When hydrogen molecules are introduced, it is found that the quenching Q of the radiation emitted from 7^3S_1 state is smaller than that of the radiation emitted from 6^3D_3 state. This difference can be explained by the assumption that Hg_2^+, upon dissociative recombination, is separated into n^3P state and the ground state atom or into n'^3F state and the ground state atom. The transition from n^3P state to 7^3S_1 state and that from n'^3F to 6^3D may be the radiative transition, because A_p and A_f are found to be independent of the static pressure of the mercury vapor flow. The ratio of the probability at which the recombined molecule is separated into n^3P state and the ground state atom to that

at which the recombined molecule is separated into n'^3F state and the ground state atom is estimated to be about 20.

The quenching Q_1 of the resonance radiation is found to be considerably large and depend on the static pressure, whose dependence can be quantitatively explained from that of the radiative imprisonment. The average quenching cross section $\bar{\sigma}_{q1}$ is calculated to be 6.6 $\mathring{A}^2$, which is comparable with the value obtained by M.W.Zemanski.

The quenching Q_o of the metastable atom density is found to decrease exponentially. This behavior is interpreted as the metastable atoms with a small decay constant are produced at the discharge source in a large quantity and decrease in the metastable atom density is not affected by cascade transitions in the recombination region. The average quenching cross section $\bar{\sigma}_{qo}$ of the reaction(7-19) is estimated to be $\bar{\sigma}_{qo} = 0.25\ \mathring{A}^2$.

References

1) A.C.G.Mitchell and M.W.Zemanski : Resonance Radiation and Excited Atoms (Cambridge Univ. Press, 1961)

2) W.R.Bennett, Jr.,P.J.Kinklmann and G.N.Mercer : Appl. Optics, Supplement on Chemical Lasers (1965) 34.

3) V.M.Kamshilina : Optics and Spectros. 14(1962) 252.

4) V.A.Fabrikant : Soviet Physics JETP 14(1962) 372.

5) M.Silver and R.H.Neusèl : J.appl.Phys. 38(1967) 123.

6) F.C.Fehsenfeld, E.E.Fergunson and A.L.Schmeltekopf : J.chem.Phys. 44(1966) 3022.

7) R.C.Bolden, R.S.Hemsworth, M.J.Shaw and N.D.Twiddy : J.Phys. B : Atom.Molec.Phys. 3(1970) 45.

8) R.Anderson and E.Steep : J.Opt.Soc.Amer. 53(1963) 1139.

9) M.Nishikawa, Y.Fujii-e and T.Suita : Japan J.appl.Phys. 7(1968) 442.

10) M.A.Biondi : Phys.Rev. 90(1953) 730.

11) R.Stain, W.E.Schneider and J.K.Takson : Appl.Optics 2(1963) 1151.

12) M.Nishikawa, Y.Fujii-e and T.Suita : J.Phys.Soc.Japan 30(1971) 528.

13) M.S.W.Massey : Phil.Mag.Suppl. 1(1952) 395.

14) O.P.Bochkova : Optics and Spectros. 25(1968) 456.

15) G.Herzberg : Molecular Spectra and Molecular Structure,

I. Spectra of Diatomic Molecules(D.Van Nostrand Company, Princeton, New Jersey 1950)

16) C.H.Corliss and W.R.Bozman : Experimental Transition Probabilities for Spectral Lines of Seventy Elements (Washinton N.B.S. 1962) P.152.

17) C.Kenty : Phys.Rev. 42(1932) 828.

18) A.O.McCoubrey : Phys.Rev. 93(1954) 1249.

19) The Autumnal Sectional Meeting of the Physical Society of Japan, 1969. 15pE 7.

Chapter 8.

Summary

Behaviors of excited and charged particles in the flowing mercury afterglow have been investigated spectroscopically. When the d.c. discharge was locally excited in the flow, the intensity of certain mercury lines along the flow direction exhibited rapid decrease near the discharge source followed by slow decrease somewhat distant from the source. From the dependences of these intensity decreases on the charged particle concentration at the discharge source and on the static pressure, the collision processes which predominate in the afterglow were postulated and further, those rate constants were estimated. The characteristics of the d.c. discharge in the flow are shown first. The collision processes connected with rapid decrease in intensity are described in the first half of this thesis and those connected with slow decrease are in the latter half. These results are summarized below.

The mechanism of electron release as well as ion release from the discharge source is theoretically interpreted as follows. Massive ions transferred downstream by collisions with flowing neutral atoms are released from the electric field of the discharge source much easier than electrons at first, and

consequently by the produced Coulomb force in the flow direction electrons are also released downstream to become the plasma flow. The electric field produced in the flow direction due to EGD effect decreases so rapid that decrease in intensity of Hg lines near the source is not affected by this field.

It is found that the electron density near the source increases linearly with the discharge current in the glow discharge region where the electron temperature is almost constant. The intensity of radiation emitted from highly excited levels also increases linearly with the electron density. Thus rapid decrease in intensity of Hg lines is found to be controlled by electron excitation and the line intensity is found to be proportional to the spontaneous radiation emitted from highly excited levels since the ratios of the transition probabilities estimated from the relative intensity measurements agree well with those of the values from NBS Table.

Rapid decrease in intensity of radiation emitted from highly excited levels near the discharge source is interpreted in connection with the electron diffusion to the wall and the electron attachment. The diffusion coefficient calculated from the experimental results is found to be about 4-5 times as large as the ambipolar diffusion coefficient measured in

the positive column by W.L.Granowski. This value can be interpreted as the transition from free to ambipolar diffusion under the experimental condition and as the increment of the diffusion coefficient due to the negative ion produced by the electron attachment. The limit where the transition from free to ambipolar diffusion is remarkable in mercury atoms is calculated by means of constant ratio approxmation and it can be found that the free diffusion predominates in the condition as follows.

$$T_e = D_e/\mu_e > 3.5\times10^{-7} n_e .$$

Under the present experimental conditions with $n_e = 5\times10^8$ cm^{-3} and $T_e = 2$ eV, the effective diffusion coefficient calculated by constant ratio approximation is almost equal to D_a, however, that calculated by accurate calculation will be estimated to be about 1.5 times as large as D_a. Since in non-equilibrium condition, the ambipolar diffusion coefficient is proportional to the electron temperature, the corrected effective diffusion coefficient introduced in Chapter 3 can be probably estimated to be near the ambipolar diffusion coefficient at 2 eV. This value agrees well with that calculated from the half breadth of the radial intensity profile. On the other hand, relatively slow decrease in intensity of the resonance radiation cannot be interpreted in connection

with the behavior of electrons mentioned above. This decrease is ascribed to imprisonment of radiation and quenching of 6^3P_1 states by collisions with mercury atoms. The absorption coefficient calculated from the experimental results agrees well with that given by M.W.Zemanski, and the quenching cross section of 6^3P_1 states by collisions with mercury atoms is estimated to be 0.038 $\mathring{A}^2$.

The electron attachment coefficient is estimated to be about 1.6×10^{-13} $cm^3 s^{-1}$. This electron attachment process is interpreted as the production process of short-lived negative ions, which are separated into metastable atoms and electrons, shown by U.Fano and J.W.Cooper. The possibility of this process may be supported by decrease in intensity somewhat distant from the discharge source controlled by electrons and positive ions, and supported by the maximum of the metastable atom density exhibited near the discharge source. If this process is regarded, the dissociative rate constant of the short-lived negative ions separated into metastable atoms and electrons may be estimated to be about 2×10^4 s^{-1}.

Metastable atoms may be produced in the case when the short-lived negative ions are dissociated, and also in the case when the resonance states are quenched by collisions with mercury atoms so that the metastable atom density near the discharge source will become large. Then decrease in

number density of metastable atoms with a long life time can not be affected by the cascade transitions from highly excited states to the metastable states in the recombination region. It can be interpreted as the diffusion loss and the conversion from metastable atoms to metastable diatomic molecules by collisions with mercury atoms. This conversion frequency and the diffusion coefficient of metastable atoms are estimated to be $\nu_m = 8.3\times10^2 p \quad s^{-1}$ and $D_m = 82/p \quad cm^2 s^{-1}$ respectively, when the radial dependence of flow velocity is not taken into consideration. Assuming a parabolic viscous flow, these value are estimated to be $\nu_m = 6.6\times10^2 p \quad s^{-1}$ and $D_m = 64/p \quad cm^2 s^{-1}$ respectively. The latter diffusion coefficient is agreeable to that obtained by A.O.McCoubrey and H.Coulliette. By A.O.McCoubrey the rate converted by the three body collision was estimated to be $\nu_m = 5.8\times10^2 p^2 \quad s^{-1}$ at the pressure from 0.5 to 1.5 mmHg, however, in the present experiment the conversion process is found to occur by the two body collision at the rate $\nu_m = 6.6\times10^2 p \quad s^{-1}$, whose value agrees well with the result obtained by him at about 1 mmHg. In his experimental condition, mercury gas was superheated from about 70 °C to 100 °C, on the other hand in the present experiment mercury gas was almost near the saturation temperature.

Slow decrease in intensity somewhat distant from the dis-

charge source is related to the dissociative recombination process. At the low pressure from 0.5 to 2.0 mmHg, the reciprocal characteristic length ζ is found to be independent of the discharge current. In this pressure range, the ambipolar diffusion coefficient for atomic ions and the conversion frequency at which atomic ions are converted to molecular ions by collisions with mercury atoms are obtained as $D_{a+} = 1.6\times10^{2}$ /p cm^2s^{-1} and $\nu = 1.5\times10^{2}p^{2}$ s^{-1} respectively. The conversion frequency is in comparable order with $100p^2$ estimated by M.A.Biondi. The current dependence of ζ is found to be clear at the pressure more than 2.7 mmHg. From this dependence the ambipolar diffusion coefficient for molecular ions and the dissociative recombination coefficient are estimated to be $D_{a2+} = 6.2\times10^{2}/p$ cm^2s^{-1} and $\alpha_{2+} = 3.7\times10^{-7}$ cm^3s^{-1} respectively. This recombination coefficient is about 1.5 times smaller than that measured by M.A.Biondi. From the deta of the ambipolar diffusion coefficient, the electron temperature in this region is estimated to be about 0.12 eV, which is relatively high in comparison with the electron temperature in the afterglow reported by M.A.Biondi. It may be expected that high energy electrons diffuse to the boundary layer near the wall which may be a large energy damper, and are thermalized to recombine with molecular ions. This interpretation will be supported by the radial intensity distri-

bution which is flatter than zeroth Bessel function and exhibits the emission near the wall.

In order to make the dissociative recombination clear, hydrogen molecules are introduced into the mercury afterglow plasma and depopulation of excited atoms has been observed. If atomic ion-electron recombination is predominant, the quenching Q of the radiation emitted from 7^3S_1 state may be expected to be equal to that of the radiation emitted from 6^3D_3 state, however, in the experimental results it is found that the quenching Q of the radiation emitted from 7^3S_1 state is smaller than that of the radiation emitted from 6^3D_3 state. This difference can be explained by the assumption that the recombined molecule is separated into n^3P state and the ground state atom or into n'^3F state and the ground state atom. The transition from n^3P state to 7^3S_1 state and that from n'^3F to 6^3D is estimated to be the radiative transition, because A_p and A_f are found to be independent of the static pressure of the mercury vapor flow. The ratio of the probability at which the recombined molecule is separated into n^3P state and the ground state atom to that at which the recombined molecule is separated into n'^3F state and the ground state atom is estimated to be about 20, so that the recombined molecule is almost separated into n^3P state and the ground state.

The quenching Q_1 of the resonance radiation is found to be

considerably large and depend on the static pressure, whose dependence can be quantitatively explained from that of the radiative imprisonment. The average quenching cross section $\bar{\sigma}_{q1}$ is calculated to be 6.6 $\mathring{A}^2$ which is comparable with the value obtained by M.W.Zemansky.

The quenching Q_o of the metastable atom density is found to decrease exponentially. This behavior is interpreted as follows. The metastable atoms with a small decay constant produced in a large quantity at the discharge source are not affected by cascade transitions in the recombination region. The average quenching cross section $\bar{\sigma}_{qo} = 0.25\ \mathring{A}^2$.

As mentioned above, rapid decrease in intensity of radiation emitted from highly excited states is controlled by the electron diffusion and the electron attachment. On the other hand, decrease in intensity of the resonance radiation masks rapid decrease related to the electron behavior due to the imprisonment of radiation. Slow decrease in intensity of mercury lines somewhat distant from the discharge source is found to be due to the radiative cascade transition from the upper excited states produced by the dissociative recombination.

Acknowledgements

The author would like to express his gratitude to Professor T.Suita for drawing his attention to this problem and continuing guidance and affectionate encouragement, without which this work could never have been accomplished.

The author wishes to express his sincere thanks to Professor S.Fujita for useful discussion and encouragement.

In addition, the author wishes to thank Professor T.Sano, Professor M.Shinagawa, Professor T.Sekiya and Professor S. Imoto for their warm encouragements.

The author is deeply indebted to Dr. Y.Fujii-e for frequent, stimulating, and helpful discussion.

Thanks are due also to Mr. K.Miyazaki and Mr. S.Inoue who gave constant encouragements to the author.

The author is greateful to Mr. T.Yamasaki, Mr. H.Yamasaki and Mr. K.Itahara for their technical assistance. And to the rest of the members in Suita Laboratory the author also would like to express his appreciation.

List of Papers by the Author

1) Intensity Relaxaton of Certain Hg Lines in Preionized Mercury Vapor Flow.

Japan J. appl. Phys. 7 (1968) 442.

2) Decrease in Intensity of Hg Lines near the Source in Weakly Ionized Mercury Gas Flow.

J. Phys. Soc. Japan 30 (1971) 528.

3) Flowing Mercury Afterglow Excited by d.c. Discharge.

J. Phys. Soc. Japan 31 (1971) 910.

4) Depopulation of Excited Mercury Atoms by Collisions with Hydrogen Molecules in the Flowing Mercury Afterglow.

Japan J. appl. Phys. 10 (1971) 827.

List of Lectures by the Author

1) Klein Effect in Magnetic Field.

The Autumnal Sectional Meeting of the Physical Society of Japan, 1965. 15B-3.

2) Experiment of Preionized Mercury Vapor Flow (Ⅲ).

-Decrease in Intensity of Hg Lines along the Flow-

The Autumnal Sectional Meeting of the Atomic Energy Society of Japan, 1966. B-78.

3) Experiment of Preionized Mercury Vapor Flow (Ⅴ).

-Behavior of Excited Mercury Atoms-

The Autumnal Sectional Meeting of the Atomic Energy Society of Japan, 1967. A-49.

4) Experiment of Preionized Mercury Vapor Flow (Ⅵ).

-Behavior of Excited Mercury Atoms in Magnetic Field-

The Autumnal Sectional Meeting of the Atomic Energy Society of Japan, 1967. A-50.

5) Experiment of Preionized Mercury Vapor Flow (Ⅶ).

-Radial Intensity Distribution in Mercury Afterglow Plasma-

The 8 th Annual Meeting of the Atomic Energy Society of Japan, 1968. E-32.

6) Decrease in Intensity of Hg Lines in the Preionized Mercury Vapor Flow.

The 24 th Annual Meeting of the Physical Society of Japan, 1969. 1aRH 5.

7) Flowing Mercury Afterglow (I).

The Autumnal Sectional Meeting of the Physical Society of Japan, 1969. 15pE 9.

8) Flowing Mercury Afterglow (II) .

The 25 th Annual Meeting of the Physical Society of Japan, 1970. 2pTD 6.

9) Flowing Mercury Afterglow (III).

The Autumnal Sectional Meeting of the Physical Society of Japan, 1970. 27pQ 7.

10) EGD Effect in the Case of Corona Discharge Excited in Mercury Vapor Flow.

The Autumnal Sectional Meeting of the Atomic Energy Society of Japan, 1970. D-13.

11) EGD Effect Using Contact Ionization with Atractor in Mercury Vapor Flow.

The 11 th Annual Meeting of the Atomic Energy Society of Japan, 1971. G-47.

論 文 目 録　大阪大学

報告番号・甲第1468号　氏名 西川雅弘

主論文 Behavior of Excited Mercury Atoms in the Preionized Mercury Vapor Flow
（前段電離された水銀蒸気流中の励起原子のふるまい）

（主論文のうち印刷公表したもの）

1. 題名 Intensity Relaxation of Certain Hg Lines in Preionized Mercury Vapor Flow
（前段電離された水銀蒸気流中の発光強度の減少）
Japanese Journal of Applied Physics,
Vol.7, No.4, P.442, April, 1968.

1. 〃 Decrease in Intensity of Hg Lines near the Source in Weakly Ionized Mercury Gas Flow
（弱電離された水銀ガス流中の放電源付近での発光強度の減少）
Journal of the Physical Society of Japan,
Vol.30, No.2, P.528, February, 1971.

1. 〃 Depopulation of Excited Mercury Atoms by Collisions with Hydrogen Molecules in the Flowing Mercury Afterglow
（水銀フローイングアフタグロー中で水素分子との衝突によって起る励起原子密度の減少）
Japanese Journal of Applied Physics,
Vol.10, No.7, P.827, July, 1971.

1. 〃 Flowing Mercury Afterglow Excited by D.C. Discharge
（直流放電による水銀フローイングアフタグロー）
Journal of the Physical Society of Japan,
Vol.31, No.3, P.910, September, 1971.

（主論文のうち未公表のものなし）